LAPPEENRANTA UNIVERSITY OF TECHNOLOGY
LUT School of Engineering Science
Degree Program of Chemical Engineering
Master's Thesis 2018

Vesa Mantsinen

RECYCLING OF CELLULOSE-DISSOLVING IONIC LIQUIDS

Examiners: Prof. Tuomo Sainio
D.Sc. Jari Heinonen

TIIVISTELMÄ

Lappeenrannan teknillinen yliopisto

LUT School of Engineering Science

Kemiantekniikan koulutusohjelma

Vesa Mantsinen

Selluloosaa liuottavien ionisten nesteiden kierrätys

Diplomityö, 2018

Tarkastajat: Prof. Tuomo Sainio

TkT Jari Heinonen

115 sivua, 37 kuvaa, 6 taulukkoa, 1 liite

Hakusanat: ioniset nesteet, liuottimen kierrätys, vedenpoisto, Ioncell-F, adsorptio

Puupohjaisten tekstiilikuitujen valmistus on tällä hetkellä kiivaan tutkimuksen kohteena. Yksi lupaavimmista prosesseista tällaisten kuitujen valmistukseen on selluloosan suoraliuotus ionisilla nesteillä. Olennainen osa prosessia on ionisen nesteen tehokas kierrätys, minkä kehitys on kuitenkin vielä kesken. Tämän työn tavoitteena oli tutkia ja kehittää keinoja ionisen nesteen puhdistamiseen ja kierrättämiseen tekstiilikuidun valmistusprosessissa nimeltään Ioncell-F.

Työn kirjallisuusosassa esiteltiin ionisten nesteiden yleisiä ominaisuuksia ja Ioncell-F-prosessin toimintaa. Useita tekniikoita epäpuhtauksien poistamiseen ionisista nesteistä käytiin läpi ja verrattiin toisiinsa. Kokeellisessa osassa keskityttiin vedenpoistoon 1,5-diatsabisyklo[4.3.0]non-5-enium asetaatti ([DBNH][OAc]) -liuoksista ja kehitettiin adsorptioon perustuva vedenpoistomenetelmä.

Useita kaupallisia orgaanisia ja epäorgaanisia adsorbenttejä testattiin tasapainokokeissa. Parhaat adsorbentit valittiin dynaamisiin kolonnikokeisiin. Kolonnikokeissa tutkittiin lämpötilan, partikkelikoon, virtausnopeuden ja adsorbentin regeneroinnin vaikutusta vedenpoistoon.

Ainoastaan adsorbentit, joilla oli riittävän pieni huokoskoko ja erittäin kapea huokoskokojakauma kykenivät poistamaan vettä [DBNH][OAc]-liuoksista. Niinpä vedenpoiston pääteltiin perustuvan kokoekskluusioon. Vaikka osa adsorbenteistä kykeni poistamaan veden käytännössä täydellisesti, niiden kapasiteetti oli tarkoitukseen nähden matala, minkä vuoksi niitä jouduttiin regeneroimaan tiheästi. Adsorption kinetiikka oli myöskin hidasta, joskin lämpötilan nosto ja pienempi partikkelikoko nopeuttivat sitä hieman.

Menetelmän todettiin vaativan lisäkehitystä ja -tutkimusta. Toisaalta erotusmekanismin ajateltiin olevan sovellettavissa myös muihin ionisiin nesteisiin ja niitä hyödyntäviin prosesseihin. Lopuksi todettiin, että myös muita vedenpoistotekniikoita tulisi tutkia, sillä ne saattavaisivat soveltua adsorptiota paremmin Ioncell-F-prosessiin.

ABSTRACT

Lappeenranta University of Technology

LUT School of Engineering Science

Degree Program of Chemical Engineering

Vesa Mantsinen

Recycling of cellulose-dissolving ionic liquids

Master's thesis, 2018

115 pages, 37 figures, 6 tables, 1 appendix

Examiners: Prof. Tuomo Sainio

D. Sc. (Tech.) Jari Heinonen

Keywords: ionic liquids, solvent recycling, water removal, Ioncell-F, adsorption

Production of wood-based cellulosic textile fibres is currently under intensive research. One of the most promising techniques to produce such fibres is the direct dissolution of cellulose by ionic liquid solvents. A crucial part of the process is solvent recycling, but the lack of viable recycling concepts is currently limiting the commercialisation of the process. The aim of this thesis was to find and develop methods to purify and recycle an ionic liquid in a textile fibre production process called Ioncell-F.

General properties of ionic liquids and basic concept of Ioncell-F were introduced in the literature part of this work. Numerous methods to remove impurities and water from ionic liquids were introduced and compared to each other. Water removal from 1,5-diazabicyclo[4.3.0]non-5-enium acetate ([DBNH][OAc]) solutions was chosen as the main focus in the experimental part and an adsorption-based method was developed.

Several commercial organic and inorganic adsorbents were screened by equilibrium batch experiments. The most suitable adsorbents were chosen for dynamic column experiments. The effect of temperature, particle size, flow rate and regeneration procedure on water removal performance was studied in the dynamic experiments.

It was discovered that only adsorbents with small-enough pores and a very narrow pore size distribution could remove water from [DBNH][OAc] solutions. The separation mechanism was concluded to be size exclusion. Water removal capacity of the studied adsorbents was found to be low for the purpose and frequent regeneration was required. Adsorption kinetics were found to be slow, although improved by higher temperature and smaller particle size.

Further development of the method and exploration of new adsorbents was recommended. On the other hand, the separation mechanism was thought to be applicable for other ionic liquids and processes utilising them. It was also noted that other water removal techniques should be studied because they might be more suitable for Ioncell-F.

TABLE OF CONTENTS

LITERATURE REVIEW 9
1 INTRODUCTION 9
2 IONIC LIQUIDS 13
2.1 General properties 13
2.1.1 Structure 14
2.1.2 Volatility 14
2.1.3 Viscosity 15
2.1.4 Stability 15
2.1.5 Internal interactions 16
2.2 Applications 16
3 IONCELL-F PROCESS 18
3.1 Dissolution of cellulose and preparation of the spinning dope 18
3.2 Spinning and regeneration 19
3.3 Solvent recovery 20
4 RECYCLING OF IONIC LIQUIDS 23
4.1 Removal of water 23
4.1.1 Distillation and evaporation 23
4.1.2 Pressurised carbon dioxide 24
4.1.3 Salting-out 25
4.1.4 Membrane separation 27
4.1.5 Electrodialysis and electrolysis 28
4.1.6 Sweeping with nitrogen 30
4.1.7 Adsorbents and molecular sieves 31
4.2 Removal of inorganic impurities 37
4.2.1 Crystallization 37
4.2.2 Ion exchange 38
4.3 Removal of organic impurities 38
4.3.1 Liquid-liquid extraction 39
4.3.2 Supercritical CO_2 41
4.3.3 Liquid chromatography 41
4.4 Recovery of trace amounts of ionic liquids 43
4.4.1 Membrane separation 43
4.4.2 Adsorption 44
5 SOLVENT RECYCLING CONCEPTS FOR IONCELL-F 46
5.1 Water removal strategies 47

5.2 Strategies for removing inorganic impurities 51
5.3 Strategies for removing organic impurities 52
5.4 Trace IL recovery 53
5.5 Process concepts 54
5.6 Techniques to be studied in experimental part 56
EXPERIMENTAL PART 59
6 MATERIALS AND METHODS 59
6.1 Pre-treatment of solid separation materials 59
6.2 Preparation of ionic liquid solutions 62
6.3 Water removal experiments 63
6.3.1 Equilibrium batch experiments 63
6.3.2 Kinetic experiments 63
6.3.3 Dynamic adsorption experiments 64
6.3.4 Stripping experiments 66
6.4 Chemical analyses 66
7 EQUATIONS 69
8 RESULTS AND DISCUSSION 71
8.1 Viscosity and density measurements 71
8.2 Water removal experiments 73
8.2.1 Equilibrium batch experiments 73
8.2.2 Kinetic experiments 78
8.2.3 Loading experiments 79
8.2.4 Regeneration experiments 88
8.2.5 Cyclic experiment 94
8.2.6 Stripping experiments 98
8.3 SEM-EDS studies 102
9 CONCLUSIONS 105
References 109

APPENDICES
APPENDIX I DERIVATION OF EQUATION (3)

NOMENCLATURE

Symbols

Abs.	absorbance, -
C_e	equilibrium concentration in liquid phase, mol/L
d	diameter, m
h_{bed}	height of separation material bed, m
K_d	apparent distribution coefficient, -
$m_{H_2O,removed}$	mass of water removed by a solid separation material, g
$m_{H2O,\ column}$	mass of water inside a column, g
$m_{IL,e}$	mass of ionic liquid phase in equilibrium, g
$m_{IL,i}$	initial mass of ionic liquid phase, g
m_{solid}	mass of solid separation material, g
N	speed of orbital shaker, rpm
p	pressure, Pa
q_e	concentration of a solute in solid phase, g(solute)/g(solid)
T	temperature, °C
t	time, s
T_{column}	temperature of adsorption column, °C
$t_{contact}$	contact time between solid and liquid phases, s
T_{feed}	temperature of feed solution, °C
U	voltage, V
V	volume, m^3
$\dot{V}$	flow rate, BV/h
V_{air}	volume of air, m^3
V_{feed}	volume of feed solution, m^3
V_{liquid}	volume of liquid phase, m^3
V_{tubes}	void volume of pipes and valves, m^3
$x_w(H_2O)$	water content, wt-%
$x_{w,cumulative}(H_2O)$	cumulative water content, wt-%
$x_{w,spline}$	fitted water content, wt-%
η	viscosity, Pas

Abbreviations

[Amim]Cl	1-allyl-3-methylimidazolium chloride
[APPH][OAc]	3-(aminopropyl)-2-pyrrolidine acetate
[Bmim][BF_4]	1-butyl-3-methylimidazolium tetrafluoroborate
[Bmim][CH_3SO_3]	1-butyl-3-methylimidazolium methanesulfonate
[Bmim][OAc]	1-butyl-3-methylimidazolium acetate
[Bmim][PF_6]	1-butyl-3-methylimidazolium hexafluorophosphate
[Bmim]$^+$	1-butyl-3-methylimidazolium
[Bmim]Cl	1-butyl-3-methylimidazolium chloride
[DBNH][OAc]	1,5-diazabicyclo[4.3.0]non-5-enium acetate
[Emim][$AlCl_4$]	1-ethyl-3-methylimidazolium tetrachloroaluminate
[Emim][OAc]	1-ethyl-3-methylimidazolium acetate
[Emim][Tf_2N]	1-ethyl-3-methylimidazolium bis(trifluoromethylsulfonyl)imide
[Emim]Br	1-ethyl-3-methylimidazolium bromide
[Emim]Cl	1-ethyl-3-methylimidazolium chloride
[Hmim][PF_6]	1-hexyl-3-methylimidazolium hexafluorophosphate
[Mmim][DMP]	*N*-methyl-*N*-methylimidazolium dimethyl phosphate
[Omim][PF_6]	1-octyl-3-methylimidazolium hexafluorophosphate
[TMG]L	1,1,3,3-tetramethylguanide lactate
ABS	aqueous biphasic system
AC	activated carbon
AEM	anion exchange membrane
APP	1-(3-aminopropyl)-2-pyrrolidone
APPAc	1-(3-acetamidopropyl)-2-pyrrolidone
BV	bed volume
CCT	concentrate compartment
CEM	cation exchange membrane
Cuen	cupriethylene diamine
Cuoxam	cuprammonium hydroxide
DBN	1,5-diazabicyclo[4.3.0]non-5-ene

DCT	diluate compartment
ED	electrodialysis
EDS	energy dispersive X-ray spectroscopy
ESP	electrostatic precipitator
GC	gas chromatography
HOAc	acetic acid
L_1	liquid phase 1
L_2	liquid phase 2
NMMO	*N*-methylmorpholine *N*-oxide
PA	polyacrylate
PEG	polyethylene glycol
PS-DVB	polystyrene-divinylbenzene
SAC	strong acid cation exchange resin
SBA	strong base anion exchange resin
sccm	standard cubic centimetre
$scCO_2$	supercritical carbon dioxide
SEM	scanning electron microscopy
TCD	thermal conductivity detector
UV	ultraviolet
UV-VIS	ultraviolet-visible light spectrometer
WAC	weak acid cation exchange resin

LITERATURE REVIEW

1 INTRODUCTION

World population will continue its growth in the near future and with it the demand for food is expected to increase with by 43 % by year 2030 (Hämmerle, 2011). At the same time the world textile consumption is expected to increase by 84 % (Hämmerle, 2011). A major part of textiles is produced from cotton (21.8 % in 2010), which is grown on arable lands that could be used for food production (Hämmerle, 2011). Due to this competition between food and cotton and the fact that cotton requires a lot of water to grow (10 000 L/kg of fibres) (Hämmerle, 2011), the growing textile demand cannot be satisfied by cotton alone. Some of the demand can be satisfied by synthetic textile fibres, but cellulosic fibres are still needed due to their exceptional comfort and moisture management properties (Hämmerle, 2011). Man-made cellulosic fibres have similar physical properties to cotton, but they can be made from more sustainable raw materials, such as wood fibres (Hämmerle, 2011; Hummel, et al., 2016).

Currently the most commonly used process for man-made cellulosic fibre production is the viscose process (Hummel, et al., 2016; Ahmad, et al., 2016). It uses carbon disulfide (CS_2) and sodium hydroxide (NaOH) to convert cellulose into cellulose xhantate, which is then regenerated back to cellulose with sulfuric acid (H_2SO_4) (Hauru, et al., 2014). The process consumes significant amounts of chemicals and produces toxic by-products, such as hydrogen sulfide (H_2S) and other volatile sulfuric compounds (Hummel, et al., 2016).

Another commercial process for producing man-made cellulosic fibres is the Lyocell process (Hauru, et al., 2014). Unlike in the viscose process, cellulose is not derivatized, but dissolved directly without chemical modification with a solvent called *N*-methylmorpholine *N*-oxide monohydrate (NMMO · 1 H_2O) (Hummel, et al., 2016). After dissolution, cellulose is spun and regenerated with water (Hummel, et al., 2016). The solvent can then be recovered almost completely (>99 %) by evaporation and used again (Parviainen, et al., 2015). The major drawback of the process is the thermal instability of NMMO, which is why stabilizer chemicals are needed in the process (Parviainen, et al., 2015; Wang, et al., 2012a). There is also a risk of thermal runaway reaction (Rosenau, et al., 2002), which makes the process

inherently unsafe. Several other non-derivatizing solvents have been developed, such as cupriethylene diamine (Cuen), cuprammonium hydroxide (Cuoxam) and phosphoric acid, but none of them are used commercially (Hummel, et al., 2016).

Due to the toxic chemicals used in the viscose process and the instability of the NMMO-solvent, a new sustainable process for cellulosic fibre production is needed. In 2002 Swatloski et al. discovered that cellulose could be dissolved with ionic liquids. Ionic liquids (ILs) are defined as salts that have a low melting point (<100 °C) (Hummel, et al., 2016) and thus can be used in liquid form in most processes. They exhibit excellent solvent capabilities and are often referred as "designer solvents" due to the huge number of possible cation-anion pairs (Pucheault & Vaultler, 2009). Some of them have unique properties, such as low to non-existent vapour pressure, non-flammability, high thermal stability and low toxicity (Tan & MacFarlane, 2009). Due to their low vapour pressure, ionic liquids are often referred also as green solvents since they do not emit volatile organic compounds (VOCs) (Tan & MacFarlane, 2009).

Since the discovery of their cellulose dissolution capability in 2002, ionic liquids for cellulose dissolution have been under intensive research. Recently researches from University of Helsinki and Aalto University developed a process for the production of man-made cellulose fibres based on a novel ionic liquid (Michud, et al., 2014). The process is called Ioncell-F and it uses an ionic liquid called 1,5-diazabicyclo[4.3.0]non-5-enium acetate ([DBNH][OAc]) as a solvent (Sixta, et al., 2015). The process is very similar to the Lyocell process and the strength of the produced fibres is similar or better than that of Lyocell fibres (Hauru, et al., 2014). [DBNH][OAc] has several advantages over NMMO, such as the possibility to use lower temperatures in dissolution, spinning and regeneration, which leads to energy savings and reduced cellulose and solvent degradation (Sixta, et al., 2015). The ionic liquid solvent is also more stable, which makes the process safer (Ahmad, et al., 2016; Sixta, et al., 2015). These advantages make the Ioncell-F process very appealing both from economic and environmental point of view.

Despite having many advantages over the Lyocell process, Ioncell-F has not yet been commercialized. A major challenge is the recycling of the ionic liquid solvent, which is a vital part of the process because the price of ionic liquids can be very high (Sixta, et al.,

2015; Ahmad, et al., 2016; Parviainen, et al., 2015). In Ioncell-F, the water content of the solvent needs to be considerably lower (<4 wt%) (Parviainen, et al., 2015) than in the Lyocell process (~13 %) (Sixta, et al., 2015), which means that water removal capacity needs to be higher. Low water content is required as water hydrolyses [DBNH][OAc] and thus weakens its cellulose dissolving power (Ahmad, et al., 2016). Also impurities originating from the raw material and solvent degradation need to be removed from the solvent to obtain high final product quality (Ahmad, et al., 2016).

No studies dealing with the removal of impurities from [DBNH][OAc] solutions have been carried out. Water removal on the other hand has been studied (Ahmad, et al., 2016). It has been reported that water can be evaporated away from [DBNH][OAc], but the hydrolysis reactions, which are accelerated by heat make the evaporation challenging (Ahmad, et al., 2016). Some of the solvent is lost with the distillate and reaching low-enough water content by evaporation has proven difficult (Ahmad, et al., 2016). The evaporation needs to be carried out in low pressure (<3 kPa) (Ahmad, et al., 2016), which increases energy and equipment costs.

The aim of this thesis is to develop alternative methods to evaporation for removing water from [DBNH][OAc] and to explore methods to remove impurities from the IL. The thesis consists of a literature review and an experimental part.

The literature review will introduce ionic liquids and their properties and give an overview of the Ioncell-F process. Different methods for ionic liquid recycling will be reviewed focusing on chemical separation methods, such as chromatography and adsorption. The applicability of each method for the Ioncell-F process will be shortly evaluated.

Water removal from [DBNH][OAc] will be studied in the experimental part of this work. The main focus will be on adsorption-based processes and adsorbent screening by equilibrium and kinetic experiments. The most suitable adsorbents will be tested in dynamic adsorption experiments. The effect of temperature, feed solution water content and adsorbent particle size on water removal will be studied in the dynamic experiments. The stability of the best adsorbents in [DBNH][OAc] will be studied by scanning electron microscopy (SEM).

Stripping by air will also be briefly studied as an alternative for the adsorption-based process. The performance of stripping and adsorption will be shortly compared, and the advantages and disadvantages of both processes evaluated.

2 IONIC LIQUIDS

As already mentioned, ionic liquids are generally described as salts that have a melting point lower than 100 °C (Lei, et al., 2017). Many ILs are liquids even at room temperatures (Mallakpour & Dinari, 2012). The difference between an electrolyte solution and an ionic liquid is that an ionic liquid is composed completely of ions and does not contain a separate solvent.

Ionic liquids were first discovered in 1914 by Paul Walden, who described them as molten salts (Kirchner, 2009). After that, ionic liquids received little research interest until the 1980s (Lei, et al., 2017; Kirchner, 2009). Since then, the amount of research on ionic liquids has increased significantly, particularly in the last 20 years (Lei, et al., 2017).

In 1982, Wilkes et al. introduced what is now called the first generation of ionic liquids (Kirchner, 2009). These ILs were based on 1-alkyl-3-methylimidazolium cations and tetrachloroaluminate anion ($AlCl_4^-$) (Wilkes, et al., 1982). In 1990s, water-stable ILs were developed by changing the tetrachloroaluminate anion to more stable anions (Vekariya, 2017). The third generation of ILs was introduced in 2004 and named task-specific ILs (TSILs) (Davis, 2004). The basic idea of TSILs is that the cation, anion or both contain a functional group, which affects the properties of the IL (Vekariya, 2017). By changing the functional group or the whole cation or anion, one can tune the physical and chemical properties of the IL (Vekariya, 2017). The almost endless tunability is perhaps the main reason for the current research interest in ILs.

2.1 General properties

Originally it was thought that all ionic liquids would have similar properties, but research in recent years has proved otherwise (Clare, et al., 2009). Many studies in the past suggested that ILs are “green solvents”, because of their negligible vapour pressure, non-flammability, and non-toxicity (Ranke, et al., 2007). However, their greenness has been questioned since some ILs are distillable (Kirchner, 2009), somewhat flammable (Fox, et al., 2008) and quite toxic (Ranke, et al., 2007). One might also think that ILs would be highly polar and hydrophilic since they consist of ions, but it has been proven that many ILs are only

moderately polar (Wakai, et al., 2005). There are also many hydrophobic ILs (Tan & MacFarlane, 2009). Generally however, ILs are considered to be greener and have better properties than conventional solvents or catalysts (Lei, et al., 2017). The greenness of the IL can be affected by a careful choice of the cation-anion pair.

2.1.1 Structure

Ionic liquids typically consist of a relatively large organic cation and an organic or inorganic anion (Vekariya, 2017). Typically, the cations are based on positively charged nitrogen or phosphorus with hydrocarbon chains or cyclic structures attached to them (Clare, et al., 2009; Tan & MacFarlane, 2009). Common cations are based on ammonium, imidazolium, pyridinium or phosphonium structures (Clare, et al., 2009). The anions are often rather small and weakly basic with a scattered or obscured negative charge (Clare, et al., 2009; Mallakpour & Dinari, 2012). Some of the most commonly used anions are chloride (Cl^-), acetate (CH_3COO^- or $[OAc]^-$) and tetrafluoroborate (BF_4^-) (Clare, et al., 2009).

Both cations and anions should be asymmetrical so that they cannot pack into a solid structure (Krossing, et al., 2006). The number of possible cation-anion pairs that will form an ionic liquid has been estimated to be as high as 10^{18} (Katritzky, et al., 2002). Each of them has slightly different properties, which means that they have a massive number of potential applications. Modifying the cation affects the melting point, viscosity and solubility with other solvents (Clare, et al., 2009; Mallakpour & Dinari, 2012). Changing the anion affects all of the aforementioned properties, but the anion also affects water and air stability of the IL (Mallakpour & Dinari, 2012).

2.1.2 Volatility

As mentioned earlier, ILs are said to have negligible vapour pressures (Mallakpour & Dinari, 2012; Tan & MacFarlane, 2009). This is true in ambient temperatures and pressures (Mallakpour & Dinari, 2012), but some ILs can be distilled under reduced pressure (<15 kPa) (Ahmad, et al., 2016). It has also been shown that some ILs will burn at elevated temperatures and have similar flammability characteristics with aliphatic hydrocarbon plastics (Fox, et al., 2008). However, under ambient pressure and moderate temperatures

(<200 °C) ILs can be considered as non-volatile and non-flammable (Mallakpour & Dinari, 2012).

2.1.3 Viscosity

Most ILs have considerably higher viscosities at room temperature (roughly 10–500 $mPas^{-1}$) (Mallakpour & Dinari, 2012) than conventional solvents (0.3–5 $mPas^{-1}$) (Sigma-Aldrich, 2017). High viscosities are caused by electrostatic interactions between the ions, such as hydrogen bonding and van der Waals forces (Mallakpour & Dinari, 2012). High viscosity slows down the diffusion of substances in ILs and increases the energy consumption of pumping and mixing (Mallakpour & Dinari, 2012), which is why ILs with low viscosities are usually preferred.

2.1.4 Stability

The first generation of ILs were sensitive to moisture and air (Wilkes, et al., 1982). Since then, more stable ILs have been developed (Kirchner, 2009). Still, many ILs will decompose in the presence of water (Mallakpour & Dinari, 2012; Ahmad, et al., 2016). Halogen containing ILs might even release acidic compounds like HF and HCl (Mallakpour & Dinari, 2012). Water can dramatically change the properties of ILs, such as solvation power and reactivity (Mallakpour & Dinari, 2012; Parviainen, et al., 2015). The anion seems to be largely responsible for the interactions between water and IL and the hydrophilicity of the IL (Mallakpour & Dinari, 2012). To avoid problems with water, ILs are often dried before use (Mallakpour & Dinari, 2012).

ILs are usually regarded as being thermally very stable (Mallakpour & Dinari, 2012; Pucheault & Vaultler, 2009). Some ILs can indeed tolerate temperatures of over 400 °C, but some will start to decompose already at 200 °C (Mallakpour & Dinari, 2012). Even much lower temperatures (<100 °C) can promote the degradation of ILs, especially in the presence of water (Parviainen, et al., 2015). Therefore all ILs cannot be regarded as stable even at mild conditions.

2.1.5 Internal interactions

In early studies, ILs were treated like conventional organic solvents with the capability to transport ions (Taubert, 2009). Nowadays however ILs have been identified as very complex compounds with a large number of interactions, such as liquid crystal formation, complex hydrogen bond networks and microscopic polar and non-polar areas (Taubert, 2009). The complexity of ILs makes it difficult to fully understand their properties and interactions with other substances (Taubert, 2009). On the other hand, the complexity also gives them unique properties that cannot be found in other substances, such as excellent solvent power and the ability to act simultaneously as a solvent and a catalyst (Vekariya, 2017; Maase, et al., 2005).

2.2 Applications

Due to the wide spectrum of properties, ILs have a large number of potential applications. These include their use as solvents, catalysts, electrolytes, separation materials, and extraction agents (Vekariya, 2017). The first industrial application of ionic liquids was the BASIL™-process by BASF (Maase, et al., 2005). It uses 1-methylimidazole to scavenge hydrochloric acid (HCl) from the reaction mixture in the production diethoxyphenylphosphine (Maase, et al., 2005). 1-methylimidazole reacts with the acid to form an ionic liquid that can be separated from the reaction product (Maase, et al., 2005). The formed ionic liquid also acts as a nucleophilic catalyst accelerating the reaction and reducing the size of reaction equipment (Maase, et al., 2005).

Currently one of the most intensively studied application of ionic liquids is the dissolution and conversion of cellulose and other biopolymers (Wang, et al., 2012a; Tan & MacFarlane, 2009). Cellulose dissolving ionic liquids were first discovered in 2002 (Swatloski, et al., 2002) and since then a large number of studies about ionic liquids as cellulose dissolving agents have been published (Wang, et al., 2012a). Ionic liquids can dissolve cellulose with very little degradation, which enables the production of regenerated cellulosic fibres (Hummel, et al., 2016). These fibres can then be used to produce textile fibres (Hummel, et al., 2016).

Anions of ILs seem to be largely responsible for their ability to dissolve cellulose. The generally accepted theory is that the anions of ILs can compete with the hydrogen bonds of cellulose and break the hydrogen bond network between cellulose molecules. This is supported by the fact that anions with higher hydrogen bond basicity and dipolarity dissolve more cellulose. The cation also has an influence on the solubility of cellulose, but the interactions between cellulose and cations of ILs are not fully understood. (Wang, et al., 2012a)

3 IONCELL-F PROCESS

Since the discovery of cellulose dissolving ILs, most of the research in the area focused on imidazolium-based ionic liquids (Sixta, et al., 2015; Wang, et al., 2012a). Although fibres with equal properties to Lyocell fibres could be produced with these liquids (Bentivoglio, et al., 2006), it was soon discovered that they react with cellulose (Ebner, et al., 2008). At temperatures over 90 °C, cellulose could degrade quite severely (Sixta, et al., 2015). Corrosion of process equipment was also seen as an issue (Ebner, et al., 2008), mainly because the used anions were often halides (Sixta, et al., 2015). Imidazolium-based ILs with non-halide anions were later developed and one of the best ones was 1-ethyl-3-methylimidazolium acetate ([Emim][OAc]) due to its low viscosity and good cellulose dissolving power (Sixta, et al., 2015). Its problem was however the difficulty to achieve suitable viscoelastic properties for spinning (Sixta, et al., 2015).

In 2014, a novel non-imidazolium-based IL solvent for cellulose dissolution was introduced by researchers from Helsinki University and Aalto University (Michud, et al., 2014). The solvent was a superbase-based IL called 1,5-diazabicyclo[4.3.0]non-5-enium acetate ([DBNH][OAc]). It was used to produce regenerated cellulose fibres in a dry-jet wet spinning process, which was named as Ioncell-F process and the fibres produced by the process were called Ioncell-F fibres (Sixta, et al., 2015). The process was able to produce strong fibres (Sixta, et al., 2015) with reportedly non-existent cellulose degradation (Parviainen, et al., 2015).

3.1 Dissolution of cellulose and preparation of the spinning dope

The Ioncell-F process begins with the milling of the raw material, which is often air-dry dissolving pulp (Sixta, et al., 2015; Parviainen, et al., 2015; Hummel, et al., 2016; Bulota, et al., 2016). The solvent is heated to 70 °C to keep it in liquid form and cellulose is gradually added until a 13 wt-% cellulose solution is obtained (Sixta, et al., 2015; Hummel, et al., 2016). The solution is then moved into a kneader system for 90–180 min, which operates at elevated temperature (80 °C) and low pressure (50–200 mbar) (Hauru, et al., 2014; Sixta, et al., 2015; Bulota, et al., 2016). Low pressure is used to remove air bubbles from the solution (Hauru, et al., 2014). After all of the cellulose has dissolved, the solution is filtered by a

press filter at high pressure (1–2 MPa) and temperature (80–100 °C) to remove undissolved impurities (Sixta, et al., 2015; Hummel, et al., 2016; Hauru, et al., 2014; Bulota, et al., 2016). After filtration, the solution is ready for spinning.

3.2 Spinning and regeneration

The solution from filtration is transferred to a spinning unit (figure 1), which consists of a cylinder, a multihole spinneret, a coagulation bath and a godet couple, which collects the fibres (Hummel, et al., 2016). The solution is first transferred into the cylinder of the spinning unit and heated to 70 °C (Hauru, et al., 2014). Next, the solution is extruded through the multihole spinneret at 75–80 °C to form filaments (Hauru, et al., 2014; Hummel, et al., 2016). The filaments go through a 1 cm air-gap before entering the coagulation bath (Hauru, et al., 2014; Hummel, et al., 2016). The coagulation bath is cold water (15 °C) (Sixta, et al., 2015), which causes cellulose to precipitate from the IL (Tan & MacFarlane, 2009). The godet couple collects the fibres from the coagulation bath and the fibres can then be further processed into yarn (Hummel, et al., 2016).

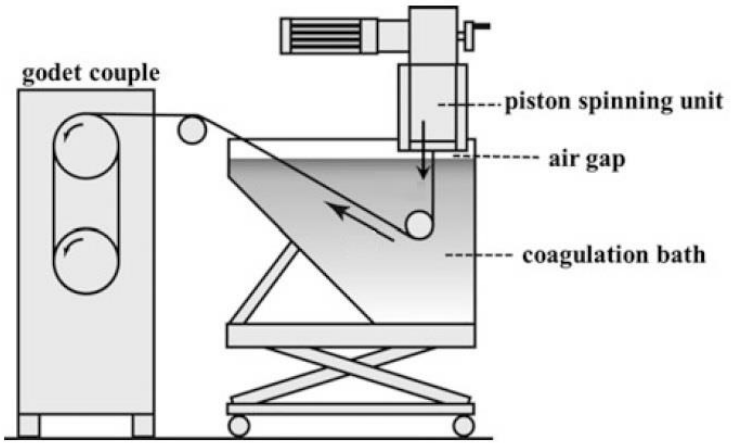

Figure 1 A laboratory-scale spinning unit used in the Ioncell-F process. Adapted from (Hummel, et al., 2016).

3.3 Solvent recovery

After fibre regeneration, the IL solvent remains in the coagulation solution. Due to the high price of the solvent (30–120 €/kg) (Parviainen, et al., 2013), it should be recycled almost completely (>99 %) to make the process competitive (Parviainen, et al., 2015). The water content of the IL is approximately 80 wt-% after it has gone through the Ioncell-F process (Ahmad, et al., 2016).

Water in [DBNH][OAc] causes it to undergo reversible hydrolysis into 1-(3-aminopropyl)-2-pyrrolidone (APP), which then forms 3-(aminopropyl)-2-pyrrolidine acetate ([APPH][OAc]) (Ahmad, et al., 2016). [APPH][OAc] can then irreversibly decompose into 1-(3-acetamidopropyl)-2-pyrrolidone (APPAc) (figure 2) (Ahmad, et al., 2016). To avoid excessive hydrolysis and loss of cellulose dissolution power as a result, the water content of the solvent should be less than 4 wt-% (Parviainen, et al., 2015). This means that substantial amounts of water need to be removed from the solvent before it can be reused.

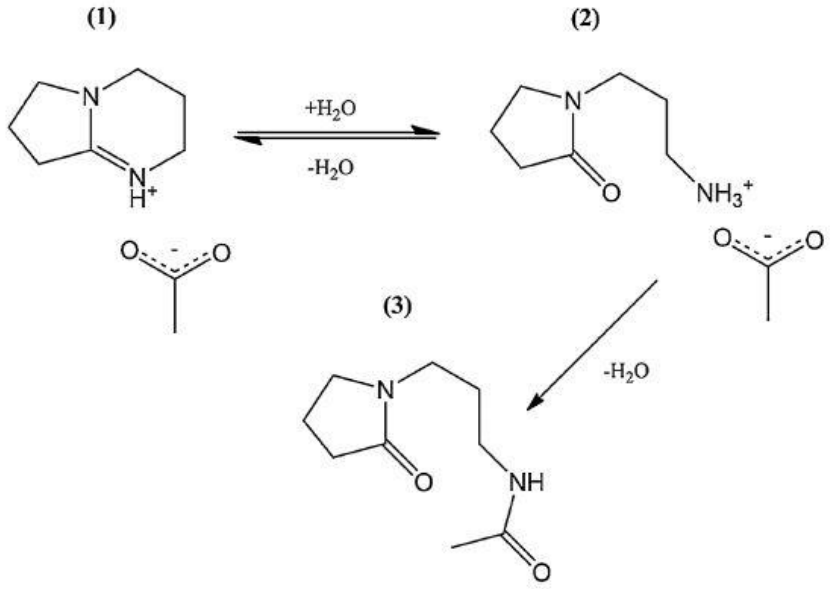

Figure 2 Hydrolysis of [DBNH][OAc] (1) into [APPH][OAc] (2) and further decomposition into APPAc (3) (Ahmad, et al., 2016).

In addition to hydrolysis, [DBNH][OAc] can form neutral DBN and acetic acid (Ostonen, et al., 2016a). This makes recycling the solvent difficult, because the neutral species will interact differently compared to the ionic species (Ostonen, et al., 2016a). The conversion to

neutral components was originally thought to be a useful phenomenon as the IL could be distilled as neutral components (Parviainen, et al., 2013). However, when distillation behaviour of pure [DBNH][OAc] was studied, it was discovered that about 40 % of the IL evaporated as almost pure (≥98.9 wt-%) DBN, while the rest of the solvent formed two different complexes with 3:2 and 5:3 HOAc:DBN molar ratios (Ahmad, et al., 2016). This makes the purification of [DBNH][OAc] by distillation difficult (Ostonen, et al., 2016b).

To study the feasibility of evaporation as a technique to remove water from [DBNH][OAc], experiments with an agitated thin-film evaporator were conducted by Ahmad et al. (2016). They used a solution containing 80 wt-% water and 20 wt-% [DBNH][OAc] as a feed solution. Water was collected as the distillate and [DBNH][OAc] as the distillation residue. Several experiments were conducted with different heating jacket temperatures (77–94 °C) and pressures (1.6–3.1 kPa). (Ahmad, et al., 2016)

Evaporation was able to lower the water content of [DBNH][OAc] to 5.0–11.7 wt-%. The amount of hydrolysis product ($APP/APPH^+$) in the feed was 0.59 wt-% with no APPAc. After evaporation, the amount of hydrolysis product in the [DBNH][OAc] fraction (residue) was 3.4–6.0 wt-% with no traces of APPAc. Increasing residence time in the heated (50 °C) feed vessel seemed to increase the amount of hydrolysis product. It was noted that the presence of the hydrolysis product may not be an issue, since the hydrolysis reaction (figure 2) is reversible and no traces of the irreversible hydrolysis product APPAc were found in the distillation residue. Small amounts of [DBNH][OAc] (0.06–0.11 wt-%) and hydrolysis product (0.27–1.11 wt-%) were found in the distillate. The experiment with the lowest water content (5.0 wt-%) in the residue also had the highest amounts of hydrolysis product in both the distillate (1.11 wt-%) and the residue (6.0 wt-%). Also, the highest amount of [DBNH][OAc] in the distillate (0.11 wt-%) was observed in that experiment. (Ahmad, et al., 2016)

The results of the evaporation experiments indicate that low-enough water contents may not be achievable by evaporation. It was noted though that further optimization of the process parameters might enable lower water contents to be achieved (Ahmad, et al., 2016). However, to achieve high enough recovery rates, [DBNH][OAc] and its hydrolysis product

should be recovered from the distillate. The hydrolysis product should not be regarded as waste, since it can be reacted back to [DBNH][OAc], if the water content is low-enough.

In addition to water removal, impurities from the raw material and solvent degradation products must be removed from the solvent (Ahmad, et al., 2016). The composition of all of these impurities is not yet known, but at least inorganic substances (salts) start to accumulate in the solvent when it is recycled (Parviainen, et al., 2015). Approximately 0.05–0.1 wt-% of inorganic substances is accumulated in every dissolution-solvent regeneration cycle (Parviainen, et al., 2015). It was also expected that some oligosaccharides might be present in the solvent due to cellulose degradation, but no such compounds were found (Parviainen, et al., 2015). However, during solvent recycling experiments it was found that the colour of the produced fibres would change from bright white to slightly yellow or brown when the raw material was treated with recycled [DBNH][OAc] (Parviainen, et al., 2015). This was thought to be due to degradation products either form the solvent or from the raw material (Parviainen, et al., 2015).

It is clear that other techniques besides evaporation are needed for the recycling of [DBNH][OAc] in the Ioncell-F process. The next section will review some of the techniques that have been reported in literature for ionic liquid recycling. The main focus will be on removal of water, inorganic and organic impurities.

4 RECYCLING OF IONIC LIQUIDS

Recycling and reusing ionic liquids is vital for any process utilizing them (Wu, et al., 2009; Tan & MacFarlane, 2009). In addition to being expensive, some ILs can be harmful to aquatic environments because of their toxicity and non-biodegradability (Wu, et al., 2009). Ionic liquids are often said to be easily recyclable (Wu, et al., 2009), but it has proven to be more difficult than originally thought (Kuzmina, 2016). Hydrophobic ILs are generally much easier to purify and recycle than hydrophilic ILs (Wu, et al., 2009). Since [DBNH][OAc] is a hydrophilic IL, this section will concentrate mostly on the recycling of hydrophilic ILs.

4.1 Removal of water

Water is a common impurity in ILs (Clare, et al., 2009) and as in the case of Ioncell-F, most of it needs to be removed before the IL can be used (Parviainen, et al., 2015). Several techniques to remove water from ILs have been suggested in the literature, but so far none of them has been proven superior over others.

4.1.1 Distillation and evaporation

Usually the first suggested method for water removal is evaporation or distillation (Kuzmina, 2016; Clare, et al., 2009). Since ILs have very low vapour pressure, water can be evaporated out of the IL at low pressure and elevated temperature (Kuzmina, 2016; Parviainen, et al., 2015). Rotary evaporators are normally used in lab-scale to evaporate water (Kuzmina, 2016; Parviainen, et al., 2015), but it may take from few hours to even weeks to purify a batch of IL (Clare, et al., 2009). Purification times can be shortened by using more advanced equipment, such as an agitated thin-film evaporator (Ahmad, et al., 2016). Regardless of the equipment, low pressure is needed to efficiently evaporate water, which consumes a lot of energy (Kuzmina, 2016). Another disadvantage of the method is that heating the IL causes it to decompose more rapidly (Clare, et al., 2009), which was observed also in the case of [DBNH][OAc] (Ahmad, et al., 2016). Water can also be so strongly bound to the IL that a low-enough water content cannot be reached by evaporation (Clare, et al., 2009).

It has been reported that some ILs can be converted to neutral species, which can be then distilled and converted back to the IL form (Kuzmina, 2016; Abu-Eishah, 2011). This method can be applied if the IL has a protonated and alkylated cation (Kuzmina, 2016). For example, an imidazolium-based IL can be deprotonated with a base to form a carbene (figure 3) (Kuzmina, 2016). The carbene, which is much more volatile than the IL, can then be distilled and regenerated back to imidazolium by reacting it with an acid (Kuzmina, 2016). The same idea was suggested for [DBNH][OAc] to convert it back to DBN and acetic acid, which would be easy to distil (Ostonen, et al., 2016b). However, as mentioned in chapter 0, it proved that [DBNH][OAc] would distil in two different fractions and form complexes, which makes distillation difficult (Ostonen, et al., 2016b).

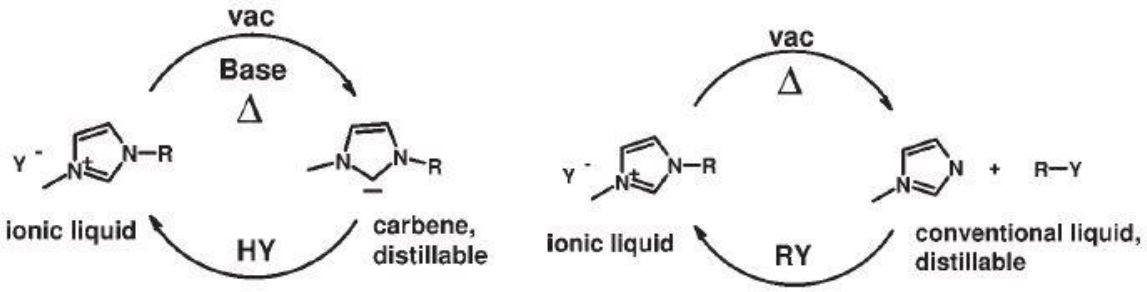

Figure 3 Possible ways to neutralize and regenerate ILs with protonated and alkylated cations (Abu-Eishah, 2011).

4.1.2 Pressurised carbon dioxide

Carbon dioxide forms a supercritical fluid at near-ambient temperature (>31.1 °C) and high pressure (>7.39 MPa) (Mai, et al., 2014). Supercritical carbon dioxide ($scCO_2$) is soluble in ILs, but ILs are not soluble in $scCO_2$ (Blanchard, et al., 2001a). Thus, ILs and $scCO_2$ form separate IL and $scCO_2$ phases (Blanchard, et al., 2001a). Due to this phase separation behaviour, carbon dioxide has been used to separate ILs from organic mixtures and aqueous solutions (Scurto, et al., 2003).

Even gaseous CO_2 has been reported to form a three-phase system with water and ILs (figure 4) at high pressure (3–5.5 MPa) and close to ambient temperature (15–25 °C). The bottom liquid (L_1 in figure 4) is rich in IL, the second liquid is rich in water and the vapour phase consists mainly of CO_2 with small amounts of water. (Scurto, et al., 2003)

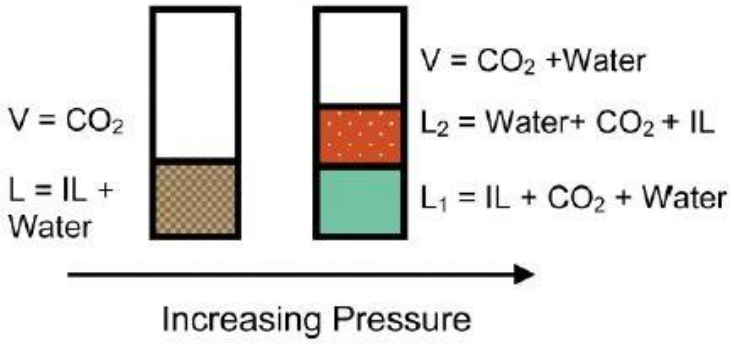

Figure 4 Separation of IL and water by CO_2. Adapted from (Scurto, et al., 2003).

Both hydrophobic and hydrophilic ILs were studied and it turned out that hydrophobic ILs were easier to separate with the method (Scurto, et al., 2003). A hydrophilic ionic liquid (1-butyl-3-methylimidazolium tetrafluoroborate, [Bmim][BF_4]) could be separated from water only when the concentration of the IL was 1.58–9.3 mol-% (Scurto, et al., 2003). Complete separation with this method was not found possible, since a part of the IL is remained in the lighter liquid phase (L_2) and some water and CO_2 were present in the bottom liquid phase (L_1) (Wu, et al., 2009). Maximum purity for the IL in the bottom phase was 75.63 wt-% (Wu, et al., 2009).

Mechanism of the separation is not entirely clear. Scurto et al. (2003) suggested that the second liquid phase might appear because of pH changes in the solution, which affects the solubility of water and IL. Also a decrease in dielectric constant was observed when adding CO_2 into the system (Scurto, et al., 2003). Later Wu et al. (2009) speculated that the phase separation might be due to the formation of carbonate (CO_3^{2-}) when CO_2 reacts with water (Wu, et al., 2009). The carbonate could then cause a salting-out effect (Wu, et al., 2008).

4.1.3 Salting-out

In 2003, Gutowski et al. discovered that a hydrophilic IL ([Bmim]Cl) could be separated from water with a concentrated solution of potassium phosphate (K_3PO_4). Contacting these two liquids causes two aqueous phases to appear with the upper phase being rich in IL and the lower phase rich in K_3PO_4. These type of systems are called aqueous biphasic systems

(ABS). K_3PO_4 is a water-structuring (kosmotropic) salt, because the phosphate ion attracts water molecules very strongly. (Gutowski, et al., 2003)

According to Gutowski et. al. (2003), when a kosmotropic salt is added to an aqueous solution of an IL, its anion (PO_4^{3-}) attracts the water molecules stronger than the IL. The anion increases the hydrogen bond network of water and thus makes water more organized. More energy is therefore required to hydrate the larger and less hydrophilic cation, and at a certain phosphate concentration, the cation will move to a separate phase taking the less structuring anion (Cl^-) with it to remain electroneutrality. Correspondingly, the potassium ion stays in the same phase with the phosphate ion to remain electroneutrality in that phase. (Gutowski, et al., 2003)

The separation can also be explained by an increase in the dielectric constant of the solution, which forces the low dielectric organic cation ($[Bmim]^+$) and the less water structuring anion (Cl^-) to move to another phase. The concentration of the IL in the upper phase increases with increasing K_3PO_4 concentration. (Gutowski, et al., 2003)

Shahriari et al. (2012) further studied the salting-out phenomenon of ILs and concluded that it was entropically driven. They found out that an increase in the entropy of hydration caused the formation of separate phases. The kosmotropic salts are able to form hydration complexes with water, which causes the ILs to dehydrate. It was also found out that the kosmotropic nature of anions follows the Hofmeister series, which describes the ability of ions to salt-out proteins. (Shahriari, et al., 2012)

High IL recovery rates have been achieved with salting-out technique (Deng, et al., 2009; Li, et al., 2010b). Deng et al. (2009) recovered 96.80 % of [Amim]Cl with a 46.48 wt-% K_2HPO_4 solution. Li et al. (2010b) managed to recover 98.77 % of $[Bmim][BF_4]$ with a 16.94 wt-% Na_2CO_3 solution. Unfortunately, no data about water removal rates were given in either of the studies.

The main disadvantage of the method is the need for additional chemicals (salts), which increases the costs of the separation and creates a waste stream (Kuzmina, 2016). Recycling the kosmotropic salt is expected to be difficult (Wu, et al., 2009). Using sucrose instead of

salts was studied by Wu et al. (2008). The separation behaviour was similar to that of K_3PO_4 and it was thought that sucrose would be a more environmentally friendly separation agent (Wu, et al., 2009). However, the recovery rate of the IL was only 74 % at its best (Wu, et al., 2008). Several other chemicals that will promote the salting-out effect have been studied, but in most cases recycling the salting-out agent efficiently has turned out to be difficult (Kuzmina, 2016).

4.1.4 Membrane separation

Membrane separation is another technique that has been studied for the separation of ILs and water (Wu, et al., 2009). Membrane separation is based on a barrier that separates two phases from each other and selectively allows only certain types of molecules or ions to pass through it (Strathmann, 2011). It has been said that membrane separation is a very efficient technique in the removal of ionic species and that only distillation can reach similar levels of purity (Wu, et al., 2009). Membrane separations are also said to have lower energy consumption compared to evaporation or distillation (Haerens, et al., 2010).

Haerens et al. (2010) studied the separation of water and a deep eutectic solvent called Ethaline200 (which they called an ionic liquid) by three different membrane separation techniques: nanofiltration, reverse osmosis and pervaporation. Nanofiltration and reverse osmosis are pressure-driven techniques, where high pressure is applied to a solution to push it through a membrane (Strathmann, 2011). Molecules or ions larger than the pore size of the membrane are retained in the feed solution whereas smaller molecules and ions pass through the membrane (Strathmann, 2011). Pervaporation is a technique that combines evaporation and membrane separation (Strathmann, 2011). A membrane is placed between a liquid phase and a gas phase, which then controls the diffusion of volatile components into the gas phase (Strathmann, 2011).

Haerens et al. (2010) found out that nanofiltration and reverse osmosis could only reach a maximum IL concentration of 30 vol-% in water. The limiting factor was the osmotic pressure of the solution. Pervaporation on the other hand was found to suffer from low water fluxes through the membrane leading to long processing times or large membrane areas. The flux of water through the membrane was observed to decrease significantly as the water

content decreased. For example, at 70 wt-% water content the water flux was about 600 g/m^{2}h, but at 30 wt-% water content the flux was only 100 g/m^{2}h. It was noted that the only benefit of pervaporation over conventional evaporation is the possibility to operate at lower temperatures and at pressures closer to ambient pressure. (Haerens, et al., 2010)

Schäfer et al. (2001) reported that 99.2 % of water could be removed from 1-butyl-3-methylimidazolium hexafluorophosphate ([Bmim][PF_6]) by pervaporation. However, about 50 h at 50°C was needed to reach such removal rates (Schäfer, et al., 2001). Sun et al. (2017) on the other hand were able to lower the water content of [Emim][OAc] from 80 wt-% to 1 wt-% in just four hours at 100 °C. Lowering the temperature had a major effect on the water removal: at 80 °C, only a 20 wt-% water content could be reached in 6 h, and at 50 °C, no water removal was observed (Sun, et al., 2017). Very small IL losses (<0.1 wt-%) were reported, which was seen as a major benefit over evaporation (Sun, et al., 2017). The membranes were reported to be quite durable since the same membrane could be used for 60 IL recovery cycles (Sun, et al., 2017).

The high viscosity of most ILs is found to be an issue in membrane separation processes as it makes it difficult to achieve high fluxes. The viscosity of an IL can be lowered by adding small amounts of methanol or ethanol, which can lead to 10–20 times higher fluxes through a membrane. After the membrane separation, the added methanol or ethanol can then easily be evaporated from the IL. However, using organic solvents makes the process less environmentally friendly. (Kuzmina, 2016)

4.1.5 Electrodialysis and electrolysis

Another membrane-based separation technique is electrodialysis (ED). It uses electricity to transport ions selectively through ion-exchange membranes (Wang, et al., 2012b). Cation-exchange membranes (CEM) and anion-exchange membranes (AEM) are placed between two electrodes in alternating series (Strathmann, 2011) (figure 5). Each space between

cation- and anion-exchange membranes can be considered as an individual cell (Strathmann, 2011).

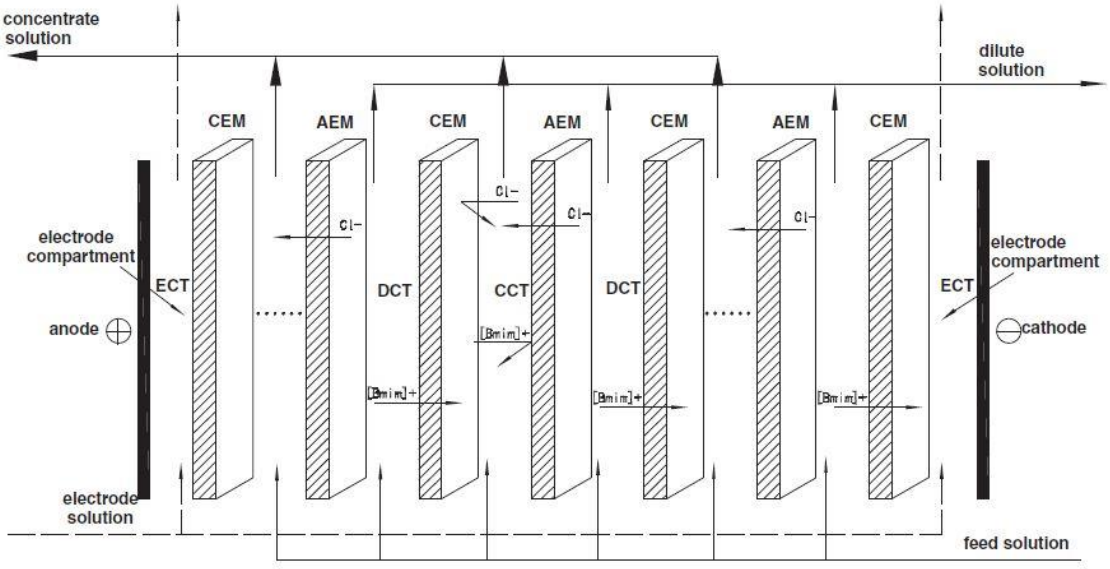

Figure 5 Principle of IL concentration by electrodialysis (Wang, et al., 2012b).

The feed solution is fed into the cells and electric current is applied. The cations of the solution start to move towards the cathode and the anions towards the anode. Cations can move through the cation-exchange membranes, but not through anion-exchange membranes. Correspondingly, anions can move through the anion exchange membranes, but not through the cation exchange membranes. This behaviour causes ions to accumulate into every other cell, which are called concentrate compartments (CCT), where they can be collected as a concentrated stream (figure 5). The other cells are called diluate compartments (DCT) from which the dilute solution can be collected. (Strathmann, 2011)

Wang et al. (2012b) studied the use of electrodialysis to separate an ionic liquid ([Bmim]Cl) from water. The feed solution could be concentrated by 1.3–1.8 times depending on the applied voltage, initial concentration and initial volume of the solution (Wang, et al., 2012b). When the feed solution contained 0.3 mol/L of [Bmim]Cl, its concentration could be increased to about 0.5 mol/L and about 60 % of water could be removed (Wang, et al., 2012b). However, the concentrated solution was still quite dilute and <70 % of the IL could be recovered. Even the highest reported IL recovery rate was only 85.2 % (Wang, et al., 2012b).

Trinh et al. (2013) studied the recovery of the same IL as Wang et. al. (2012b) by electrodialysis from a lignocellulosic hydrolysate. They used electrodialysis only to recover the IL instead of removing water from it. IL concentration actually decreased in their electrodialysis process, because distilled water was used to initially fill the diluate compartments. They could still only recover 64.0 % of the IL and noted that membrane fouling is an issue in the electrodialysis processes (Trinh, et al., 2013).

A different way of utilising electricity to remove water from ILs was studied by Islam et al. (2008). They reported that water could be removed by electrolysing it into hydrogen (H_2) and oxygen (O_2). An ammonium-based IL (*N*,*N*,*N*-trimethyl-*N*-propylammonium bis-(trifluoromethanesulfonyl)imide) containing 2.2 wt-% water was placed in an electrolytic cell with a platinum (Pt) cathode and a glassy carbon anode. Oxygen was developed at the cathode while hydrogen was developed at the anode. The removal of these gases was helped by stirring the solution and blowing nitrogen (N_2) gas into it. The electrolysis treatment was able to lower the water content of the IL to 0.06 wt-%. (Islam, et al., 2008)

4.1.6 Sweeping with nitrogen

Another technique for removing water from ionic liquids was suggested by Ren et al. (2010). They used nitrogen to blow out (sweep) water and organic solvents from ionic liquids. The technique was compared to what they called a traditional technique of drying the IL in a vacuum oven. It was found out that the sweeping technique could achieve lower water contents much faster at similar temperatures. For example, a 1,1,3,3-tetramethylguanide lactate ([TMG]L) sample containing 5.3 wt-% water was dried to a water content of 1.9 wt-% in 48 h by the traditional vacuum oven method (p = 665 Pa, T = 70 °C). The sweeping method could decrease the water content of the same IL from 5.3 wt-% to 0.25 wt-% in 5 h 20 min at the same temperature (70 °C) and at ambient pressure. Water removal was enhanced by higher temperatures and higher nitrogen flow rates. (Ren, et al., 2010)

The faster removal of water compared to the vacuum drying method was explained by the reduced vapour pressure of water. In vacuum drying, a saturated vapour layer first develops over the surface of the IL. Due to lowered pressure, the saturated vapour starts to diffuse

away from the surface and into the bulk gas phase. New water molecules then evaporate from the liquid phase to replace the diffused molecules in the saturated vapour layer. The process is controlled by diffusion, which makes it quite slow. When nitrogen is blown into the liquid, the vapour-liquid equilibrium at the surface of the liquid is broken. The nitrogen gas dilutes the surface layer and lowers the vapour pressure of water thus causing more and more water molecules to evaporate out of the solution. The phenomenon is illustrated in figure 6. (Ren, et al., 2010)

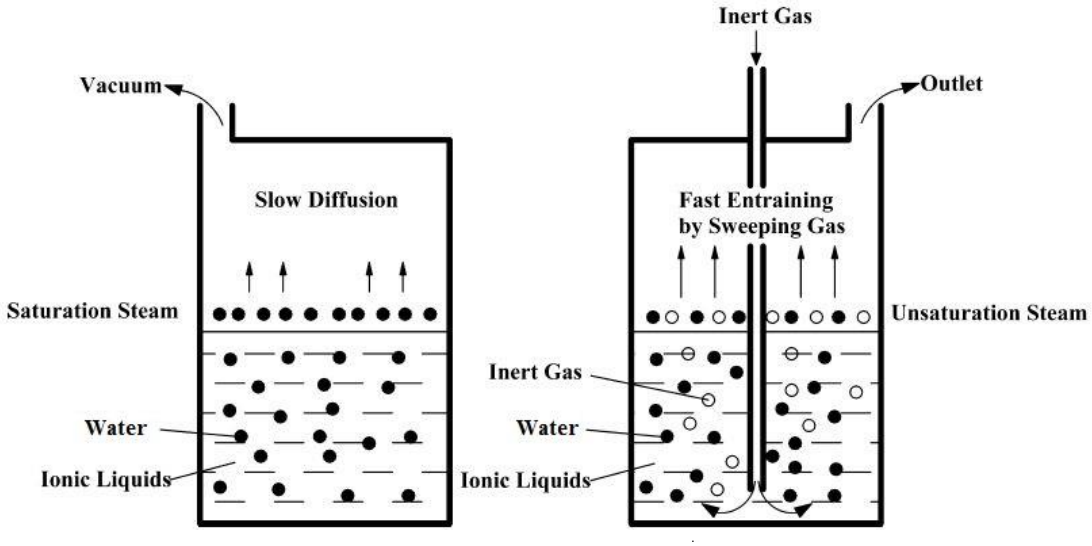

Figure 6 The principles of vacuum drying and solvent sweeping methods. Adapted from (Ren, et al., 2010).

4.1.7 Adsorbents and molecular sieves

Molecular sieves have been suggested as one possibility to remove water from ionic liquids (Clare, et al., 2009). Molecular sieves are typically different types of zeolites (aluminosilicates) or other silicates with a porous three-dimensional structure (Davis, 1991). Their pores are very uniform in size, and more importantly, the size of the pores is close to the size of small molecules (Davis, 1991). Molecular sieves can therefore separate molecules based on their size (Davis, 1991). Molecules smaller than the pores of the sieve can enter the structure of the sieve while molecules bigger than the pores cannot (Davis, 1991). Molecular sieves are often hydrophilic and are used for example to remove moisture from natural gas (Davis, 1991).

Since at least the cations in ILs are larger than water molecules, it should be possible to remove water from ILs with molecular sieves. However, it was shown by Clare et al. (2008) that alumina and silica adsorbents can contaminate ILs with microscopic (100–1000 nm) particles. These particles are said to be difficult to remove due to their small size (Clare, et al., 2008). In most cases however the amount of solid particles in the IL was low (<10 ppm) (Clare, et al., 2008), but it has been shown that even small amounts of inorganic impurities can affect the electrochemical responses of ILs (Enders, et al., 2006).

There are at least two patents (Wymore, 1966; Kiser, 1987) and a few studies (Sinegra & Carta, 1987; Joshi & Fair, 1991; Tiihonen, et al., 1999) about the use of organic ion exchange resins to remove water from organic liquids. Organic ion exchange resins consist of crosslinked hydrocarbon chains with fixed ionic groups (Helfferich, 1995). The fixed ionic groups are always accompanied by mobile ions (counter ions) of the opposite charge, which can be exchanged for a stoichiometric amount of other ions (Helfferich, 1995). Resins with cations as exchangeable ions are called cation exchange resins and resins with anions as exchangeable ions are called anion exchange resins.

Ion exchange resins are said to be in a certain ionic form based on which exchangeable ions they contain. For example, a resin containing exchangeable sodium ions is said to be in sodium form. Unlike molecular sieves, the structure of ion exchange resins is irregular and elastic. They cannot be dissolved by solvents because of their crosslinked network, but they can take up solvent, which causes them to swell. (Helfferich, 1995)

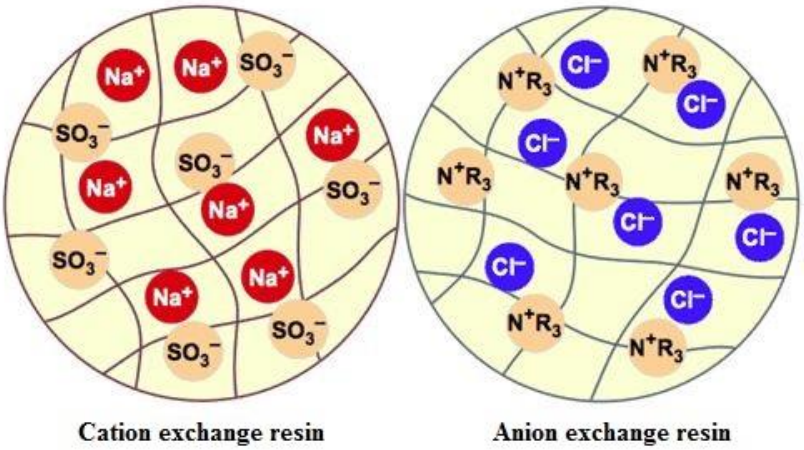

Figure 7 Illustration of the structure of organic cation and anion exchange resins. Adapted from (de Dardel, 2016).

The solvent (water) uptake of ion exchange resins is due to two main reasons. Firstly, both the fixed and the mobile ions have a tendency to surround themselves with solvent and form solvation shells. Secondly, the inside of ion exchange resin can be thought as a concentrated electrolyte solution, which tends to dilute itself by taking up solvent from a more dilute external solution. Another way expressing the same phenomenon is that there is a difference in osmotic pressure between the inside of ion exchange resin and the external solution. The solvent uptake is limited by the elastic forces of the hydrocarbon network. As more and more solvent is taken up by the resin, the elastic forces of the hydrocarbon network become stronger and start to push the solvent out. Equilibrium is reached when the solvent uptake tendency is counterbalanced by the elastic forces (Helfferich, 1995).

Water inside ion exchange resins is often divided into two different states: water of hydration and free water. Water of hydration means the water that is bound to ions as solvation shells. Free water on the other hand is not bound to ions. Water exists preferentially as water of hydration and only after nearly all of the ions have been hydrated as free water. (Helfferich, 1995)

The ionic form of the ion exchange resin has a major effect on the water adsorption capacity of gel type resins (Nandan, et al., 1993; Toteja, et al., 1997). For example, a microporous strong acid cation exchange resin (Dowex 50WX4) in H^+ form has a water adsorption capacity of 20.98 mol/equiv (at water activity 1.0), but in Ba^{2+} form the capacity is only 9.28 mol/equiv (Toteja, et al., 1997). The lower capacity in the divalent Ba^{2+} form is because

there are twice as much cations in the H^+ form of the resin than there are cations in the Ba^{2+} form (Helfferich, 1995). Since there are less ions to interact with water, less water is taken up by the resin.

Besides valence, the size and solvation tendency of the counter ion affect the water adsorption capacity (Helfferich, 1995). Li^+ forms of moderately (<12 %) crosslinked resins have a higher water adsorption capacity than K^+ forms (Nandan, et al., 1993), because the hydration number of Li^+ is larger (3.3 vs. 0.6) meaning that there are more water molecules surrounding the cation and there is less free water (Helfferich, 1995). The hydrated water is more tightly packed than free water and thus requires a smaller volume (Helfferich, 1995). The Li^+ form therefore contains more water in the same volume of resin compared to the K^+ form. Also the degree of crosslinking of the resin affects the water adsorption capacity (Nandan, et al., 1993; Toteja, et al., 1997), since resins with lower degree of crosslinking can swell more and thus take up more solvent (Helfferich, 1995).

The water adsorption of capacity of macroporous resins on the other hand does not seem to depend quite so much on the ionic form. For example, a macroporous resin (Amberlyst-15) in H^+-form has a water adsorption capacity of 11.64 mol/equiv and in Ba^{2+}-form the capacity is 11.23 mol/equiv. Toteja et. al. (1997) speculated that the similar capacities might be due to water filling the pores of the macroporous resin. (Toteja, et al., 1997)

The Dow Chemical Company advertises some of their strong acid cation exchange resins (Dowex Marathon C) for removing water from organic solvents (The Dow Chemical Company, 2017). A patent by Wymore (1966) suggests that after the adsorption of water into a carboxylate cation exchange resin, the resin could be regenerated (dried) by blowing dry, hot (105–200 °C), unreactive gas, such as CO_2 or N_2 through the resin. It was also noted that the resin should be in alkali metal or ammonium form (Wymore, 1966). Also the Dow Chemical Company (2017) suggests that that the resins could dried by heating to about 150 °C. It was also pointed out that the resin should be in Na^+ or K^+ form (The Dow Chemical Company, 2017).

Kiser (1987) on the other hand suggested that instead of heating the resin, water could be removed from it by passing a low molecular weight hydrophilic solvent (e.g. methanol,

acetone or propanol) through the resin, which would desorb the water. It was also said that both strong acid cation (e.g. Dowex 50WX2, Amberilte IR-120) and strong base anion exchange resins (Dowex 1X2, 1X8) could be used (Kiser, 1987).

Organic solvents and ionic liquids have very different properties and characteristics as already mentioned in chapter 0. Most notably organic solvents consist of neutral species whereas ionic liquids are composed of ionic species. One might think therefore that ion exchange resins would be unsuitable for removing water from ILs, because the mobile ions of the resins would be exchanged for the ions of the IL. However, this can be avoided by changing the ion exchange resin into the same ionic form as the IL. In that case the chemical composition of the IL will not change even if ion exchange does take place. The polar water molecules should be attracted by the ionic groups of the resin and water removal should take place. Unfortunately, there is no water adsorption data available for ion exchange resins in $[DBNH]^+$ or $[OAc]^-$ forms.

Another group of adsorbents that might be able to remove water from ILs are non-ionic hypercrosslinked polystyrenes. As the name suggests, they are highly cross-linked (degree of crosslinking 100–200 %) polymers, which have a nanoporous structure (Tsyurupa & Davankov, 2006). Typical pore diameters are between 0.4 and 30 nm at dry state (Tsyurupa & Davankov, 2006). The pore size distribution is usually quite narrow, which enables the separation of molecules based on their size (Laatikainen, et al., 2007a). Hypercrosslinked polystyrene has been shown to be able to separate even simple electrolytes from each other, such as HCl and NaCl, HCl and $CaCl_2$ (Laatikainen, et al., 2007a; Laatikainen, et al., 2007b). It was noted that in the case of electrolytes, the separation is not only based on size, but other factors, such as activity of the electrolytes, have an effect on the separation (Laatikainen, et al., 2007b).

Due to their nanoporous structure, hypercrosslinked polystyrenes might be able to act similarly to molecular sieves and separate water form ILs. Unlike ion exchange resins, hypercrosslinked polystyrenes do not need to be pre-treated with the ions of the IL, which leads to lower chemical consumption. However, the lack of ionic groups also leads to low water adsorption capacity (Belyakova, et al., 1986). It was discovered by Belyakova et al. (1986) that a hypercrosslinked polystyrene without ionic groups had a maximum water

vapour adsorption capacity of about 2 mmol/g of resin, whereas a sulfonated version of the same resin had a capacity of >40 mmol/g. When amines were added to the resin, the maximum capacity was >30 mmol/g (Belyakova, et al., 1986). However, the resin was reported to lose its porous structure during sulfonation (Belyakova, et al., 1986). Adding amine groups to the resin on the other hand retained the porous structure (Belyakova, et al., 1986).

Regenerating hypercrosslinked polystyrenes should be possible with the same methods as with ion exchange resins. It has been reported that water can be desorbed from sulfonated hypercrosslinked polystyrene easily even at room temperature whereas the neutral from of the resin cannot be completely desorbed from water at room temperature (Belyakova, et al., 1986). However, no studies regarding the use ion exchange resins or hypercrosslinked polystyrenes for IL dehydration have been made.

4.2 Removal of inorganic impurities

Inorganic impurities are common in ionic liquids (Clare, et al., 2009). Halide and metal salts may remain in the IL from the synthesis (Clare, et al., 2009) and in IL recycling operations a build-up of salts is often observed (Parviainen, et al., 2015). In the case of hydrophobic ILs, removing the salts is quite straightforward since the IL can simply be washed with water (Clare, et al., 2009). As in the case of water removal, hydrophilic ILs are more difficult to purify. Some of the methods described in the previous section will remove at least a part of the inorganic impurities. However, many methods, like electrodialysis, might suffer from them.

4.2.1 Crystallization

Crystallization is commonly used to purify common ionic compounds (Sklavounos, et al., 2016). Ionic liquids are less often purified by crystallization (Sklavounos, et al., 2016), due to their tendency to supercool and form glasses (Holbrey & Seddon, 1999). However, when crystallization can be carried out, it can produce very high purity ILs (>99.9 %) (König, et al., 2008).

Melt crystallization is said to be a suitable technique for purifying ILs. The idea of the technique is to cool the IL so that crystals start to appear. The crystals will be purer than the feed solution due to the very organized structure of the crystals. Only certain sized and shaped molecules can fit into the crystal structure. The molecules that do not fit into the structure remain in the liquid phase and can thus be easily separated. (König, et al., 2008)

Melt crystallization includes several methods such as zone melting, static and dynamic layer crystallization, dry sweating and suspension crystallization (König, et al., 2008). All of them were successfully used to purify [Emim]Cl and [Emim]Br from a purity level of 93–98 % to >99.9 % purity (König, et al., 2008). Nearly all of the studies about IL purification by crystallization seem to focus on producing very high purity ILs from already rather high purity feeds (>95.0 %) (Sklavounos, et al., 2016).

A more industrially relevant study was made by Solà Cervera and König (2010). They studied the recycling of a mixture consisting of an IL (1-ethyl-3-methylimidazolium bis(trifluoromethylsulfonyl)imide, [Emim][Tf_2N]) and aluminium chloride ($AlCl_3$) from an aluminium electrodeposition process. According to the authors, high purity could be achieved by crystallizing both compounds as [Emim][$AlCl_4$]. However, no exact purity numbers were given, and make-up chemicals had to be added before the purified IL/$AlCl_3$ mixture could be reused. Yields were reported to be >65 %. (Solà Cervera & König, 2010)

4.2.2 Ion exchange

Ion exchange is commonly used to purify water from different salts (Helfferich, 1995). It can be used to either completely demineralize water (Helfferich, 1995) or selectively remove certain species (El-Sayed, et al., 2014). For ionic liquids however, there are very few reports regarding their purification by ion exchange. Using ion exchange with ionic liquids might seem a bit difficult as already mentioned in chapter 4.1.7, but with selective-enough resins, removal of metals and other ionic impurities should be possible. Due to the large size and rather low polarity of the IL cations, smaller metal ions should be preferred by the resins (Helfferich, 1995). A recent project by the Finnish Bioeconomy Cluster (FIBIC) suggested that strong acidic cation exchange resins could remove magnesium almost completely from the spinning bath solution of Ioncell-F (FIBIC Oy, 2014). It was also said that weak acid cation exchangers were less effective in removing magnesium (FIBIC Oy, 2014).

4.3 Removal of organic impurities

Organic impurities are a common impurity in ILs and they can originate from the production of the IL (Clare, et al., 2009) or from the process that utilizes the IL. Organic compounds are of course present when biomasses are treated with ILs. However, processing biomass with ILs often creates unwanted organic by-products, such as cellulose degradation products (Sixta, et al., 2015), which can be harmful to the process (Parviainen, et al., 2015).

4.3.1 Liquid-liquid extraction

Liquid-liquid extraction or solvent extraction can be used to remove both hydrophilic and hydrophobic compounds from ionic liquids (Sklavounos, et al., 2016). The technique utilizes the low solubility of some ILs to organic solvents and water (Kuzmina, 2016). Hydrophobic ILs can be used to extract metals from aqueous solutions (Wei, et al., 2003). After extraction the ILs can be purified by changing the pH of the IL (Wei, et al., 2003).

Purifying hydrophilic ILs with liquid-liquid extraction is more difficult, since water cannot be used to extract the impurities. However, organic impurities can be extracted from hydrophilic ILs with organic solvents such as acetonitrile, dichloromethane and ethyl acetate (Dibble, et al., 2011). However, as noted earlier, using organic solvents makes the process less green due to their volatility and toxicity (Kuzmina, 2016).

Dibble et al. (2011) studied the separation of several organic compounds from [Emim][OAc] that was used to dissolve corn stover. They used a mixture of acetone and ethanol to first precipitate the dissolved biomass out of the IL solution. After precipitation there were several organic components, such as sugars, lignin and extractives, remaining in the IL/acetone/ethanol solution. These compounds were separated in a multi-stage distillation/extraction process, which utilised the adjustable solubility of [Emim][OAc] to acetone/ethanol mixtures. Pure acetone and [Emim][OAc] are miscible, but when 1.0 wt-% of water is added, the solubility of [Emim][OAc] to acetone reduces to <0.05 wt-%. By adding ethanol or other alcohols, the solubility can be restored. The formation of two phases and their regeneration back to one phase can therefore be easily controlled by adding water or ethanol. (Dibble, et al., 2011)

The first step of the solvent recovery process was to distil acetone and alcohols out of the used IL solution. A small amount of water was left in the liquid IL phase. Next, acetone was added to the IL solution and two phases were formed due to the residual water in the IL. Non-polar substances, such as long-chain aliphatic alcohols, aromatics and sterols, were extracted into the acetone phase. The acetone phase was separated, and water was added to it to remove any traces of IL. The acetone phase was then distilled out with the extracted

compounds. The IL phase from the acetone extraction was treated with 2-propanol, which caused a lignin-rich solid to precipitate out of the solution. The solid was separated from the liquid and residual alcohol, acetone and water were removed from the IL by vacuum distillation. (Dibble, et al., 2011)

Dibble et al. (2011) proposed that the formation of two phases is caused by hydrophilic interactions between the IL and water. As the second phase (acetone) starts to appear, the IL starts to move away from the acetone phase and towards the more polar water-containing phase. The destruction of the second phase by alcohol addition was explained by the formation of IL-water-alcohol complexes, which have a higher solubility in acetone than IL-water complexes. (Dibble, et al., 2011)

Li et al. (2010a) used solvent extraction to extract hydrophobic organic compounds from an aqueous solution of 1-allyl-3-methylimidazolium chloride ([Amim]Cl) that was used in acid-catalysed hydrolysis of wood. They used ethyl acetate as the organic phase and were able to extract phenols, furans and lignin degradation products out of the IL solution (Li, et al., 2010a).

Rodríquez et al. (2009) demonstrated that at least some lignin could be extracted from [Emim]Cl with polyethylene glycol (PEG). High molecular weight PEG (PEG-1500, PEG-2000 and PEG- 3400) forms a biphasic system with [Emim]Cl (Rodríquez, et al., 2009). PEG is an interesting compound for solvent extraction, because it eliminates many problems associated with organic solvents: it is non-volatile, biodegradable, inexpensive and has low-toxicity (Rodríquez, et al., 2009).

The formation of two phases in mixtures of IL and lower molecular weight PEGs can be induced by the addition of water (Tomé, et al., 2014). Tomé et al. (2014) studied the mechanism of two-phase formation in such systems. They suggested that water solvates the anion of the IL and breaks the hydrogen bonds between the anions and the hydroxyl groups of PEG (Tomé, et al., 2014). This then causes the polymer to form a separate phase (Tomé, et al., 2014). The phenomenon was called washing-out to separate it from the salting-out phenomenon since washing-out is caused by water and salting-out by salts (Tomé, et al.,

2014). It should be noted that washing-out cannot be used for water removal, because water preferentially hydrates the IL anions over PEG (Tomé, et al., 2014).

4.3.2 Supercritical CO_2

As mentioned in chapter 4.1.2, $scCO_2$ is soluble in ILs, but ILs are not soluble in $scCO_2$ (Blanchard, et al., 2001a). This unusual behaviour can be used to first extract organic compounds from the IL phase into $scCO_2$ (Mai, et al., 2014). The extraction is very efficient due to the good solubility of $scCO_2$ into the IL, which enables good contact with the compounds to be extracted, and also because dissolved CO_2 lowers the viscosity of the IL (Blanchard, et al., 2001a). After extraction, the system is depressurized, which transforms the $scCO_2$ into gas and takes the extracted compounds with it (Mai, et al., 2014). Also the dissolved CO_2 in the IL phase is removed (Blanchard, et al., 2001a). Since the IL is not soluble in $scCO_2$, no IL is lost with the gas stream (Blanchard, et al., 2001a).

Blanchard and Brennecke (2001b) were able to extract several organic compounds, including benzene, aniline and phenol, from [Bmim][PF_6] with $scCO_2$. A yield of 95 % could be achieved for each compound with varying amounts of $scCO_2$ (Blanchard & Brennecke, 2001b). The major drawback of using $scCO_2$ is the need for high pressure equipment, which increases the costs of the process and is a potential safety risk.

4.3.3 Liquid chromatography

Liquid chromatography is a separation technique that uses a stationary separation material to separate solute components from liquids. The solid separation material is packed into a column and a carrier liquid (eluent) is pumped constantly through it. The solution that contains the components to be separated is injected to the eluent stream and fed to the column (Scott, 2003). Different components in the liquid stream will interact in different ways with the separation material and propagate through the column at different velocities (Scott, 2003). Those that interact more strongly with the separation material will remain in the

column longer than those that interact less strongly. Different components can therefore be collected from the outlet of the column at different times as individual fractions.

Liquid chromatography has been used to separate ILs and sugars from lignocellulosic hydrolysates (Binder & Raines, 2010; Feng, et al., 2011; Caes, et al., 2013; Mai, et al., 2012). Binder & Raines (2010) used a strong cation exchange resin (Dowex 50) in $[Emim]^+$ form to separate [Emim]Cl from glucose and xylose. Since the resin was in the same ionic form as the IL, the IL was excluded from the resin and eluted out of the column before the non-ionic sugars (Binder & Raines, 2010). The technique is called ion exclusion (Helfferich, 1995). More than 95 % of the IL was recovered while the recovery rates for glucose and xylose were 94 and 88 % (Binder & Raines, 2010).

Feng et al. (2011) used alumina (Al_2O_3) as a separation material to separate *N*-methyl-*N*-methylimidazolium dimethyl phosphate ([Mmim][DMP]) from glucose. Recovery rates of over 90 % were achieved for both the IL and glucose (Feng, et al., 2011). However, it was discovered that methanol had to be added to the eluent in order to achieve high enough recovery rates (Feng, et al., 2011). The use of methanol, which is a toxic and volatile chemical, and the fact that alumina adsorbents are prone to abrasion in ILs (Clare, et al., 2008) makes the process unattractive.

Both studies by Binder & Raines (2010) and by Feng et al. (2011) used simple single-column batchwise chromatography. More complicated multi-column simulated moving bed (SMB) systems were studied by Caes et al. (2013) and Mai et al. (2012). Both utilised the principle of ion-exclusion chromatography to separate IL ([Emim][OAc] and [Bmim]Cl) from sugars (Caes, et al., 2013; Mai, et al., 2012). Recovery rates of the ILs were reported to be 99.82 % (Mai, et al., 2012) and >99 % (Caes, et al., 2013).

It is clear that ion exclusion chromatography is an effective way to separate sugars and other organic compounds from ionic liquids. In the case of Ioncell-F, the composition of the organic impurities is not known (Walger, et al., 2017), but since they most likely are non-

ionic species, ion exclusion chromatography should be able to separate them from [DBNH][OAc].

4.4 Recovery of trace amounts of ionic liquids

The release of ionic liquids into natural waters is often seen as an environmental hazard due to the toxicity and non-biodegradability of some ionic liquids (Neves, et al., 2014; Fernández, et al., 2011). A few studies about the recovery of ILs from wastewater have been made (Neves, et al., 2014; Fernández, et al., 2011). In the case of Ioncell-F, small of amounts of [DBNH][OAc] and its hydrolysis products end up in the distillate stream during evaporation (Ahmad, et al., 2016). To achieve high-enough IL recovery rates, these trace amounts probably need to be recovered.

4.4.1 Membrane separation

As already mentioned in chapter 4.1.4, membranes have been used to separate water and ILs (Haerens, et al., 2010). Membranes have also been studied to recover ILs from wastewater streams (Fernández, et al., 2011). The recovery of hydrophilic ILs ([Bmim]Cl and [Bmim][OAc]) from a cellulose dissolution wastewater by nanofiltration was studied by Fernández et al. (2011). In addition to water and IL, the feed stream contained several cellulose degradation products (Fernández, et al., 2011). It was found out that the nanofiltration membranes were more selective towards the organic impurities than the IL (Fernández, et al., 2011). However, only 36 % of the impurities and 21 % of the IL were rejected by the membranes (Fernández, et al., 2011). On the other hand, it seemed that a certain type nanofiltration membrane (NF-270) could efficiently remove chromophores from the solution, because the feed solution was red or orange and permeate (solution that had gone through the membrane) was colourless (Fernández, et al., 2011). It was also discovered that organic impurities caused significant clogging of the membrane, which led to low fluxes through the membrane (Fernández, et al., 2011).

4.4.2 Adsorption

Several studies about adsorption of ILs from aqueous solutions have been made with nearly all of them focusing on adsorption by activated carbon (AC) (Palomar, et al., 2009; Neves, et al., 2014; Lemus, et al., 2012; Anthony, et al., 2001). It was noted by Anthony et al. (2001) that while AC could remove IL ([Bmim][PF_6]) from water to an undetectable level, the amount of AC needed was about 50 times more than that required for removing the same amount of toluene. It was also said that the IL could not be recovered from the AC (Anthony, et al., 2001).

Palomar et al. (2009) suggested that ILs could be desorbed from AC by acetone. Also Lemus et al. (2012) suggested the use of acetone and added that acetone could by removed from the desorbed IL by evaporation at atmospheric pressure. Both authors noticed that AC was better at adsorbing less polar ILs, such as 1-octyl-3-methylimidazolium hexafluorophosphate ([Omim][PF_6]) and 1-hexyl-3-methylimidazolium hexafluorophosphate ([Hmim][PF_6]) compared to more polar ILs like [Bmim][PF_6] (Palomar, et al., 2009; Lemus, et al., 2012). It was also discovered that the adsorption of polar ILs could be enhanced by introducing hydroxyl groups or other polar groups to the surface of the AC, which would form hydrogen bonds with the ILs (Palomar, et al., 2009; Lemus, et al., 2012).

Neves et al. (2014) suggested that the adsorption of hydrophilic ILs, such as [Bmim]Cl could be enhanced by adding sodium sulphate (Na_2SO_4) to the IL solution. The addition of Na_2SO_4 induced a salting-out phenomenon leaving the salt in the liquid phase and transferring the IL into the AC. The addition of Na_2SO_4 could increase the apparent distribution coefficient (K_d) of [Bmim]Cl and [Bmim][CH_3SO_3] up to 5.5 times. The highest distribution coefficients were obtained at the highest Na_2SO_4 concentrations (1.75 mol/kg). The apparent distribution coefficient is defined as the ratio of equilibrium concentrations in the liquid phase (C_e) and the solid phase (q_e). (Neves, et al., 2014)

$$K_d = \frac{q_e}{C_e} \quad (1)$$

Despite most of the authors claiming AC as an effective adsorbent for ILs (Palomar, et al., 2009; Lemus, et al., 2012; Neves, et al., 2014), ion exchange resins would most likely be more effective due to their ionic nature (Anthony, et al., 2001). In the case of Ioncell-F, the distillate from evaporation most likely contains [DBNH][OAc] and its hydrolysis product [APPH][OAc] as the only ionic species. It is therefore likely that they could be selectively recovered from the distillate with ion exchange resins in the same way as salt is removed from drinking water.

5 SOLVENT RECYCLING CONCEPTS FOR IONCELL-F

To make Ioncell-F economically feasible, an efficient solvent recycling system is needed. Based on the methods described in the previous chapter, this chapter will introduce possible solvent recycling concepts for Ioncell-F.

The cellulose dissolution and fibre spinning part of Ioncell-F is well-studied and it can produce high-quality cellulosic fibres (Sixta, et al., 2015). However, the solvent recycling part is still under development. Only water removal by evaporation and solvent purification by distillation have been studied so far (Ahmad, et al., 2016; Ostonen, et al., 2016b). Distillation has turned out to be challenging as described in chapter 4.1.1 and evaporation might not be able to reach low-enough water contents. Removal of organic and inorganic impurities by other methods than distillation has not been studied. A simplified block diagram of the Ioncell-F process is presented in figure 8.

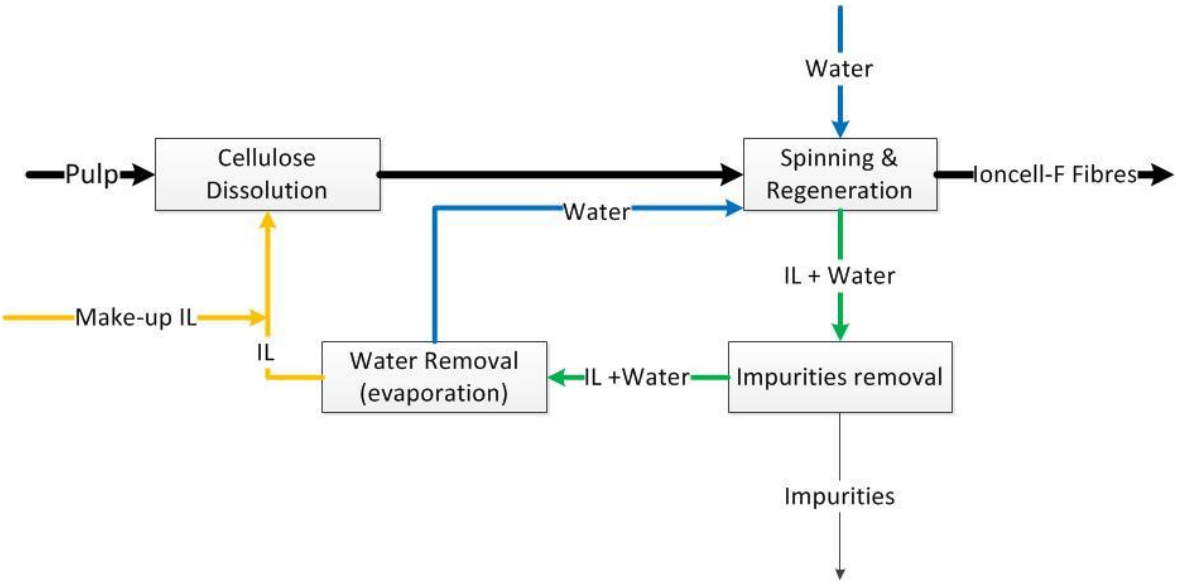

Figure 8 Simplified block diagram of the Ioncell-F process.

One of the drawbacks of evaporation is that it leaves non-volatile impurities in the IL (Kuzmina, 2016). Therefore, the impurities need to be removed before or after evaporation. In the case of [DBNH][OAc] it has been shown that some of the IL and its hydrolysis product end up in the distillate (Ahmad, et al., 2016). To remain high-enough IL recovery rates, [DBNH][OAc] and its hydrolysis product will probably need to be recovered from the distillate. On the other hand, if the distillate water is reused in the coagulation bath,

recovering the IL might not be necessary, since the IL lost in evaporation will return to the solvent recycle stream as depicted in figure 8.

5.1 Water removal strategies

Of the water removal techniques presented in chapter 4.1, perhaps the most interesting ones are evaporation, pervaporation, salting-out, sweeping with nitrogen (stripping), electrolysis, molecular sieves, ion exchange resins and hypercrosslinked polystyrene desiccants. Evaporation is suitable for removing most of the water (bulk water), but struggles to reach low-enough water contents (Ahmad, et al., 2016). It also promotes hydrolysis of [DBNH][OAc] and the amount of hydrolysis product increases with decreasing water content (Ahmad, et al., 2016). Pervaporation allows the use of lower temperatures and has lower IL losses (Sun, et al., 2017), but seems to suffer from low fluxes, long processing times and the need for large membrane areas. It might therefore be better to lower the water content to a moderately low level (~10 wt-%) by evaporation and then use some other method to lower the water content to the level needed for cellulose dissolution (<4 wt-%).

Salting-out is a powerful technique for water removal, but it requires the use of additional chemicals (salts), which should also be recycled (Kuzmina, 2016). On the other hand, using a cheap enough salting-out agent might remove the need for recycling. For example, sodium sulphate (Na_2SO_4) is generated in large amounts in recovery boilers of Kraft pulp mills as electrostatic precipitator dust (ESP-dust) (Vakkilainen, 2005). The amount of ESP-dust a recovery boiler generates is about 5–12 % of black liquor dry solids flow (Vakkilainen, 2005). Most of it is recycled to the evaporation plant (Vakkilainen, 2005), but some of it may need to be removed from the process to adjust the amount of sulphur in the chemical recovery cycle.

Sodium sulphate has been reported to work as a salting-out agent for ILs, although not being as strong as phosphate salts (Trindade, et al., 2007). It is however stronger than acetate (Shahriari, et al., 2012), which is why it might be possible to dehydrate [DBNH][OAc] with Na_2SO_4. If an Ioncell-F plant was built next to a Kraft pulp mill, Na_2SO_4 from recovery boiler could at least theoretically be used to remove water from [DBNH][OAc], after which it could be returned back to the pulp mill. This way one could utilize a by-product of a pulp

mill and not generate additional waste streams. On the other hand, as with any salting-out agent, there is a risk of contaminating the IL and anion exchange between the IL and salting-out agent might take place (Sklavounos, et al., 2016).

Another challenge in using ESP-dust as a source of Na_2SO_4 is the presence of impurities, which may affect the salting-out ability and contaminate the IL. Typical ESP-dust contains about 40–60 wt-% sulphate and 25–33 wt-% sodium (Öhman, et al., 2014). In addition, carbonate (2–22 wt-%), chloride (1–2.5 wt-%), potassium (2–32 wt-%) are present in significant amounts (Öhman, et al., 2014). Also trace amounts (<0.05 wt-%) of calcium, iron and manganese may be present in the dust (Öhman, et al., 2014).

Another source of sodium sulphate in a pulp mill would be the saltcake from ClO_2 production, which contains very low levels (<0.003 wt-%) of impurities (Öhman, et al., 2014). The amount of saltcake a ClO_2 plant produces depends on the process type and conditions, but it is often about 1.1 ton of Na_2SO_4/1 ton of ClO_2 (Öhman, et al., 2014). However, the saltcake often consists of sodium sesquisulphate ($Na_3H(SO_4)_2$), which is acidic (Öhman, et al., 2014) and should be neutralized before contacting it with [DBNH][OAc]. Protons from an acidic solution might induce the conversion of acetate ($[OAc]^-$) to acetic acid (HOAc), which would at least partly remove the ionic nature of the solvent.

Using ion exchange resins or hypercrosslinked polystyrenes as drying agents might also be an interesting option, although they have not been studied for ILs. Being solid and reusable materials, they do not create a waste stream like salting-out agents. However, the high viscosity of ILs at low water contents (10–500 $mPas^{-1}$ as pure IL at room temperature) (Mallakpour & Dinari, 2012) and the strong interactions between water and hydrophilic ionic liquids (Khan, et al., 2014) might cause difficulties with solid separation materials.

The high viscosity will probably make pumping the IL through a column difficult if not impossible and pumping will consume a lot of energy. The strong interactions between water and IL decrease the activity of water in IL with lowering water concentrations (Khan, et al., 2014). Low water activity then leads to low water adsorption capacity (Nandan, et al., 1993; Toteja, et al., 1997), which means that larger amounts of the adsorbent are needed. On the other hand, at low water activities, the difference in adsorption capacity between resins in

different ionic forms and with different crosslinking densities becomes smaller (Nandan, et al., 1993; Toteja, et al., 1997; Gregor, et al., 1952). So does the capacity difference between ionic and non-ionic forms of hypercrosslinked polystyrene (Belyakova, et al., 1986).

Another challenge with ion exchange resins and polystyrene adsorbents is the regeneration (drying) of the adsorbent. As mentioned in chapter 4.1.7, a wet ion exchange resin can be dried either by heating (The Dow Chemical Company, 2017; Wymore, 1966) or by passing a polar hydrophilic solvent through it (Kiser, 1987). The needed heat for regeneration is reported to be around 4190 kJ/kg of water at 135–149 °C (The Dow Chemical Company, 2017), which is almost twice as high compared to the heat of vaporization of water at 100 °C and ambient pressure (~2260 kJ/kg of water) (CRC Press, 2017). This is due to the fact that in addition to water, the resin itself needs be heated up to the desired temperature. The high temperature during drying also means that the resin bed needs to be cooled down before the feed liquid is introduced to the system (The Dow Chemical Company, 2017). It is therefore likely that the energy consumption of the drying process will be rather high.

Iborra et. al. (2000) reported that macroporous ion exchange resins (Amberlyst 15, Bayer K-2631, Lewatit SPC 112) in H^+ form could be dried with air even at 25 °C. It was shown however that at higher temperatures the rate of drying is faster and the final (equilibrium) moisture content is lower (Iborra, et al., 2000). For example, after drying a Bayer K-2631 resin contained 3.44 mol of water/equiv at 25 °C, but at 93 °C it contained only 0.35 mol of water/equiv (Iborra, et al., 2000).

Using a non-ionic adsorbent might lead to lower energy consumption in the drying compared to ion exchange resins since there are no ion-dipole interactions between the adsorbent and water. It might also mean that they can be dried to a lower water content, since in the study by Iborra et. al. (2000), the water that was not removed from the resin even at the highest temperature (93 °C) was said to be bonded to the ionic groups of the resin. The result also suggests that during drying of ion exchange resins, free water is removed first and water of hydration last. In other words, drying seems to advance in reversed order compared to water adsorption and water of hydration seems to be more difficult to remove than free water.

Using organic solvents for regeneration instead of heat will probably lower the energy consumption since the water adsorption and resin regeneration can be carried out even at room temperature (Kiser, 1987). However, using an organic solvent creates an additional waste stream. The solvent could be recovered by distillation or evaporation and reused, but it would also require additional process steps and equipment. There is also a risk of contaminating the IL with the solvents (Kuzmina, 2016). Kiser (1987) suggested that after regenerating the resin with methanol, nitrogen gas could be blown through the resin to remove methanol from the resin. However, some methanol still ended up in the dried solvent (ethanol) (Kiser, 1987).

A simpler water removal method compared to salting-out and adsorbents is sweeping (stripping) with nitrogen. It has been demonstrated to remove water almost completely from several different ILs (Ren, et al., 2010). It is also a faster method compared to vacuum evaporation (Ren, et al., 2010). However, it has been reported that to lower the water content of [Bmim][BF_4] from 5.5 wt-% to ~0.1 wt-% at 50 °C, about 2800 mL of nitrogen is needed per gram of IL (Ren, et al., 2010). High nitrogen consumption is due the non-polar nature of nitrogen, which is why it does not attract water very strongly. Producing large amounts of nitrogen is quite expensive and energy intensive. Air would be a cheaper option, but because air is not much more polar than nitrogen, the stripping gas consumption would probably still be high. IL oxidation might also be an issue when using air as the stripping gas.

Electrolysis is another potential water removal technique. Very low water contents can be achieved by it (<0.1 wt-%) (Islam, et al., 2008), but it is also likely to be an energy-intensive technique. Breaking water into hydrogen and oxygen consumes a lot of energy. If inorganic impurities (metals) are present, they might be reduced in the electrolytic cell, which would further increase the energy consumption. On the other hand, it would remove the need for a separate inorganic impurity removal step. Also producing hydrogen and oxygen might be profitable if they could be sold as a by-product.

Table I summarizes the advantages and disadvantages of the most potential water removal techniques. Reported IL recoveries are given when available to demonstrate the potential of each technique.

Table I Summary of the advantages and disadvantages of different water removal techniques.

Technique	Advantages	Disadvantages	IL Recovery
Evaporation	Simple, no additional chemicals needed	Energy intensive, promotes hydrolysis	[DBNH][OAc]: 95.7–98.9 % (including the hydrolysis product)
Pervaporation	Smaller IL losses & milder conditions than in evaporation	Low fluxes, large membrane areas, fouling & membrane durability?	[Emim][OAc]: ≥99.9 %
Salting-out	High recovery rates, no need for elevated *T* or *p*	Uses chemicals (salts), challenging recycling, contamination of the IL	[Bmim][BF_4]: 98.77 %, [Amim]Cl: 96.80 %
IX resins, hypercross-linked PS, molecular sieves	Relatively simple process, reusable separation materials	Not studied for ILs, regeneration & energy consumption?	N/A
Electrolysis	No additional chemicals, production of H_2, possibility to simultaneously separate metals	Energy consumption (?), safety (H_2 and O_2 gases)	N/A
Stripping (sweeping)	Simple process, no harmful chemicals, faster than evaporation	Energy and gas consumption	N/A

5.2 Strategies for removing inorganic impurities

Of the two methods to remove inorganic impurities presented in chapter 0, ion exchange has to be the more promising one. Although crystallization can produce very high purity ILs (>99.9 %) it can be difficult to apply for some ILs and it requires cooling of the IL to form crystals (König, et al., 2008), which consumes energy. Ion exchange on the other hand is widely applied for removing salts from aqueous solutions (Helfferich, 1995) and has been reported to be efficient in removing at least magnesium from Ioncell-F spinning solutions (FIBIC Oy, 2014). Of course, being able to reach such high purities, crystallization could be

used as final purification step after most impurities have been removed by other methods. Table II summarizes the advantages and disadvantages of crystallization and ion exchange.

Table II Summary of the advantages and disadvantages of different techniques for the removal of inorganic impurities.

Technique	Advantages	Disadvantages	IL Recovery
Ion exchange	High selectivity & recovery, simple to operate	Need for regeneration chemicals, not studied for ILs	N/A
Crystallization	High purities possible	Supercooling and glass formation, suitable for relatively pure IL feeds	N/A

5.3 Strategies for removing organic impurities

Liquid chromatography utilizing ion exclusion has proven to be very effective in separating ILs from sugars (Binder & Raines, 2010; Caes, et al., 2013; Feng, et al., 2011; Mai, et al., 2012). As mentioned earlier, it might be able to separate non-ionic organic impurities from [DBNH][OAc]. In Ioncell-F, it should be located before evaporation since it uses water as eluent and might dilute the IL slightly. Also inorganic impurities should preferably be removed before ion exclusion chromatography to avoid changing the ionic form of the resin used in the separation.

Liquid-liquid extraction with a suitable organic solvent might also be able to extract organic compounds from [DBNH][OAc]. Acetone has proven to be able to extract several organic compounds, such as fatty acids, sterols, aromatics and triglycerides from [Emim][OAc] that has been used to dissolve corn stover (Dibble, et al., 2011). Since acetone forms a separate phase with [Emim][OAc] when water is present at >1 wt-%, it might be possible extract organic impurities from [DBNH][OAc] with acetone before evaporation. Acetone could then be recovered from the extracted impurities by evaporation and reused as described by Dibble et al. (2011).

PEG is a more environmentally friendly compound and it has been shown to be able to extract some lignin from [Emim]Cl, but no exact numbers have been given (Rodríquez, et al., 2009). ILs can form biphasic systems with pure molten PEG (Rodríquez, et al., 2009) or

with aqueous PEG solutions (Tomé, et al., 2014). It might therefore be possible to extract some organic impurities form [DBNH][OAc] with PEG. However, since the composition of the impurities (Walger, et al., 2017) and the extraction ability of PEG are not known, it is uncertain whether the IL can actually be purified with PEG.

Extraction with supercritical CO_2 is an efficient technique for removing several organic compounds from [Bmim][PF_6] (Blanchard & Brennecke, 2001b). One of its advantages is that IL losses are minimal, because ILs are not soluble in scCO_2 (Blanchard, et al., 2001a). However, the need for very high-pressure equipment (p >7.39 MPa) and the energy intensive pressurization-depressurization cycles increase the costs of the process. The advantages and disadvantages of each organic impurity removal technique are given in table III.

Table III Summary of the advantages and disadvantages of different techniques for the removal of organic impurities.

Technique	**Advantages**	**Disadvantages**	**IL Recovery**
Liquid-liquid extraction	Simple to operate, good selectivity	Additional chemicals, cross-contamination risk	[Emim][OAc]: 89 %
Supercritical CO_2	Non-toxic, no IL losses, moderate temperatures	High pressure equipment needed	[Bmim][PF_6]: ~100 %
Chromatography (ion exclusion)	Separates electrolytes and non-electrolytes, high purities, no additional chemicals, mild conditions	Requires careful design, dilution of the products	[Emim]Cl: >95 % [Emim][OAc]: 99.82 & 98% [Bmim]Cl: >95 %

5.4 Trace IL recovery

Membranes and adsorbents have been suggested as separation methods to recover ILs from aqueous solutions. Recovering [DBNH][OAc] and its hydrolysis product from the distillate after evaporation should be quite straightforward with ion exchange resins since the distillate probably does not contain any other ionic species.

Membranes could also be used, especially since the viscosity of the solution should be quite low due to the low IL (0.06–0.11 wt-%) and hydrolysis product concentrations (0.27–1.11 wt-%) (Ahmad, et al., 2016). However, the results by Fernández et al. (2011) indicated that

<50 % of [Bmim]Cl and [Bmim][OAc] could be recovered by nanofiltration membranes. Their feed solution contained several organic components from the dissolution and regeneration of cellulose (Fernández, et al., 2011), which of course affect the results. In any case, ion exchange resins should be a reliable option, although they have not been studied for recovering ILs from aqueous solutions.

5.5 Process concepts

To illustrate the possible combinations of solvent recycling techniques, several different block diagrams of the Ioncell-F process will be presented in this chapter. In all of the configurations, bulk water removal is done by evaporation and the recovery of IL from distillate by ion exchange. First, a configuration that uses ion exchange to remove inorganic impurities, ion exclusion chromatography to remove organic impurities and ion exchange resins to remove residual water, is presented (figure 9).

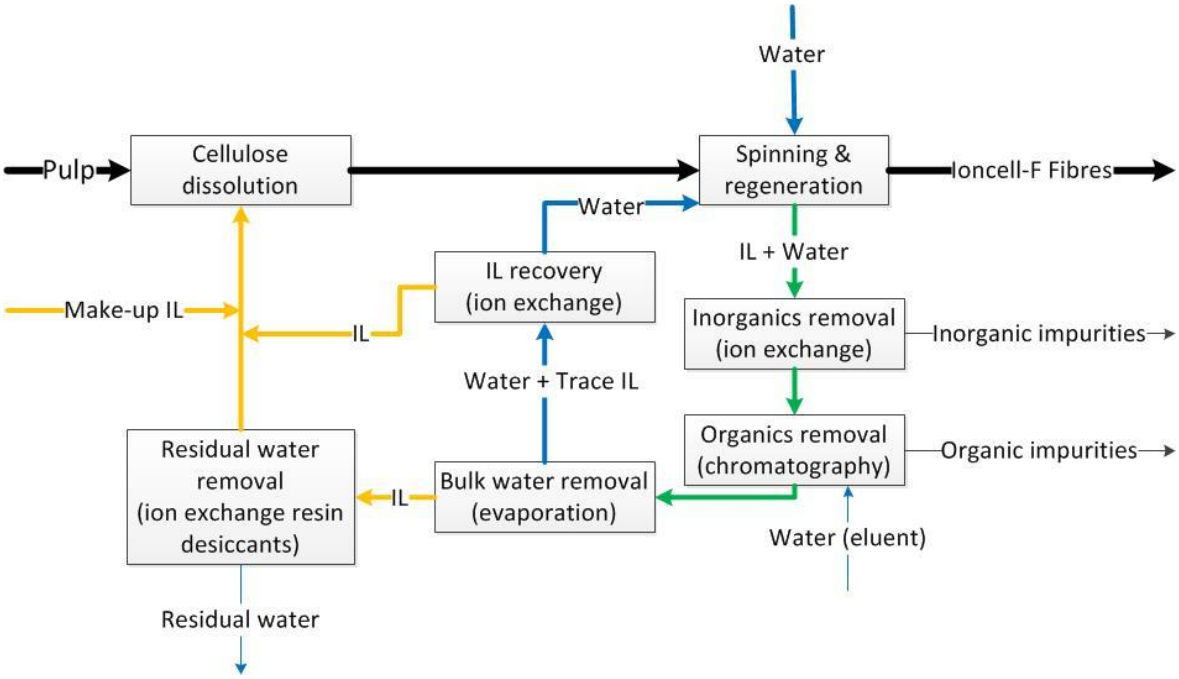

Figure 9 A conceptual solvent recycling configuration for Ioncell-F process.

The removal of inorganic impurities is located before the removal of organic impurities to avoid changing the ionic form of the ion exchange resin in the organics removal stage. Next, a configuration where residual water removal and inorganic impurities removal are combined in electrolysis, is presented (figure 10).

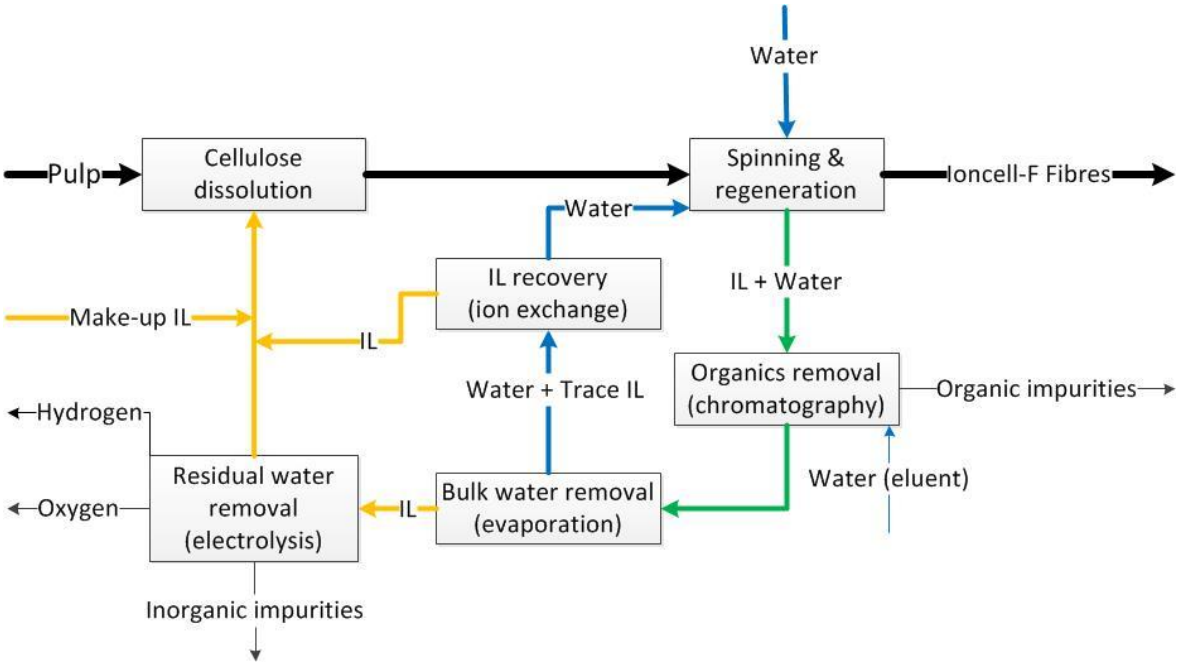

Figure 10 A conceptual solvent recycling configuration for Ioncell-F process.

Using electrolysis as a way to remove residual water enables the integrated production of hydrogen and oxygen. Also metal cations could be reduced in the electrolytic cell and removed from the process. However, this will most likely increase energy consumption. To avoid wasting electricity for metal reduction, the metals could be separated with ion exchange before electrolysis. The process flowsheet would then be similar to the one in figure 9 except for the residual water removal being done by electrolysis instead of ion exchange resins.

A third configuration, where residual water removal is carried out with Na_2SO_4 from a pulp mill is presented in figure 11. The idea is that the Ioncell-F process is located next to a pulp mill and Na_2SO_4 from the recovery boiler or the ClO_2 plant is used as a salting-out agent. After use, the salt is returned back to the pulp mill, so that it does not upset the sulphur balance of the mill.

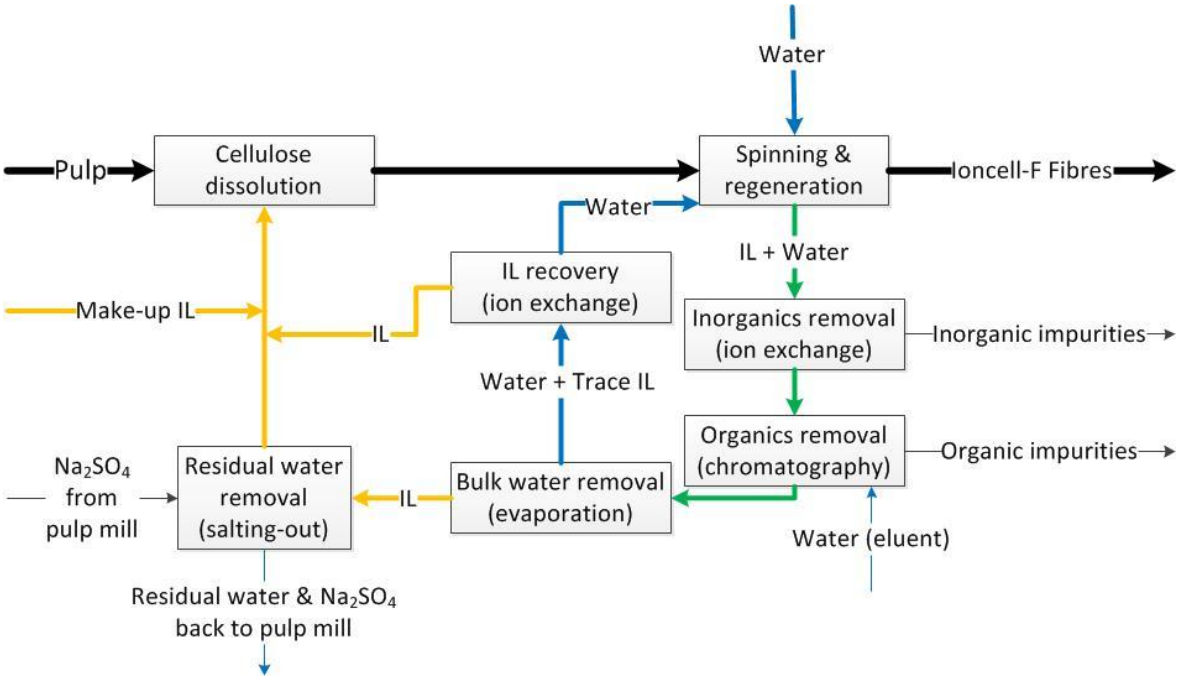

Figure 11 A conceptual solvent recycling configuration for Ioncell-F process.

If the sodium sulphate comes from a ClO_2 plant and it is acidic, a separate neutralization stage is needed before feeding the salt to the residual water removal stage. On the other hand, due to the superbase-nature of the cation (Parviainen, et al., 2013), the IL itself might be able to neutralize the acidity.

5.6 Techniques to be studied in experimental part

As shown above, solvent recycling in Ioncell-F will most likely consist of many process steps and nearly all of them can be done with several techniques. Experimentally studying all possible techniques for all process steps would be very time-consuming and labour intensive. On the other hand, because the composition of organic and inorganic impurities is not known at the moment (Parviainen, et al., 2015; Walger, et al., 2017), studying their removal would be difficult. For these reasons, only water removal from [DBNH][OAc] will be studied in the experimental part of this work.

The main focus of the experimental part will be on adsorptive water removal, because it has not been studied for ionic liquids earlier. Several types of adsorbents will be tested, including ion exchange resins, non-functionalized polystyrene, aluminium oxide and molecular sieves (zeolites). Initial testing will be carried out by equilibrium batch experiments and the most

suitable adsorbents will be studied in dynamic adsorption experiments. Effect of processing conditions, such as temperature and feed solution water content will be studied in the dynamic experiments.

Stripping with air will also be studied briefly as an alternative water removal method. Based on the results, it will be compared to adsorption and recommendations for future studies will be made.

EXPERIMENTAL PART

6 MATERIALS AND METHODS

6.1 Pre-treatment of solid separation materials

Three different types of solid porous separation materials were used in this work; organic polystyrene-divinylbenzene (PS-DVB) and polyacrylate (PA) based resins, aluminium oxide (Al_2O_3) and inorganic molecular sieves. Organic resins included strong acid cation exchangers (SAC), a strong base anion exchanger (SBA), a weak acid cation exchanger (WAC) and a non-ionic hypercrosslinked polystyrene. SAC resins were used in four different ionic forms and with three different degrees of crosslinking. Properties of each resin are given in table IV.

Table IV Organic resins used in this work and their properties.

Resin	Manufacturer	Type	Gel/Macroporous	Degree of Crosslinking	Ionic form
CS16GC	Finex	Strong acid cation exchanger	Gel	8	$[DBNH]^+$
CS16GC	Finex	Strong acid cation exchanger	Gel	8	Na^+
CS16GC	Finex	Strong acid cation exchanger	Gel	8	Ca^{2+}
CS9.6GC	Finex	Strong acid cation exchanger	Gel	4.3	$[DBNH]^+$
CA16GC	Finex	Weak acid cation exchanger	Gel	8	$[DBNH]^+$
Dowex 1x8	Dow Chemical Company	Strong base anion exchanger	Gel	8*	$[OAc]^-$
Macronet MN500	Purolite	Strong acid cation exchanger	Macroporous	Hyper-crosslinked	H^+
Macronet MN200	Purolite	Non-ionic adsorbent	Macroporous	Hyper-crosslinked	-

*The actual degree of crosslinking is higher due to secondary crosslinking between resin's amine groups

The gel type SAC resins (CS16GC & CS9.6GC) were converted from K^+/Na^+ and the WAC resin (CA16GC) from Na^+ form to $[DBNH]^+$ form to avoid changing the chemical composition of [DBNH][OAc] upon contact with the resin. The conversion was done by passing 750 mL of an aqueous solution containing about 10 wt-% of [DBNH][OAc] through the resin. Conversion was verified by measuring the electrical conductivity of the solution with Consort C3020 multi-parameter analyser before and after contact with the resin.

With the SAC resins, the electrical conductivity of the liquid that had passed through the resin was initially higher (~23 mS/cm at 22 °C) than of the feed liquid (17.80 mS/cm at 21.8 °C). After about 700 mL of the solution had been passed through the resin, the conductivity after contact with the resin had lowered to the same level (17.70–17.80 mS/cm) as the feed solution. Similar phenomenon was observed with the WAC resin, with the conductivity of the feed solution being 30.0 mS/cm (23.5 °C) while the first sample collected from the solution that had passed through the resin had a conductivity of 31.2 mS/cm (23.1 °C).

Acetic acid (100.3 %, analytical reagent, VWR), NaCl (100.3 %, analytical reagent, VWR) and $CaCl_2$ (≥99 %, analytical reagent, Sigma-Aldrich) were used in the preparation of solutions for the conversion SBA and SAC resins' ionic form. The SBA resin was converted to acetate ($[OAc]^-$) form by passing 350 mL of 1 mol/L acetic acid through the resin. Conversion of SAC resin to Na^+ form was done with 500 mL of 1 mol/L NaCl solution and conversion to Ca^{2+} form was done with 0.8 mol/L $CaCl_2$ solution. Conversion was verified in the same manner as described above. All resins were rinsed thoroughly with purified water after conversion.

The hypercrosslinked SAC (Macronet MN500) was provided in H^+ form, so no conversion of the ionic form was required. No conversion was required for the MN200 resin either, since it had no ionic groups. Both resins were however thoroughly washed with purified water to remove any adsorbed impurities. All of the organic resins were dried in a vacuum oven at 40 °C and 40–70 mbar for 24–48 h before use.

In addition to organic resins, molecular sieves of types 3A, 4A, 5A and 13X and weakly acidic aluminium oxide were also used as separation materials. The properties of the inorganic separation materials are given in table V.

Table V Inorganic separation materials used in this work.

Material	**Manufacturer**	**Composition** (Sigma-Aldrich, 2018)	**Mean micropore diameter, Å**	**Mean particle diameter, mm**
Molecular sieve type 3A	Fluka Chemika	0.6 K_2O: 0.40 Na_2O : 1 Al_2O_3 : 2.0 ± 0.1SiO_2 : x H_2O	3	1.0–1.7
Molecular sieve type 3A	Alfa Aesar	0.6 K_2O: 0.40 Na_2O : 1 Al_2O_3 : 2.0 ± 0.1SiO_2 : x H_2O	3	1–2
Molecular sieve type 4A	Alfa Aesar	1 Na_2O: 1 Al_2O_3: 2.0 ± 0.1 SiO_2 : x H_2O	4	1–2
Molecular sieve type 4A	Alfa Aesar	1 Na_2O: 1 Al_2O_3: 2.0 ± 0.1 SiO_2 : x H_2O	4	0.4–0.8
Molecular sieve type 5A	Sigma Chemical CO.	1 Na_2O: 1 Al_2O_3: 2.0 ± 0.1 SiO_2 : x H_2O	5	1.7–2.4
Molecular sieve type 13X	Sigma Chemical CO.	1 Na_2O: 1 Al_2O_3 : 2.8 ± 0.2 SiO_2 : xH_2O	10	1.7–2.4
Aluminium oxide, weakly acidic	Acros Organics	Al_2O_3	60	0.05–0.2

Although molecular sieves (zeolites) are ion exchangers (Helfferich, 1995), the ionic form of the molecular sieves was not changed before use. This is because the ionic form affects the pore size of the molecular sieve (Helfferich, 1995; Sigma-Aldrich, 2018) and on the other hand, the ion exchange capacity of molecular sieves is said to be low (Helfferich, 1995). It was also assumed that with small enough pore size, the IL will not be able enter the micropores and thus little ion exchange should take place. As with organic resins, also the inorganic separation materials were thoroughly washed with purified water and dried at 170 °C under vacuum (40–70 mbar) before use.

6.2 Preparation of ionic liquid solutions

[DBNH][OAc] was provided by Aalto University and it was used without further purification. Solutions were prepared by weighing a desired amount of solid [DBNH][OAc]

and adding a suitable amount of purified water. The mixture was heated to about 60–80 °C and mixed with a magnetic stirrer to melt the IL and to dissolve water in it.

6.3 Water removal experiments

6.3.1 Equilibrium batch experiments

Equilibrium batch experiments were carried out for all solid separation materials in 12 mL glass test tubes. 7.0–9.2 g of [DBNH][OAc] solution was first weighed into the tube and after that 1.8–4.2 g the solid material was added. A plastic cap was added to the tube and parafilm was wrapped around the cap to prevent ambient moisture from getting into the tube.

The tubes were placed into an incubator, which was equipped with a shaker (Heidolph Incubator 1000/Unimax 1010). The incubator was preheated to 50 °C and the tubes were shaken in at 400 rpm for 4.5–16 h. After shaking, the tubes were removed from the incubator, the parafilm seal was removed and a sample was taken with a plastic pipette from the liquid phase. The sample was filtered with a 0.4 µm PTFE flat membrane syringe filter (Phenex) to remove any solid particles before analysis.

6.3.2 Kinetic experiments

Kinetic experiments were carried out for CS16GC, CA16GC and Dowex 1x8 resins and for type 3A zeolite (Sigma) in the same incubator/shaker as the equilibrium batch experiments. About 40–70 g of [DBNH][OAc] was weighed into a capped 100 mL glass bottle and preheated in the incubator to 50 °C. After heating the IL, about 13–28 g of a solid separation material was added to the bottle and shaking at 400 rpm was started. Liquid phase samples were taken by stopping the shaker, removing the cap from the plastic bottle and pulling out 2 mL of liquid phase with a syringe. The samples were filtered with a 0.4 µm PTFE flat membrane syringe filter before analysis.

6.3.3 Dynamic adsorption experiments

Loading experiments were carried out for molecular sieves of type 3A and 4A in two different types of columns. First, a jacketed glass column (Kronlab ECO SR 15/120M3K-K) with a diameter (d) of 15 mm and a bed height (h_{bed}) of 20 cm was used. The column was packed with dry separation material and heated to 50 °C with a water circulation thermostat (Lauda MT) before each experiment. A HPLC pump (Knauer Azura P 4.1 S) was used to pump the IL through the column. The direction of liquid flow was from the bottom of column to the top to avoid flow channelling. The liquid flow rate was determined from the weight of the feed vessel measured at different points during the experiment and from the density of the feed solution measured prior to the experiment. The density was measured with Anton Paar DMA 4500 density meter.

A fraction collector (GE Healthcare Frac-920) and a plastic four-way valve were connected to the column outlet and another plastic four-way valve was connected to the column inlet. The fraction collector was used to collect liquid samples from the column outlet and the four-way valves were used to direct liquid or air in and out of the column.

For the regeneration of the molecular sieve, a supply of synthetic air (AGA, 79 % N_2, 21 % O_2, purity ≥99.999 %) was connected to the column outlet (top) via the four-way valve. Air could be blown through the column to remove moisture from the separation material. Air mass flow was monitored with an electronic mass flow meter (Hewlett-Packard 5182-3494), which measured the mass flow in standard cubic centimetres (mass of 1 cm^3 of air at 1 atm and 0 °C).

The column was heated to 70 °C for the regeneration stage. To collect the moist air and remove water from it, a cold trap was connected to the column inlet (bottom). The cold trap consisted of a refrigerated circulating water bath with thermostat control (Lauda PROLINE RP 855) and a gas washing bottle, which was immersed in the refrigerated (T = -15 °C) water/ethanol bath of the thermostat. The moisture coming with the air from the column was condensed inside the gas washing bottle.

A flowsheet of the experimental setup with glass column in both feed (a) and regeneration (b) configuration is presented in figure 12. The four-way valve at the column outlet (top) is presented as a three-way valve since only three of the four ways were used. Red line represents the flow path of IL and blue line the flow path of air in the system.

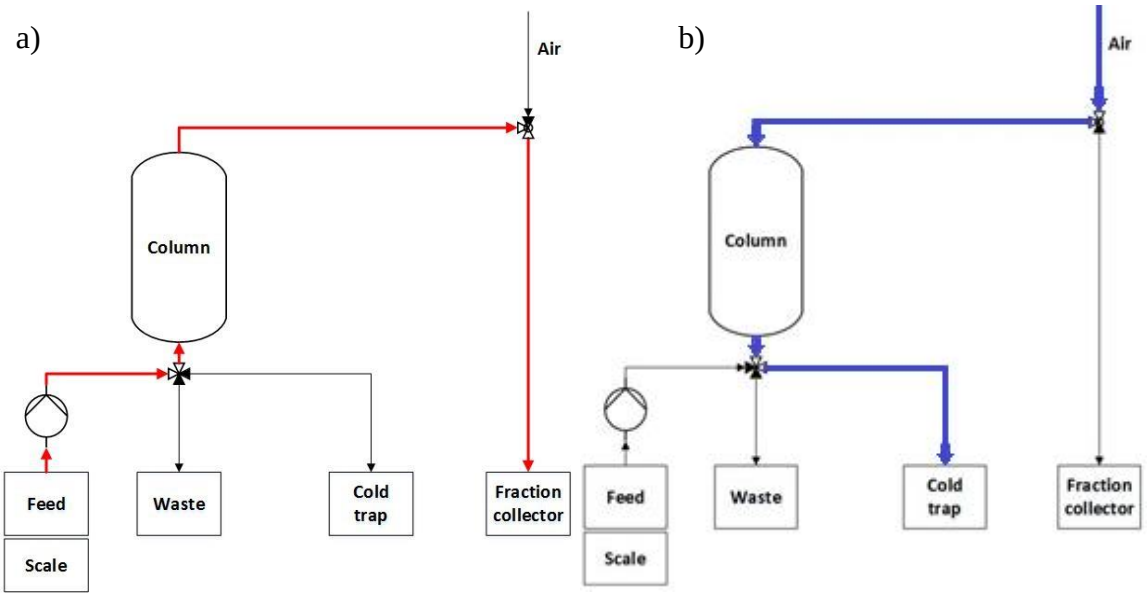

Figure 12 Flowsheets of the experimental setup with a glass column. a) = feed configuration, b) = regeneration configuration.

In addition to the experiments with the glass column, experiments with a stainless steel column (d = 20 mm, h_{bed} = 30 cm) were carried out, because it could withstand higher regeneration temperatures (up to 230 °C). Since the steel column had no heating jacket, the column was placed inside an oven (Memmert UL 40) that was used for temperature control. The experimental setup was also modified so that air could be blown in either direction through the column. A thermometer was also added to monitor the temperature of air coming out of the column during regeneration and the electronic flowmeter was replaced with a rotameter (Brooks Sho-rate, tube size R-2-15-A) to allow higher flowrates (>550 sccm) to be measured. The regeneration procedure was also modified so that after pumping the IL had been stopped, the column was washed by pumping 5–6 BV of pure water through it. Drying/blowing stage was started after washing had been completed. Flowsheet of the modified setup is presented in figure 13.

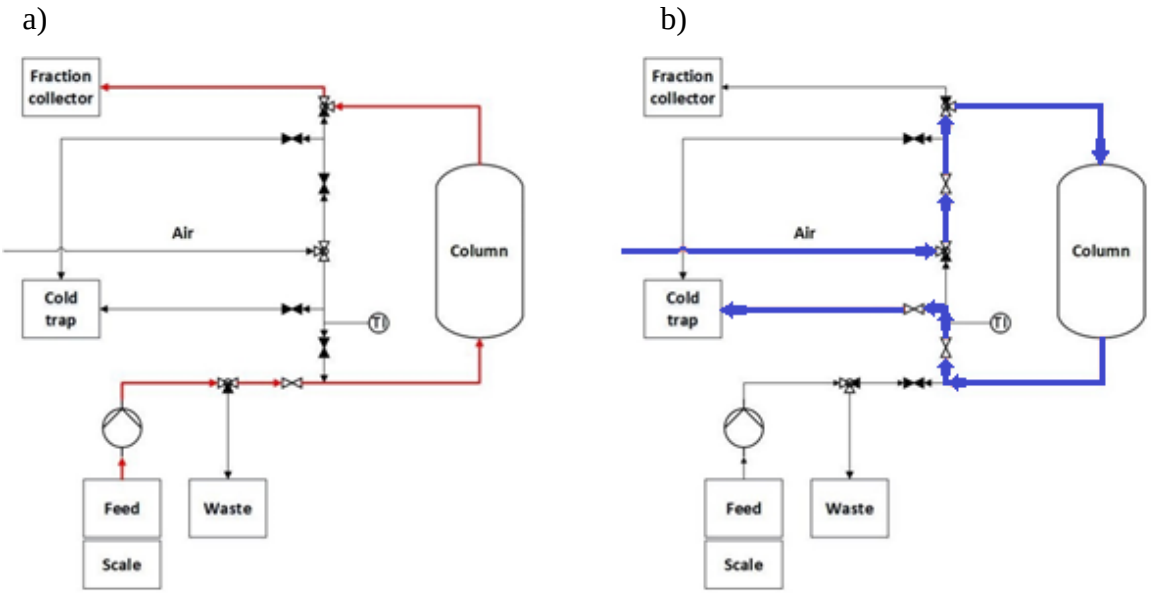

Figure 13 Flowsheets of the experimental setup with a steel column. a) = feed/wash configuration, b) = regeneration configuration.

6.3.4 Stripping experiments

Stripping water away from [DBNH][OAc] with synthetic air was briefly studied as an alternative water removal method to the adsorption-based process. Two stripping experiments were carried out with the setup presented in figure 12b. The setup was modified so that air was blown from the bottom of the column to the top from where it was directed to the cold trap. The glass column was partially filled with IL and air was blown through it. Air flow was measured with an electronic mass flow meter (Hewlett Packard 5182-3494). Samples were taken from the solution by closing the air inlet valve, removing the top adapter of the column and drawing about 1 mL of the IL with a plastic pipette.

6.4 Chemical analyses

Water content of [DBNH][OAc] was determined using gas chromatography (Agilent Technologies 6890 N) equipped with a thermal conductivity detector (TCD). Zebron ZB-WAX plus -column (Phenomenex, length = 30 m, internal diameter = 0.32 mm, film thickness = 0.50 µm) was used as a stationary phase, He (≥99.996 %) as a carrier gas (flow 2.3 mL/min) and N_2 (≥99.996 %) as a reference gas at the detector. The inlet of device was heated to 200 °C and the TCD detector to 250 °C. The column was initially held at 50 °C for

4.75 min, then heated to 220 °C at a rate of 100 °C/min and held at 220 °C for 4.5 min. All samples were diluted with ethanol (≥ 99.9 %, analytical reagent, Merck) with a dilution factor of approximately three to lower the viscosity of the IL to a suitable level for the GC. Calibration of the device was done with ethanol solutions containing 1–15 wt-% water.

Viscosities of [DBNH][OAc] at different water contents (3.6–17.0 wt-%) were determined with a rheometer (Anton Paar MCR 302 modular compact rheometer). Viscosities were measured at 50 and 60 °C with shear rates of 1–100 1/s. The samples were equilibrated for 5 min without mixing before measurement, and after that mixed at 10 1/s for 3 min.

Void volumes of the pipes and valves (V_{tubes}) of the experimental setups described in chapter 6.3.3 were measured by removing the column from the system and pumping a 0.4 g/L Blue Dextran 2000 polymer (GE Healthcare) solution through the setup at 0.88 mL/min. A UV-VIS spectrometer (Agilent Technologies Cary 8454) with a flow-through cell was connected to the system to measure the time needed for the solution to flow through the system. The spectrometer measured the absorbance of the solution at 260 nm at 1 second intervals. Before feeding the Blue Dextran 2000 solution, the system was flushed with purified water and its absorbance (blank) was measured. The polymer solution was then pumped continuously until the measured absorbance levelled out to the level of the feed solution. The void volume was then determined from the measured absorbance data as the inflection point of the breakthrough curve. It should be noted that the void volume of the adapters of the steel column was not measured due to practical issues. This means that the measured void volume for the steel column setup is slightly smaller than in reality, but the error it causes is most likely less than 1 % due to the small volume of the adapters.

The same UV-VIS spectrometer was used to analyse samples from the column washing stage. Absorbance of the samples was measured at 195 nm. Samples were diluted with purified water to keep the absorbances in the linear region (0.3–1.4 absorbance units) of the spectrometer.

Atomic absorption spectrometer (AAS, Thermo Scientific iCE 3000 Series) was used to measure the concentration of K^+ in samples from loading experiments. Measurements were carried out according to SFS 3017 -standard (Suomen Standardisoimisliitto, 1982). Samples

were diluted with purified water and about 0.25 mL of 7 mol/L HNO_3 (65 %, analytical reagent, Merck) was added to every mL of IL to lower the pH of the samples to less than two. Finally, 0.1 mL of 0.75 mol/L CsCl (99.5 %, analytical grade, Merck) solution was added to each sample to limit the ionization of K^+ (Suomen Standardisoimisliitto, 1982). Calibration solutions were made from an atomic spectroscopy standard concentrate (1.00 g/L, Fluka Chemika) by diluting it with purified water to 0.5–2 mg/L solutions. 0.25 mL of 7 mol/L HNO_3 and 0.25 mL of 0.75 mol/L CsCl was added to each calibration solution. A wavelength of 766.5 nm was used for the measurements.

Degradation of type 3A zeolite during equilibrium, kinetic and dynamic experiments was studied with scanning electron microscopy (SEM, Hitachi SU 3500). Zeolite samples were washed with purified water and dried at 170 °C & 40–70 mbar for at least 24 h before analysis. Voltages of 3 and 15 kV were used in the analysis. The elemental composition of each sample was analysed with energy dispersive X-ray spectroscopy (EDS), which was connected to the SEM device.

7 EQUATIONS

To calculate the void volumes of the setups described in chapter 6.3.3, the inflection point of the Blue Dextran 2000 breakthrough curve needs to be calculated. A typical breakthrough curve is presented in figure 14.

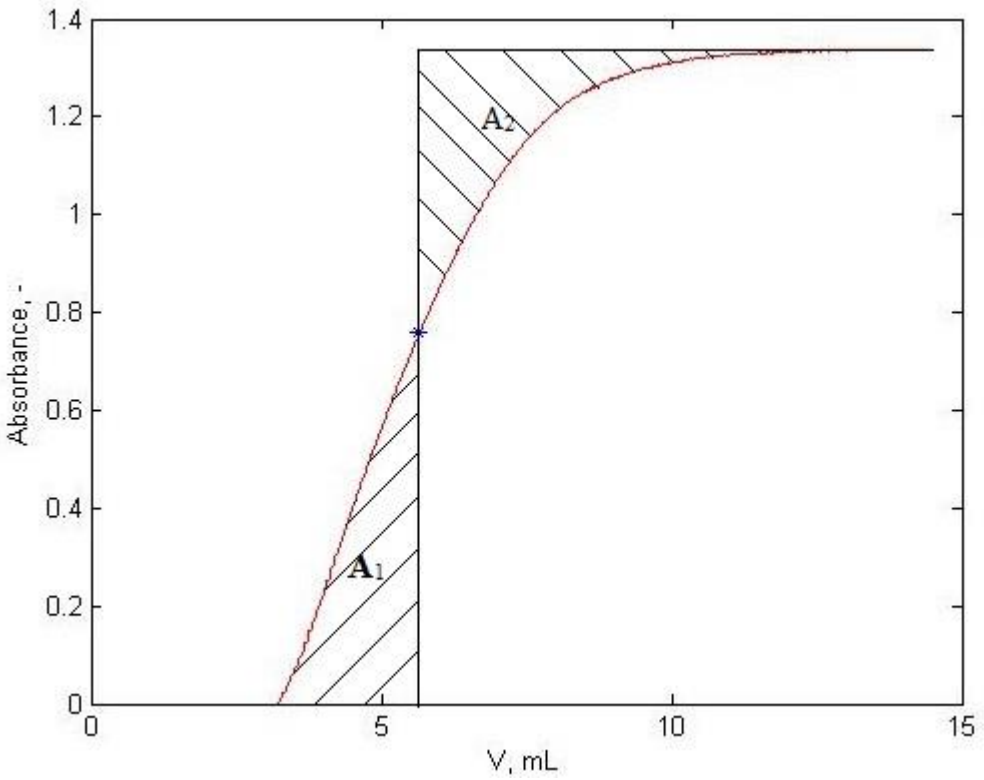

Figure 14 A typical breakthrough curve.

The inflection point of the breakthrough curve is determined as the point where areas A_1 and A_2 in figure 14 are equal. MATLAB was used to calculate the areas with its trapz-function and to determine the inflection point.

Breakthrough curves were constructed from the results of loading experiments by plotting the measured water content ($x_w(H_2O)$) as a function of the feed liquid volume (V_{feed}). To calculate the cumulative concentration ($x_{w,cumulative}(H_2O)$) at the column outlet if all of the liquid is collected into a single fraction, a spline fit ($x_{w,\,spline}(V)$) of the breakthrough curve was first done with MATLAB's csaps, spline and fnxtr -functions. The cumulative

concentration at feed volume V_{feed} was then calculated from the fitted curve according to the following equation:

$$x_{\mathrm{w,cumulative}}(\mathrm{H_2O}) = \frac{\int_0^{V_{\mathrm{feed}}} x_{\mathrm{w,spline}}(V)dV}{V_{\mathrm{feed}}} \tag{2}$$

Integration of the spline fit was done with MATLAB's trapz-function.

The amount of water in a solid separation material (q_e) was calculated from the measured mass of the dry solid (m_{solid}), measured mass of the liquid (m_{IL}) and water contents of the liquid phase before ($x_w(H_2O)_i$) and after contact with the solid ($x_w(H_2O)_e$).

$$q_{\mathrm{e}} = \frac{m_{\mathrm{IL}}\left(1 - \frac{1 - \frac{x_{\mathrm{w}}(\mathrm{H_2O})_{\mathrm{i}}}{100}}{1 - \frac{x_{\mathrm{w}}(\mathrm{H_2O})_{\mathrm{e}}}{100}}\right)}{m_{\mathrm{solid}}} \tag{3}$$

It was assumed that only water was adsorbed onto the separation material. A detailed presentation on the derivation of Eq. (3) is presented in APPENDIX I.

8 RESULTS AND DISCUSSION

8.1 Viscosity and density measurements

Viscosity of [DBNH][OAc] solutions at different water contents (3.6–17.0 wt-%) were measured to see how water affects the viscosity of the IL and to evaluate whether the viscosity was suitable for the HPLC pumps. Measurements were done at 50 and 60 °C to see the effect of temperature on viscosity. The temperatures were chosen based on the melting point of [DBNH][OAc], which was observed to be ~60 °C as dry (without added water) and about 40 °C with 3.7 wt-% water content. Solutions with over 6 wt-% water contents were liquids at room temperature.

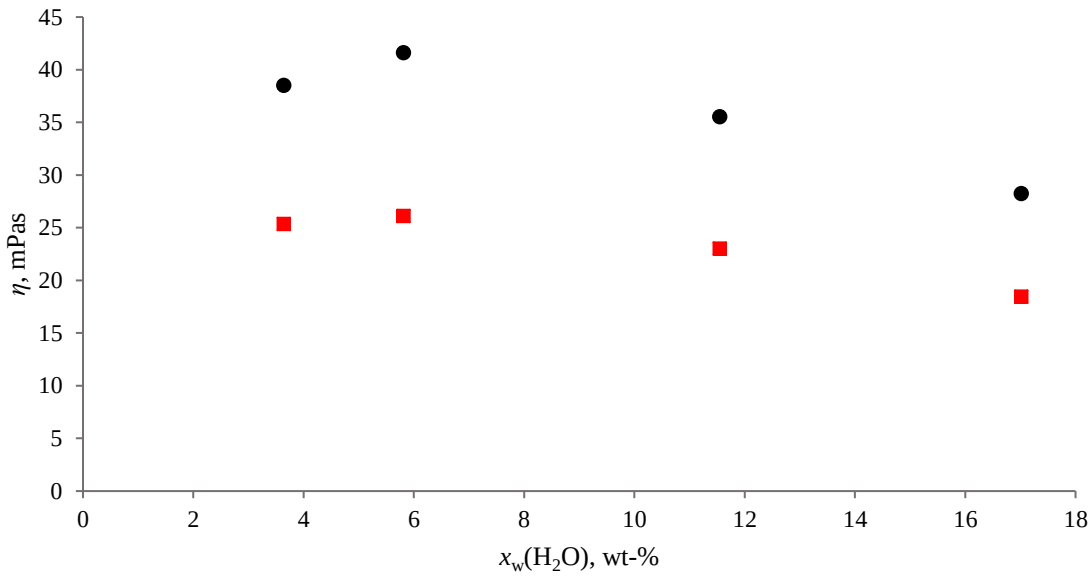

Figure 15 Measured viscosities of [DBNH][OAc] solutions at 50 °C (●) and 60 °C (■).

According to the results (figure 15), both temperature and water content affect the viscosity of [DBNH][OAc]. Increasing water content seemed to lower the viscosity except for the first points (3.6 wt-% water content). A similar phenomenon has been previously observed for [Bmim][OAc] (Yu, et al., 2012). Its viscosity was reported to increase from 139.7 to 440 mPas when water content increased from 0.0746 wt-% to 1.1003 wt-% (Yu, et al., 2012). It was speculated that the reason for such behaviour might be strong interactions between water and $[OAc]^-$ ions (Yu, et al., 2012). However, because in this case there are no more data

points available, the drop in viscosity might be a simple experimental error. For most ionic liquids, increasing water content decreases viscosity (Yu, et al., 2012).

Temperature had a strong effect on viscosity (figure 15), as viscosities at 60 °C were 9.8–13.2 mPas lower than at 50 °C. A slightly non-linear correlation between temperature and viscosity of [DBNH][OAc] has been reported earlier for pure [DBNH][OAc] (Parviainen, et al., 2013). Similar temperature dependence has been reported for other ILs, although the absolute values depend on the IL in question (Yu, et al., 2012).

To further study the physical properties of [DBNH][OAc] at different water contents, densities were measured at three different temperatures (figure 16).

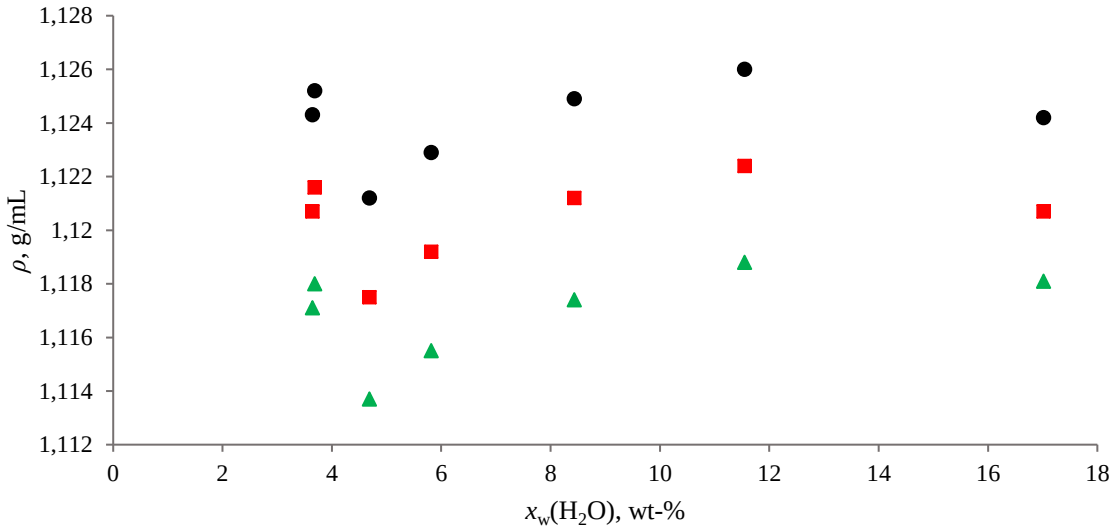

Figure 16 Measured densities of [DBNH][OAc] solutions at 45 (●), 50 (■) and 55 °C (▲).

According to the results (figure 16), there was a minimum for density at about 4.5 wt-% water content. The minimum was roughly at the same point as the maximum in viscosity, although there were more data points for density measurements. This would suggest that there actually might be some interactions between water and the IL that cause such behaviour. There is however some experimental error in the results as can been seen from the first two points in figure 16 (water content ~3.6 wt-%). The two densities were measured

from two different solution having the same water content (measured with GC) and there is a small difference (0.0009 g/mL) in the measured densities.

8.2 Water removal experiments

8.2.1 Equilibrium batch experiments

Equilibrium batch experiments were carried out for organic resins. CS16GC in $[DBNH]^+$ form, Dowex 1x8 in $[OAc]^-$ form and MN200 were tested as they should not change the chemical composition of [DBNH][OAc] as explained in chapter 4.1.7.

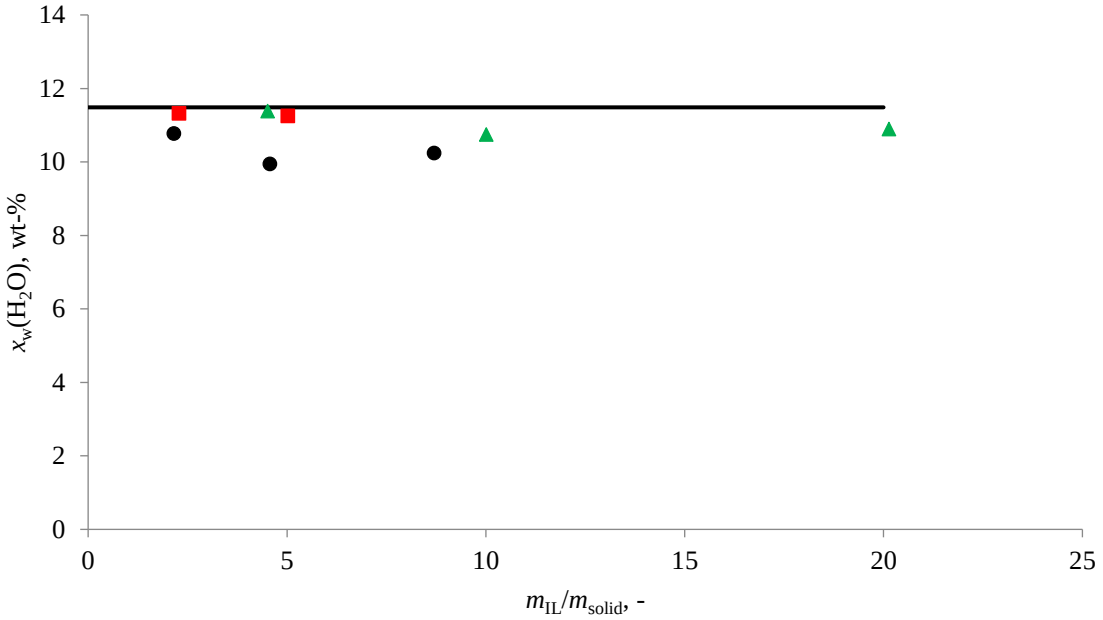

Figure 17 Water content of [DBNH][OAc] before (▬) and after contact with CS16GC in $[DBNH]^+$ form (●), Dowex 1x8 in $[OAc]^-$ form (■) and MN200 (▲). T = 50 °C, N = 250 rpm, $t_{contact}$ = 16 h.

No significant water removal took place with any of the resins at any IL-to-resin mass ratio (figure 17). MN200 was observed to heat up notably when it first came to contact with the IL, which would suggest that some adsorption did take place. However, as there was no change in water content, the resin most likely adsorbed both water and [DBNH][OAc]. Interestingly, no such heating was observed for the ion exchange resins, which would suggest that whatever was adsorbed, prefers the hydrophobic non-functionalized PS-DVB.

A slight change in the colour of the IL was observed for CS16GC and Dowex 1x8. There was some variation in the colour of the delivered IL batches. The IL used in the experiment shown in figure 17 was slightly redder in colour than other batches. The colour is caused by an oxidation product of [DBNH][OAc], but its composition is not known (Hellstén, 2017). The red colour was removed by CS16GC and Dowex 1x8, but not by MN200 (figure 18), which suggests that the oxidation product prefers the hydrophilic ion exchange resins. If the oxidation product was ionic, it could have been changed for $[DBNH]^+$ by the CS16GC resin and for $[OAc]^-$ ions by the Dowex 1x8 resin, which would explain the colour removal.

a) b)

Figure 18 Colour of [DBNH][OAc] solution after contact with a) CS16GC in $[DBNH]^+$ form and b) MN200. Experimental conditions: see caption to figure 17.

As mentioned in chapter 4.1.7, the ionic of form of an ion exchange resin has a major effect on water adsorption capacity (Toteja, et al., 1997). Another factor is the degree of crosslinking as highly crosslinked resins have lower water adsorption capacity compared to resins with a lower degree of crosslinking (Helfferich, 1995). To study the effect of ionic form and degree of crosslinking, batch experiments were carried out with CS9.6GC (4.3 % crosslinking) in $[DBNH]^+$ form, CS16GC (8 % crosslinking) in Na^+ form and CS16GC in Ca^{2+} form as separation materials.

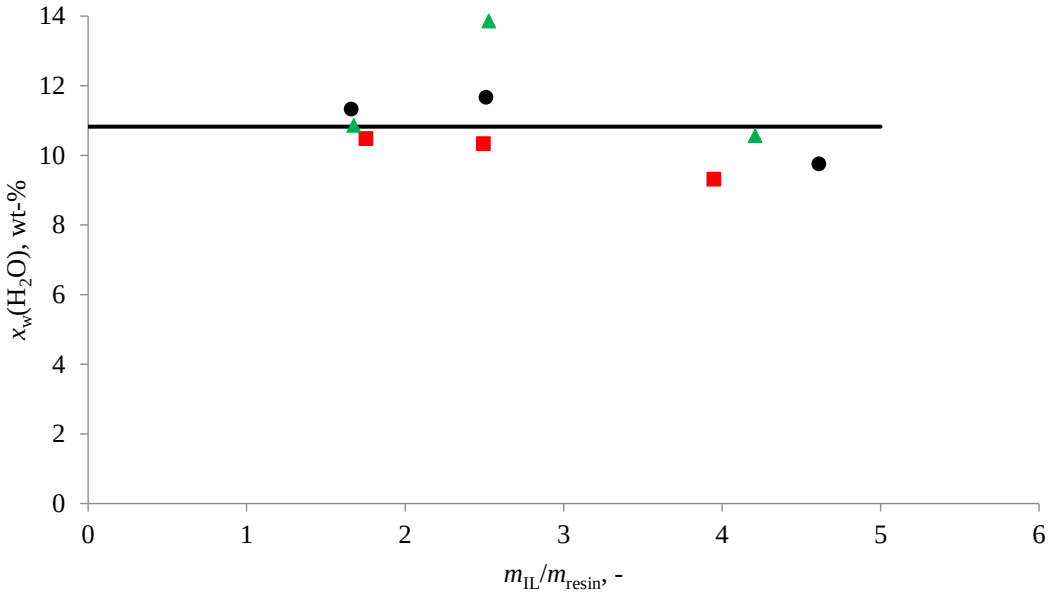

Figure 19 Water content of [DBNH][OAc] before (▬) and after contact with CS9.6GC in $[DBNH]^+$ form (●), CS16GC in Na^+ form (■) and CS16GC in Ca^{2+} form (▲). T = 50 °C, N = 400 rpm, $t_{contact}$ = 4.5 h.

Changing the ionic form or the degree of crosslinking had no effect on water removal (figure 19). Variation in the data points is most likely caused by experimental noise as there is no clear trend in the results. Based on the results of figures 17 and 19, it can be concluded that organic PS-DVB resins cannot separate water from [DBNH][OAc].

To further confirm the result, an experiment with hypercrosslinked MN500 resin in H^+ form was carried out. Conditions and experimental procedure were the same as in the experiment of figure 19. Initial water content of the IL was 10.0 wt-%. Water contents after the experiment were 14.5–16.4 wt-%, which would indicate that [DBNH][OAc] was adsorbed preferentially over water. However, there might also have been other phenomena affecting the results, such as ion exchange between the IL and the resin. In any case, the MN500 resin was not able to remove water from [DBNH][OAc].

The reason for the lack of separation by PS-DVB resins is most likely the low activity of water in [DBNH][OAc] solutions. According to vapor-liquid equilibrium measurements and an NRTL-model, the activity coefficient of water in a [DBNH][OAc] solution containing 10 wt-% water is 0.19–0.26 (Ahmad, et al., 2016). This means that the solution is highly unideal

and water is bound very tightly to the IL (Khan, et al., 2014), which is probably why the resins cannot separate water from [DBNH][OAc].

To study if water could be separated from [DBNH][OAc] by size exclusion, experiments were carried out with molecular sieves (zeolites) of type 3A, 4A and 5A. All of them have the same basic structure with the only difference being the exchangeable ion (Sigma-Aldrich, 2018). Type 4A is the basic form with Na^+ ions as exchangeable ions (Sigma-Aldrich, 2018). Type 3A is made by substituting some of the Na^+ ions with K^+ ions and type 5A by substituting the Na^+ ions with Ca^{2+} ions (Sigma-Aldrich, 2018). The substitution changes the micropore diameter of the zeolite (Sigma-Aldrich, 2018) as can be seen from table V.

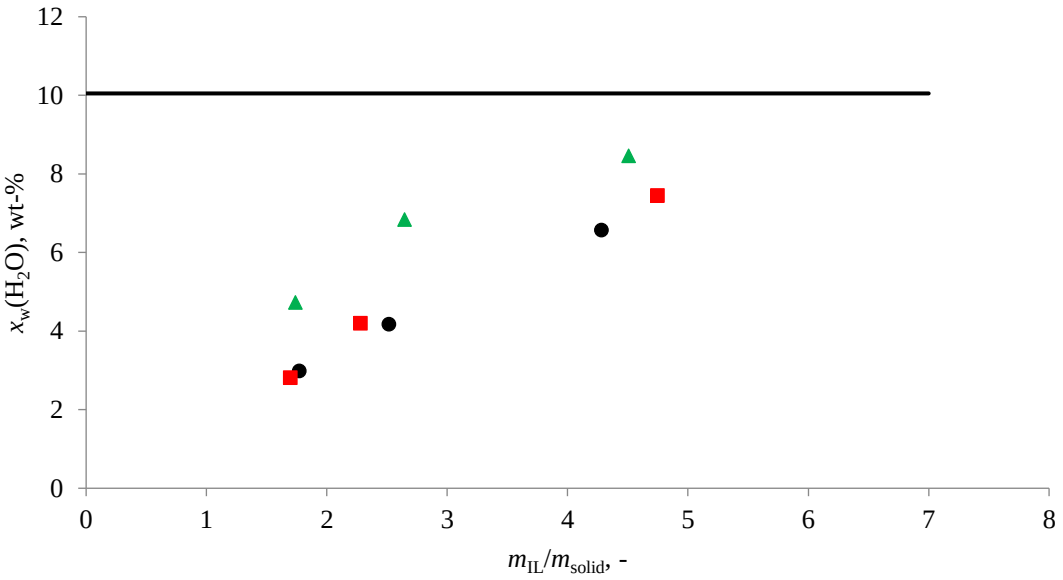

Figure 20 Water content of [DBNH][OAc] before (—) and after contact with zeolite 3A (Alfa Aesar) (●), zeolite 4A (Alfa Aesar) (■) and zeolite 5A (Sigma) (▲). T = 50 °C, N = 400 rpm, $t_{contact}$ = 4.5 h.

All of the type A zeolites were able to lower the water content of [DBNH][OAc] (figure 20). Equilibrium water content was at its lowest in samples with the lowest IL-to-adsorbent mass ratio, which was expected as a larger amount of adsorbent will most likely be able to adsorb more water. Type 3A and 4A reached similar equilibrium water contents whereas the water contents for 5A were roughly 2 %-units higher. This might be due to the larger pores of 5A zeolite, which allowed some [DBNH][OAc] to enter the pores with together with water. The result suggests that the separation of water from [DBNH][OAc] by zeolites is based on size

exclusion. On the other hand, type 5A contains less ions than types 3A and 4A because the monovalent Na^+ and K^+ ions have been substituted with divalent Ca^{2+} ions. This means that there are less ions to hydrate, which might also partly explain the lower water adsorption capacity.

To further study the effect of pore size on water removal performance, equilibrium experiments with type 13X zeolite (10 Å pore diameter) and weakly acidic Al_2O_3 (60 Å pore diameter) were carried out. The hypothesis was that less water should be removed, because they have larger pores than type A zeolites.

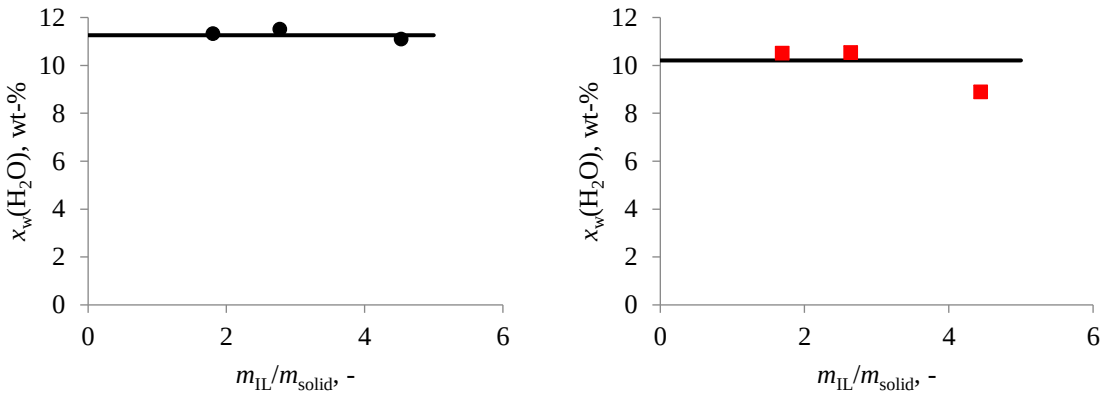

Figure 21 Water content of [DBNH][OAc] before (—) and after contact with zeolite 13X (Sigma) (●) and Al_2O_3 (■). T = 50 °C, N = 400 rpm, $t_{contact}$ = 4.5 h.

No water removal was observed with type 13X zeolite or Al_2O_3 (figure 21). Slight variation in data points is again most likely due to experimental noise. The results confirm that size exclusion is the mechanism by which water is separated from [DBNH][OAc] by zeolites. If there is no size exclusion, there is no separation either, which another reason why organic resins were not able to remove water from [DBNH][OAc]. The structure of organic resins is irregular (Helfferich, 1995) and even the very highly crosslinked MN200 resin has an average micropore diameter of 16 Å (Purolite, 2018), which is much larger than that of type 3A and 4A zeolites.

8.2.2 Kinetic experiments

Kinetic experiments were carried out to study if there are additional phenomena with organic ion exchange resins taking place that were not visible in equilibrium experiments. A weak cation exchange resin (CA16GC) was also tested to see if a resin with a hydrophilic matrix would behave differently to PS-DVB resins. A kinetic experiment was carried out also for type 3A zeolite to evaluate how fast the zeolite and IL solution reach equilibrium at 50 °C.

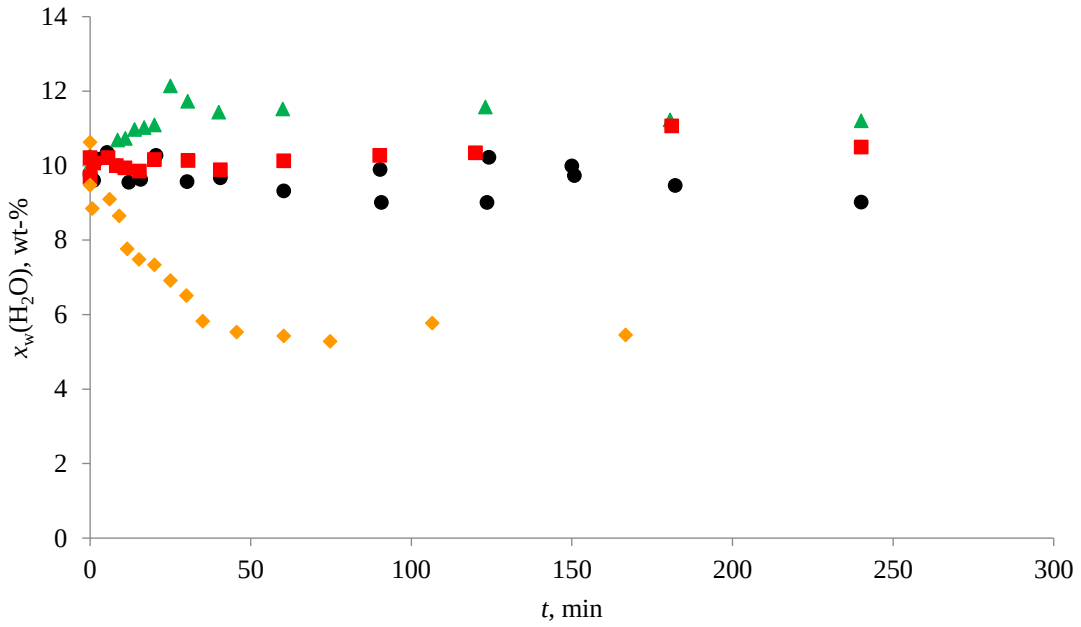

Figure 22 Water content of [DBNH][OAc] during kinetic experiments. ● = CS16GC in $[DBNH]^+$ form (m_{IL}/m_{solid} = 11.4), ■ = CA16GC in $[DBNH]^+$ form (m_{IL}/m_{solid} = 3.0), ▲ = Dowex 1x8 in $[OAc]^-$ form, (m_{IL}/m_{solid} = 2.9), ♦ = zeolite 3A (Sigma, m_{IL}/m_{solid} = 2.0). T = 50 °C, N = 400 rpm.

No water removal was observed for any of three organic ion exchange resins (figure 22). Dowex 1x8 seemed to even increase the water content slightly (from 10.3 to 11.2 wt-%), but this might also be due to experimental error.

Zeolite 3A reached equilibrium with the IL solution in about 60 min. To study if ion exchange between the zeolite and IL took place, concentration of K^+ in the liquid samples was determined with AAS. The K^+ content was found to increase from 1.2 to 2.0 ppm, meaning that very little ion exchange took place. This further confirms that the mechanism

of water removal by zeolites is based purely on size exclusion and ion exchange does not play a major role in the process.

8.2.3 Loading experiments

Based on the results of equilibrium batch experiments, type 3A and 4A zeolites were chosen as separation materials for loading experiments. An experiment with type 3A zeolite (Alfa Aesar) was carried out with the setup described in figure 12. Temperature of the column was kept at 50 °C and flow rate at 1 BV/h (0.57 mL/min). The feed solution was at room temperature (23 °C).

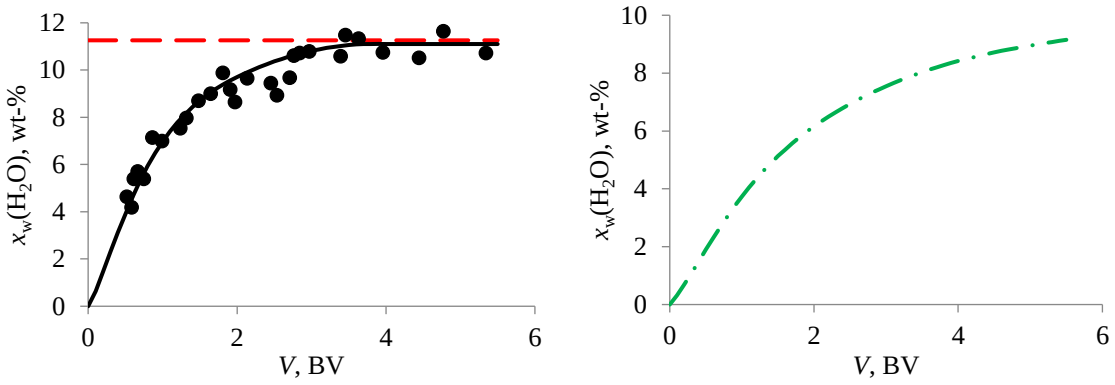

Figure 23 Measured (●), fitted (—) and cumulative (— ·) water content of [DBNH][OAc] at column outlet during a loading experiment. Dashed red line (— —) represents the feed solution. Separation material: zeolite 3A (Alfa Aesar). Experimental setup: see figure 12a. T_{column} = 50 °C, T_{feed} = 23 °C, $\dot{V}$ = 1 BV/h.

Only about 3.4 BV of [DBNH][OAc] containing 11.3 wt-% water could be fed to the column before the concentration at column outlet reached the feed concentration (figure 23). The first samples at 0.5 BV contained already about 4 wt-% water, which is roughly the point where [DBNH][OAc] loses its cellulose dissolution power (Parviainen, et al., 2015). In practice, the water content target should probably be about 3 wt-%. According to the cumulative water content curve, only about 0.8 BV could be fed to the column before 3 wt-% cumulative water content was exceeded.

A typical breakthrough curve should be S shaped (McCabe, et al., 1993), meaning that the concentration of the adsorbed species (here water) should initially be zero and then rise to

the level of the feed solution. It therefore seems that either the water content of the feed solution was too high and the capacity of the zeolite was not high enough to remove water completely, or the flow rate was too high. Too high flow rate would prevent the zeolite from reaching equilibrium with the IL.

It was also observed that as the feed solution was pumped through the dry zeolite bed, some air bubbles remained trapped between the zeolite particles (figure 24). The air bubbles prevented complete contact between the zeolite and the IL, which lowered the effective capacity of the zeolite bed. The bubbles probably also caused disturbance in the liquid flow and some mixing might have taken place. It was found that also the zeolite particles that had been wetted by the liquid would release small air bubbles. Such behaviour was caused by diffusion of air out of the pores of the zeolite and is inevitable if a dry zeolite is used.

Figure 24 Small air bubbles in a glass column during a loading experiment. Separation material: zeolite 3A (Alfa Aesar). Experimental setup: see figure 12a. T_{column} = 50 °C, T_{feed} = 23 °C, $\dot{V}$ = 1 BV/h.

The Dow Chemical Company (2017) suggests air issues could avoided by first pumping a water-free liquid upwards through the bed, which would remove air from the system.

However, in this case the direction of flow was upwards and it is unlikely that a water-free IL would remove any more air from the column than the feed solutions used in this work. Of course, some other liquid could be used for the air removal step, but this would cause chemical consumption, IL contamination and lengthen the processing time. Therefore, no additional measures were taken to remove air from the column.

To find out if a lower flow rate would affect the results, an experiment with a flow rate of 0.17 BV/h (0.10 mL/min) was carried out (figure 25). The column was packed with fresh type 3A zeolite and experimental conditions were kept the same as in previous experiment.

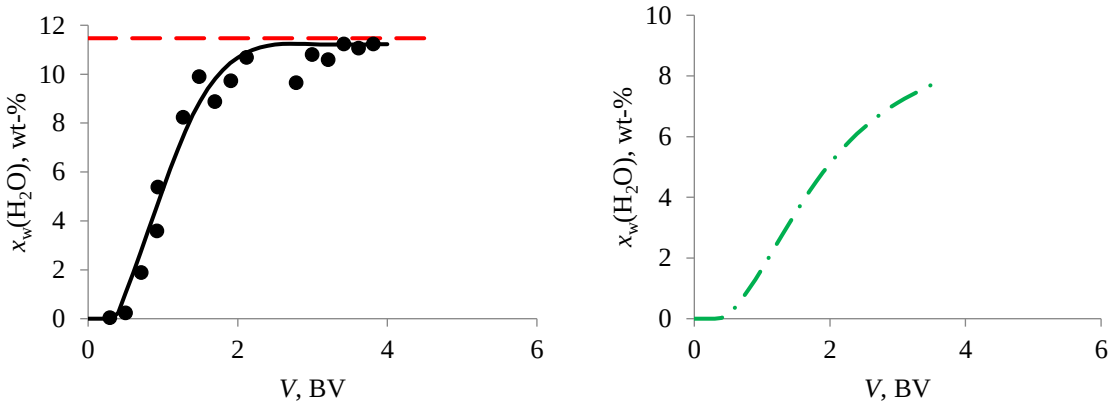

Figure 25 Measured (●), fitted (—) and cumulative (— ·) water content of [DBNH][OAc] at column outlet during a loading experiment. Dashed red line (— —) represents the feed solution. Separation material: zeolite 3A (Alfa Aesar). Experimental setup: see figure 12a. T_{column} = 50 °C, T_{feed} = 23 °C, $\dot{V}$ = 0.17 BV/h.

Lowering the flow rate did change the shape of the breakthrough curve so that it became S shaped (figure 25). However, water content started to increase soon after collecting the first samples (~0.5 BV) and reached the feed concentration at about 2.5 BV. It seems therefore that the flow rate of the first loading experiment (figure 23) was slightly too high since feed water content was reached 0.9 BV faster at the lower flow rate (figure 25). On the other hand, it also seems that the capacity of the zeolite was not sufficient, because even at the lower flow rate only about 1.4 BV of product could be collected before cumulative water content exceeded 3 wt-%.

To enable higher regeneration temperatures (up to 220 °C), the experimental setup was changed to that described in figure 13. The column dimensions were slightly different (d = 2 cm, h_{bed} = 30 cm) compared to the glass column (d = 1.5 cm, h_{bed} = 20 cm). To investigate whether changing the column affects the results, an experiment was carried out with 0.17 BV/h flow rate (figure 26).

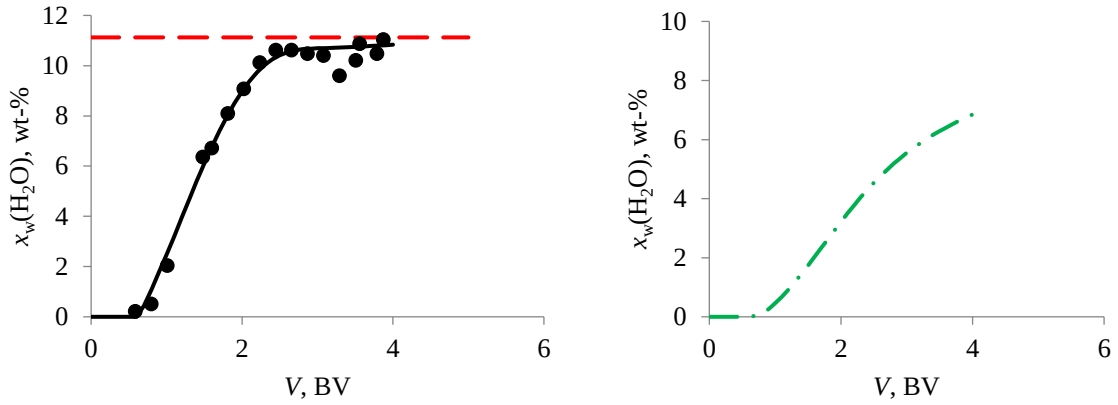

Figure 26 Measured (●), fitted (—) and cumulative (— ·) water content of [DBNH][OAc] at column outlet during a loading experiment. Dashed red line (— —) represents the feed solution. Separation material: zeolite 3A (Alfa Aesar). Experimental setup: see figure 13a. T_{column} = 50 °C, T_{feed} = 23 °C, $\dot{V}$ = 0.17 BV/h.

Changing the column had little to no effect on the results (figure 26). About 2.7 BV of IL could be fed to the column before feed concentration was reached, which is nearly the same as with the glass column (2.5 BV). Cumulative water content target (3 wt-%) was exceeded at 2 BV, which is a bit higher than with the glass column (1.4 BV). The difference is however most likely due to the slightly lower feed water content (11.1 wt-%) compared to that in the glass column experiment (11.5 wt-%). All in all, the separation efficiency with the larger (steel) column was on a similar level with the smaller (glass) column.

To study how the feed water content affects the separation, an experiment with a feed water content of 4.7 wt-% was carried out. Other conditions were kept the same as in the experiments with higher water content feed. The hypothesis was of course that a larger amount of [DBNH][OAc] could be treated before exceeding the cumulative water content target.

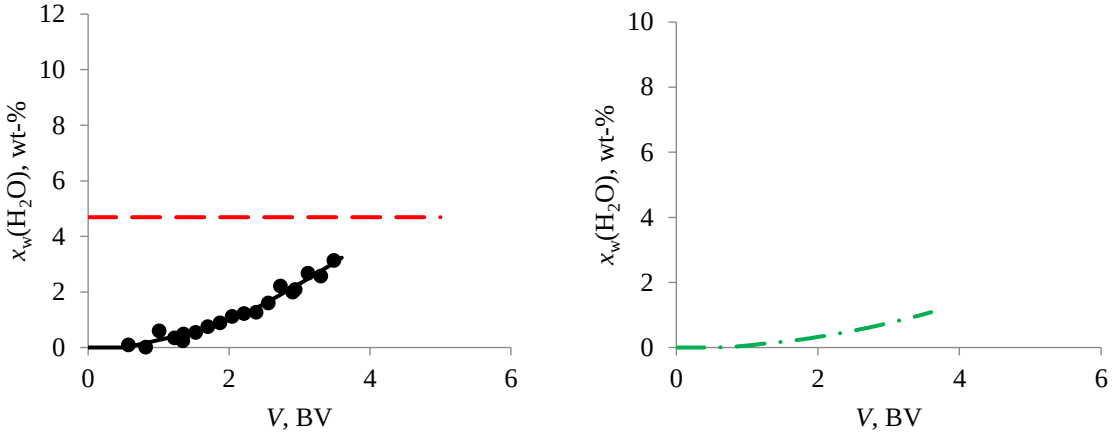

Figure 27 Measured (●), fitted (—) and cumulative (— ·) water content of [DBNH][OAc] at column outlet during a loading experiment. Dashed red line (— —) represents the feed solution. Separation material: zeolite 3A (Alfa Aesar) from previous experiment. Experimental setup: see figure 13a. T_{column} = 50 °C, T_{feed} = 23 °C, $\dot{V}$ = 0.16 BV/h.

Feed water content was not reached in 3.5 BV (figure 27). Cumulative water content also remained very low (about 1.0 at 3.5 BV) which means that a much greater amount of [DBNH][OAc] could be treated compared to experiments with higher feed water content. However, the shape of the breakthrough curve was extended and not very sharp. Even with a lower feed water content, water content at the column outlet started to increase almost immediately after collecting the first samples (0.6 BV).

The extended shape is usually a sign of mass-transfer resistance or dispersion in the system (McCabe, et al., 1993). There might have been some dispersion caused by air bubbles inside the column. However, since the experimental setup remained the same as in the higher feed water content experiment (figure 26), there should not be any additional dispersion. The shape is therefore more likely due to mass-transfer resistance, which seems to be greater at a lower feed water content.

Greater mass-transfer resistance might be partially caused by higher viscosity at lower water contents as depicted in figure 15. Another factor affecting mass-transfer is the activity of water in [DBNH][OAc], which decreases with decreasing water content (Ahmad, et al., 2016). At low activities, the difference in chemical potential of water in [DBNH][OAc] and in zeolite is small, which means that the driving force of adsorption is small. Therefore, the

rate of adsorption is lower at lower water contents, which causes the shape of the breakthrough curve to become extended. If there was no change in mass-transfer resistance, the shape of the breakthrough curve should have been the same with different feed concentrations and only the point where concentration started to increase should have been different (McCabe, et al., 1993).

No signs of increased mass-transfer resistance were observed in the kinetic experiment (figure 22) due to relatively high equilibrium water content (~5.4 wt-%). If higher amounts of the zeolite would have been used, a lower equilibrium water content would have been reached and slowing kinetics might have been visible.

Despite being able to treat well over 4 BV of [DBNH][OAc] at 4.7 wt-% feed water content, the process would still require a large amount of adsorbent due to the very low flow rate (0.17 BV/h). Also in practise, the process would require at least two adsorption columns (Thomas & Crittenden, 1998). One of the columns would be in adsorption and the other in regeneration mode (Thomas & Crittenden, 1998). Although evaporation can lower the water content of [DBNH][OAc] to around 5 wt-%, it is not necessarily desirable as IL losses and decomposition start to increase when evaporating to low water contents (<10 wt-%) (Ahmad, et al., 2016). On the other hand, using a separate adsorption process just to lower the water content from 5 to 3 wt-% does not seem very attractive either. It is therefore clear that the adsorption process must be able to handle higher flow rates and higher feed water contents.

To increase the mass-transfer rate in the system and to allow for higher flow rates and feed water contents, experiments at 80 °C were carried out. Flow rate was set to 0.95 BV/h and feed water content to 8.2 wt-%. Feed vessel was heated to 60 °C to lower the viscosity of the feed solution so that it could be pumped more easily.

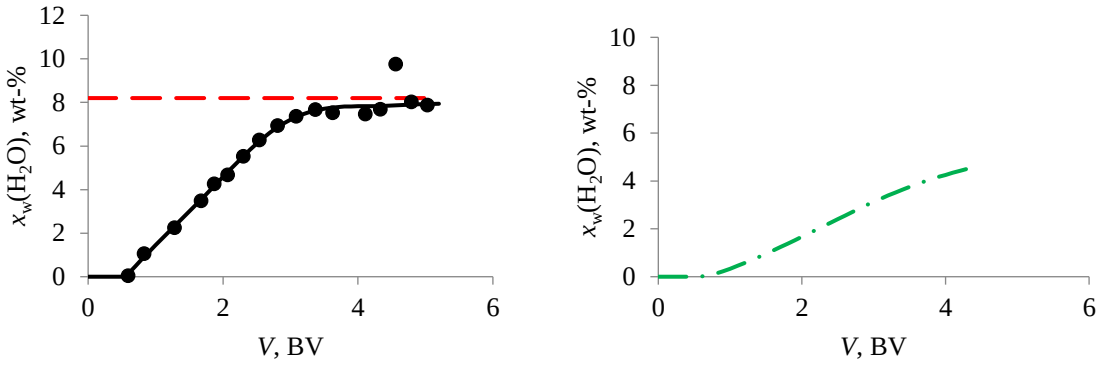

Figure 28 Measured (●), fitted (—) and cumulative (— ·) water content of [DBNH][OAc] at column outlet during a loading experiment. Dashed red line (— —) represents the feed solution. Separation material: zeolite 3A (Alfa Aesar). Experimental setup: see figure 13a. T_{column} = 80 °C, T_{feed} = 60 °C, $\dot{V}$ = 0.95 BV/h.

When comparing the results at 80 °C (figure 28) to those at 50 °C (figure 23), it is clear that increasing temperature improved water removal as the first sample (0.6 BV) was virtually water-free. Of course, different feed water contents (8.2 vs. 11.3 wt-%) make it difficult to compare the results directly. Nonetheless, about 2.9 BV of the feed solution could be treated at 80 °C before exceeding the cumulative water content target.

To find out if higher flow rates could be used, an experiment at 80 °C and 2 BV/h was carried out. The feed water content was increased slightly from 8.2 to 8.9 wt-%.

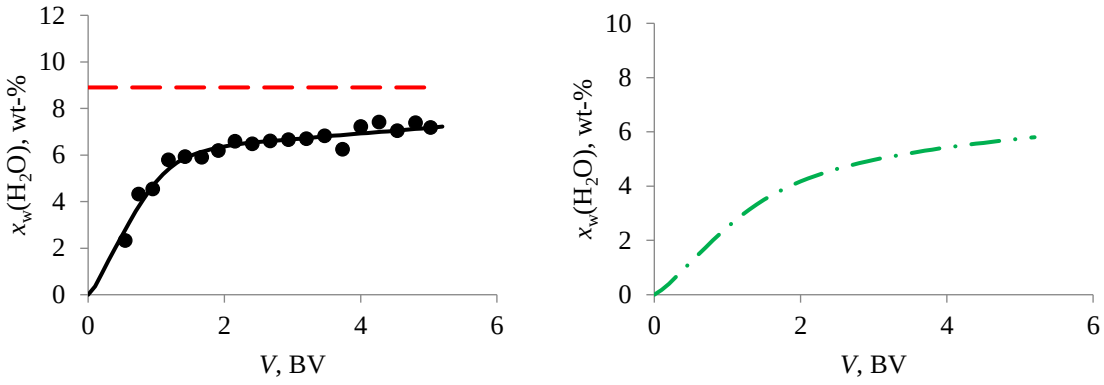

Figure 29 Measured (●), fitted (—) and cumulative (— ·) water content of [DBNH][OAc] at column outlet during a loading experiment. Dashed red line (— —) represents the feed solution. Separation material: zeolite 3A (Alfa Aesar). Experimental setup: see figure 13a. T_{column} = 80 °C, T_{feed} = 60 °C, $\dot{V}$ = 2 BV/h.

At 2 BV/h, the first sample at 0.5 BV already contained some water (2.3 wt-%) and water content at the column outlet increased quite quickly (~1.3 BV) to about 5.8 wt-% (figure 29). After that, the water content increased slowly towards the feed concentration, which however was not achieved even after 5 BV. Only about 1.2 BV could be collected before exceeding the cumulative water content target. It is therefore clear that 2 BV/h was too high a flow rate.

The shape of the breakthrough curve (figure 29) was very different to that at 1 BV/h flow rate (figure 28). It was also different compared to the curve in the experiment at 50 °C and 1 BV/h with the glass column (figure 23). It seems that at a higher flow rate, the residence time of IL in the column was too short and only partial water removal took place before the IL started to come out of the column. This probably caused the quick increase in water content at the beginning of the breakthrough curve. On the other hand, because only partial water removal had taken place, even the first parts of the zeolite bed had not become saturated with water and there was still some capacity left in the zeolite. Therefore, some water removal took place along the column long after the first part of feed solution had come through, which explains the slowly rising tail of the breakthrough curve.

Because equilibrium batch experiments suggested that type 4A zeolite should have similar water removal performance (figure 20), an experiment with type 4A zeolite was carried out.

Temperature of the column was kept at 80 °C, flow rate at 1 BV/h and feed water content was 7.1 wt-%.

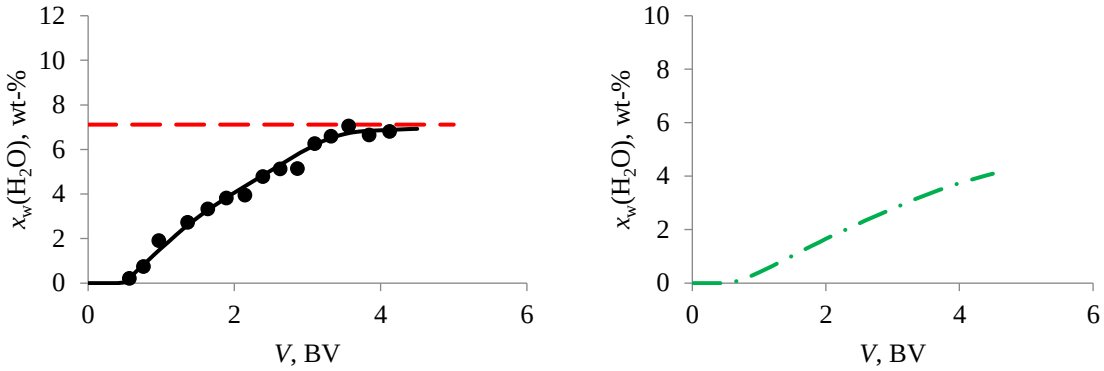

Figure 30 Measured (●), fitted (▬) and cumulative (▬ ·) water content of [DBNH][OAc] at column outlet during a loading experiment. Dashed red line (▬ ▬) represents the feed solution. Separation material: zeolite 4A (Alfa Aesar). Experimental setup: see figure 13a. T_{column} = 80 °C, T_{feed} = 60 °C, $\dot{V}$ = 1 BV/h.

Slightly different feed water contents in experiments with type 3A zeolite (figure 28) and type 4A zeolite (figure 30) make it difficult to compare the results in detail. However, it seems that as predicted by the equilibrium batch experiments, there is little difference between the two zeolite types. The shape of the breakthrough curve is very similar for both zeolites and the amount of feed liquid that can be handled is very similar (3.2 BV for type 4A and 2.9 BV for type 3A).

In addition to increasing temperature, another way to increase mass transfer rate in adsorption is to increase the interfacial area between solid and liquid phases. Smaller solid particles provide more interfacial area, which is why type 4A zeolite with an average particle diameter of 0.4–0.8 mm was tested. All other conditions were kept the same as in the experiment shown in figure 30.

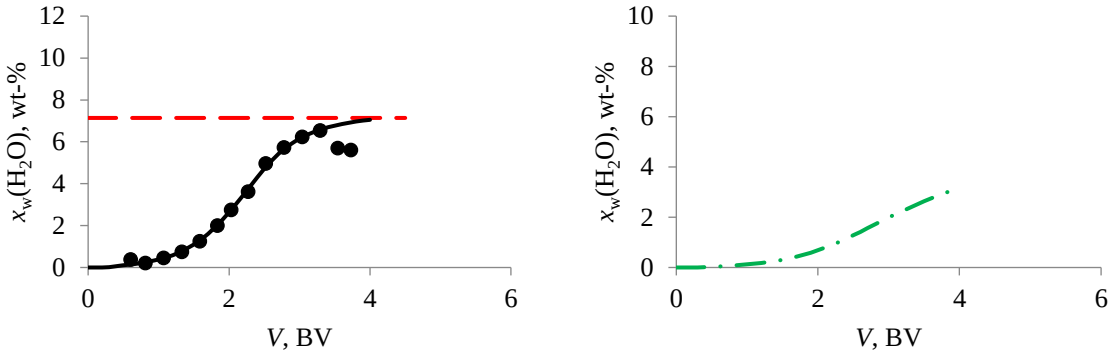

Figure 31 Measured (●), fitted (▬) and cumulative (▬ ·) water content of [DBNH][OAc] at column outlet during a loading experiment. Dashed red line (▬ ▬) represents the feed solution. Separation material: zeolite 4A (Alfa Aesar, 0.4–0.8 mm particles). Experimental setup: see figure 13a. T_{column} = 80 °C, T_{feed} = 60 °C, $\dot{V}$ = 1 BV/h.

The breakthrough curve profile was clearly S-shaped and sharper with the smaller particle size (figure 31) than with the larger particle size type 4A zeolite (figure 30). The sharper profile means that 0.7 BV more (3.9 BV in total) of the feed solution could be treated compared to the larger particle size zeolite. The better performance is due to enhanced mass transfer rate as explained earlier. The breakthrough curve was still somewhat extended, and the water content started to increase almost immediately after the first two samples (0.8 BV), which has been observed in all of the experiments. This supports the theory that adsorption of water becomes slower at lower water contents. Of course, mixing due to air bubbles might have caused some dispersion in the system, which also contributes to the extended shape.

8.2.4 Regeneration experiments

Removing water from IL (loading) is just one step in the adsorption process. After the desired amount of water has been removed, the adsorbent must be regenerated. In theory, the loaded zeolite could be regenerated simply by heating it to a high-enough temperature, because both water and [DBNH][OAc] will evaporate when sufficient heat is applied (Parviainen, et al., 2013).

A preliminary regeneration experiment was conducted with the zeolite from the experiment of figure 25 and with the setup presented in figure 12b. The glass column was heated to 70

°C and air was blown through the column at 1 bar and 540 sccm for 23 h. A small amount of brown liquid was accumulated in the column outlet tubes and about 1.1 g of clear liquid was collected in the cold trap. It was concluded that 70 °C was not enough to regenerate the zeolite, which is consistent with results in presented literature (Gabrus, et al., 2015). It has been reported that the minimum temperature for removing water from type 3A and 4A zeolites is 130 °C (Gabrus, et al., 2015).

It was found out already in the equilibrium batch experiments that heating the zeolite after contact with the IL caused the zeolite particles to turn dark brown. Also, [DBNH][OAc] exposed to such regenerated zeolite would turn brown. Such discoloration is not desirable as it may also affect the colour of the Ioncell-F fibres, which is a very important factor in textile fibre production (Parviainen, et al., 2015). The colour is most likely caused by a degradation product of [DBNH][OAc] as was speculated by Parviainen et al. (2015).

To avoid degrading [DBNH][OAc] and causing colour issues, it was decided that [DBNH][OAc] should be washed away from the column before heating. Water was used as a washing agent and it was pumped through the column after loading phase. Other chemicals, such as methanol or ethanol, could also be used, but they were not studied in this work. The advantages of water are that it is readily available in large amounts and it is non-toxic. The clear drawback on the other hand is the high heat of vaporization (~2260 kJ/kg of water at 1 atm) (CRC Press, 2017) resulting in high energy consumption.

To study if washing the zeolite would remove colour issues and to test the steel column setup, an experiment with the setup described in figure 13b was carried out. After a loading experiment (figure 26), purified water was pumped through the column at 50 °C and 3 BV/h for 2 h. After washing, air was blown through the column for 7 min at 1.5 bar and 530 sccm to remove free liquid from the column. The column was then heated to 150 °C while air was blown at 1.5 bar and 540 sccm. Blowing was continued for 16 h, after which the column was removed and weighed.

It was discovered that the column was actually slightly lighter after the regeneration cycle than it had been immediately after packing the zeolite (0.83 g difference). It seems therefore that the zeolite was completely free of water and that the zeolite might have degraded

slightly. Of course, it is also possible that the zeolite was not completely dry when it was packed into the column, but it seems unlikely since the zeolite was dried at a high temperature (170 °C) and under reduced pressure (40–70 mbar) before packing.

The colour of the regenerated zeolite was observed to be similar to fresh, unused zeolite. No [DBNH][OAc] discoloration was observed either when it was contacted with the well-washed zeolite.

To study how much the zeolite should be washed, a washing experiment was carried out after loading fresh type 3A zeolite with 4 BV of [DBNH][OAc] at 8.5 wt-% water content. Water was pumped through the steel column at 6 BV/h (9.42 mL/min) and samples were collected for 30 s (~4.7 mL) at 1 BV intervals. Absorbance of each sample was then measured with a UV-VIS device as described in chapter 6.4. Absorbance was assumed to be caused by some component of [DBNH][OAc] and it was used to estimate the amount of [DBNH][OAc] in each sample.

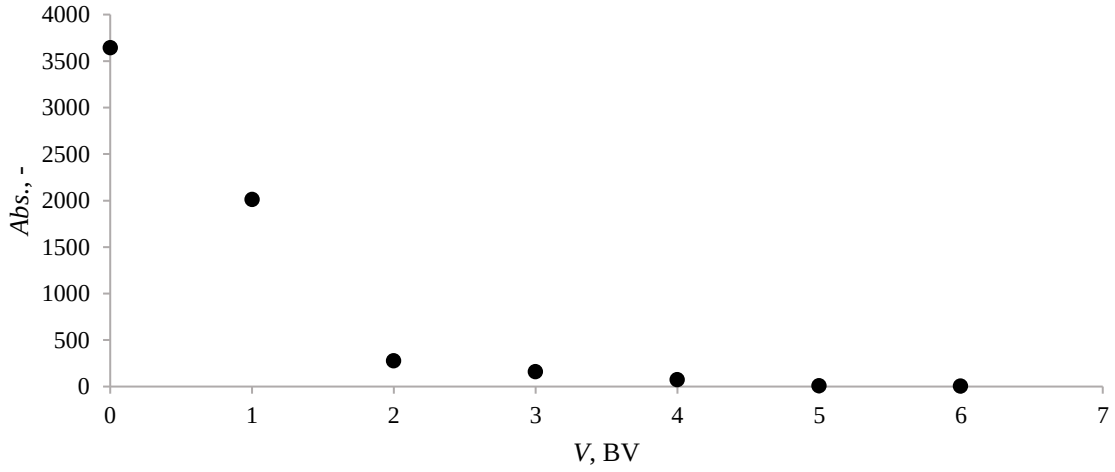

Figure 32 Measured absorbance at 195 nm at column outlet during a washing experiment with water. Separation material: zeolite 3A (Alfa Aesar). Experimental setup: see figure 13a. T_{column} = 80 °C, T_{feed} = 23 °C, $\dot{V}$ = 6 BV/h.

About 2 BV of water was able to lower the absorbance from 3645 to 276 (figure 32). After 2 BV, the absorbance continued to decrease, although at a much slower rate. The absorbances of the last two samples (5 and 6 BV) were very close to each other (7.5 and 6.8)

which indicates that all [DBNH][OAc] was removed after 5 BV. From a practical point of view, it seems that 2 BV of water should be able to remove most of the IL from the column.

The absorbance of the feed liquid that had been used in the loading phase was also measured. Its absorbance was 403, which is about nine times lower than the absorbance of the first sample in the washing experiment. The result suggests that the colour of the IL solution intensified as it went through the column. Because the zeolite was fresh, the colour is most likely caused by thermal degradation of [DBNH][OAc]. Therefore, the absorbance cannot be used as direct measure of [DBNH][OAc], but rather as a measure of colour. This makes it more difficult to estimate the amount of washing water needed to remove the IL. In any case, 5 BV should be enough to remove practically all IL components from the column.

The flow rate used in the washing stage was quite high to keep the duration of the washing stage short. If two columns are used in parallel, regeneration of one column must be done while the other is in loading stage to achieve a continuous overall flow (Thomas & Crittenden, 1998). In this case, if the flow rate in the loading phase is 1 BV/h and about 4 BV of IL is collected, the duration of the loading phase is 4 h. If the zeolite is then washed with 5 BV of water (50 min at 6 BV/h), there is 3h 10 min left for heating and cooling the column back to loading temperature.

To study the heating (drying) stage more closely, a new drying experiment was carried out. Fresh type 4A zeolite (0.4–0.8 mm particles) was packed into the steel column and the column was weighed. Water was then pumped through the column at 6 BV/h for 1 h at 80 °C. After water pumping had been stopped, the column was weighed again. The experimental setup was then switched to regeneration configuration (figure 13b) and air was blown through the column at 2 bar. Flow rate of air was initially below the detection point of the rotameter. Free liquid (not bound to zeolite) came out after 5 min of blowing. The column was weighed again, and weighing was continued at regular intervals.

Heating to 220 °C was started after free liquid had come through, and after about 25 min the oven had reached 220 °C. Air flow at the beginning of heating was 130 sccm and after 30 min the flow increased to 4590 sccm. The increased flow was caused by the weighing procedure, which included removing the column from the setup. There seemed to some

pressure build-up in the column due to evaporating water, which caused flow resistance. The pressure was let out of the column as it was removed, which is why after reconnecting the column, about 35 times higher air flows were achieved. This makes the results a bit inaccurate as the flow rate of air changed so dramatically, but at least some conclusions can be made.

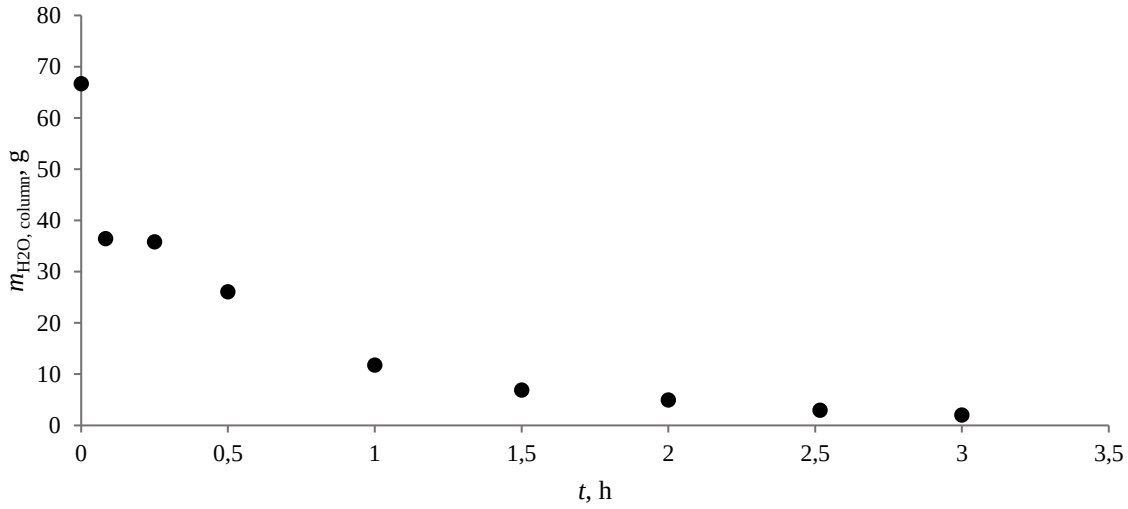

Figure 33 Amount of water inside the column during a drying experiment. Separation material: zeolite 3A (Alfa Aesar). Experimental setup: see figure 13b. T_{column} = 80–220 °C, $\dot{V}_{air}$ = 130–4590 sccm.

Immediately after water pumping had been stopped, the column contained 66.7 g of water (figure 33). About 30 g of it was free water (in liquid form), which was removed in 5 min. After that, next 24.7 g of water was removed in 1 h. After 1h, the rate of water removal started to drop and only 9.7 g of water was removed in the next 2 h. It can be concluded that complete water removal takes a lot of time (>4 h), but most of the water (92.5 % including free water) is removed in already in 2 h.

After the drying experiment, the hatch of the oven was opened and the column was let to cool down. The oven reached 80 °C in 18 min after which the column was let to cool for another 7 min. The total time for cooling was therefore 25 min.

When the 25 min cooling time is taken into account, about 2 h 45 min is left for the actual blowing/heating step. Based on the results (figure 33), less than 2.5 g of water should be left

in the column after such step. The mass of the dry zeolite in the column was 68.2 g, meaning that 0.04 g(H_2O)/g(dry zeolite) would be left in the column after the regeneration cycle. Based on the equilibrium batch experiments (figure 20), type 4A zeolite will adsorb about 0.15 g(H_2O)/g(dry zeolite) at 50 °C (calculated with equation (3)). The capacity is similar to what has been reported in literature for moisture adsorption from air by type 3A zeolite (0.19 g(H_2O)/g(dry zeolite) at 100 % humidity & 50 °C) (Lin, et al., 2015). The capacity is reported to be slightly lower at 80 °C (0.17 g(H_2O)/g(dry zeolite)) (Lin, et al., 2015).

In any case, when a new loading phase begins, there will be something between 19 and 24 % of the maximum water uptake capacity used by the residual water from previous regeneration cycle. Therefore the amount of IL that can be treated will be lower than in the loading experiments (figure 31) and the time for the loading step will be shorter.

If it is assumed that 3.5 BV of the feed IL solution can be treated with the conditions from figure 31, the loading phase will take 3.5 h. If the column is then washed for 50 min (5 BV) with water and the cooling time is assumed to be 25 min, 2 h 15 min is left for the actual blowing/heating stage. According to figure 33, about 3.5 g of water should be left in the column after such regeneration cycle. If another cycle was then carried out, even less IL could be collected. It seems therefore that the time for regeneration might be too short to maintain the process in a steady state.

However, it should be noted that the results of the drying experiment were somewhat distorted by the weighing of the column. Weighing caused the column to temporarily lose pressure and temperature, which affected the results. The drying time is also quite sensitive to setup, meaning that different tubing or column adapters will probably give different results. Therefore, not very detailed calculations should be made based on the results presented above.

8.2.5 Cyclic experiment

A cyclic experiment was carried out to test how the process would actually behave in cyclic operation. The experiment was done as a continuation to the experiment presented in figure 31. After the loading phase, the column was washed with water at 6 BV/h for 1 h while heating the column to 95 °C. Heating to 220 °C was then started and air was blown through the column at 2 bar and 41–14400 sccm. Oven heater was switched off and the hatch opened after 2h 15 min and air blowing was stopped after 2 h 36 min. The tubing between the column and the feed valve (see figure 13) was then blown for 3 min and the tube between the column and the fraction collector was blown for 1 min to remove water from the tubes. All blowing was stopped after 2h 40 min from the beginning of heating.

A new loading was then done with the same feed liquid and at the same conditions as in figure 31. The volume of the loading was 3.5 BV (3 h 30 min). The column was then washed for 50 min at 6 BV/h and while heating to 95 °C. The heating step was then done in the same manner as described above.

After the heating step was completed, another loading was done with the same feed liquid and conditions as in the previous loadings. The volume of the loading was 3.3 BV (3 h 20 min). To illustrate the time-scale of cyclic operation, a temperature profile of the cyclic experiment is presented in figure 34.

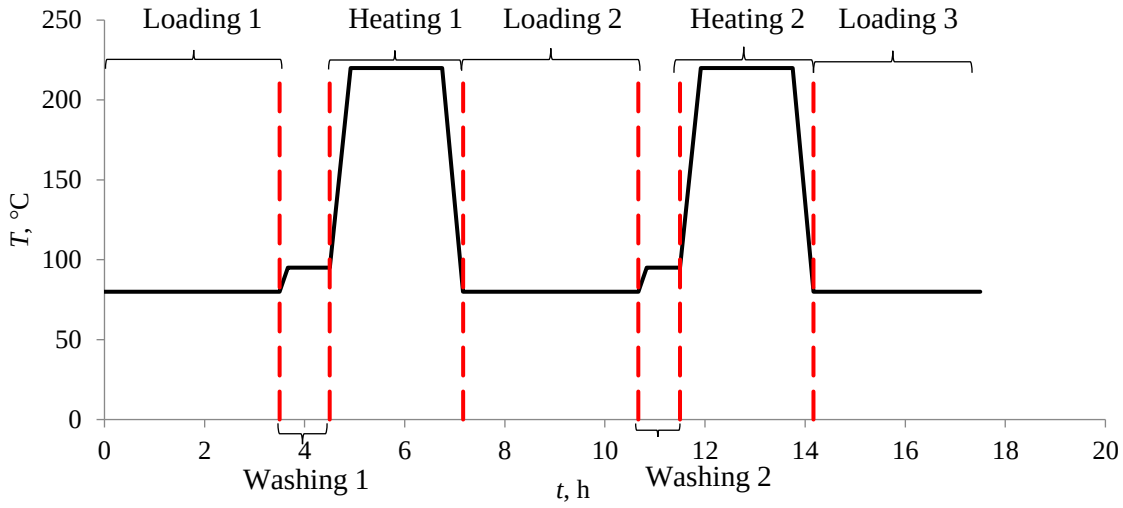

Figure 34 Column temperature during a cyclic experiment. Separation material: used zeolite 4A (Alfa Aesar, 0.4–0.8 mm particles). Experimental setup: see figure 13. $\dot{V}$ = 1 BV/h.

The 1st regeneration step (washing + heating) was slightly longer (10 min) than the 1st loading step, which is why the 2nd washing step was shortened by 10 min. This way, the process could be operated continuously with two columns.

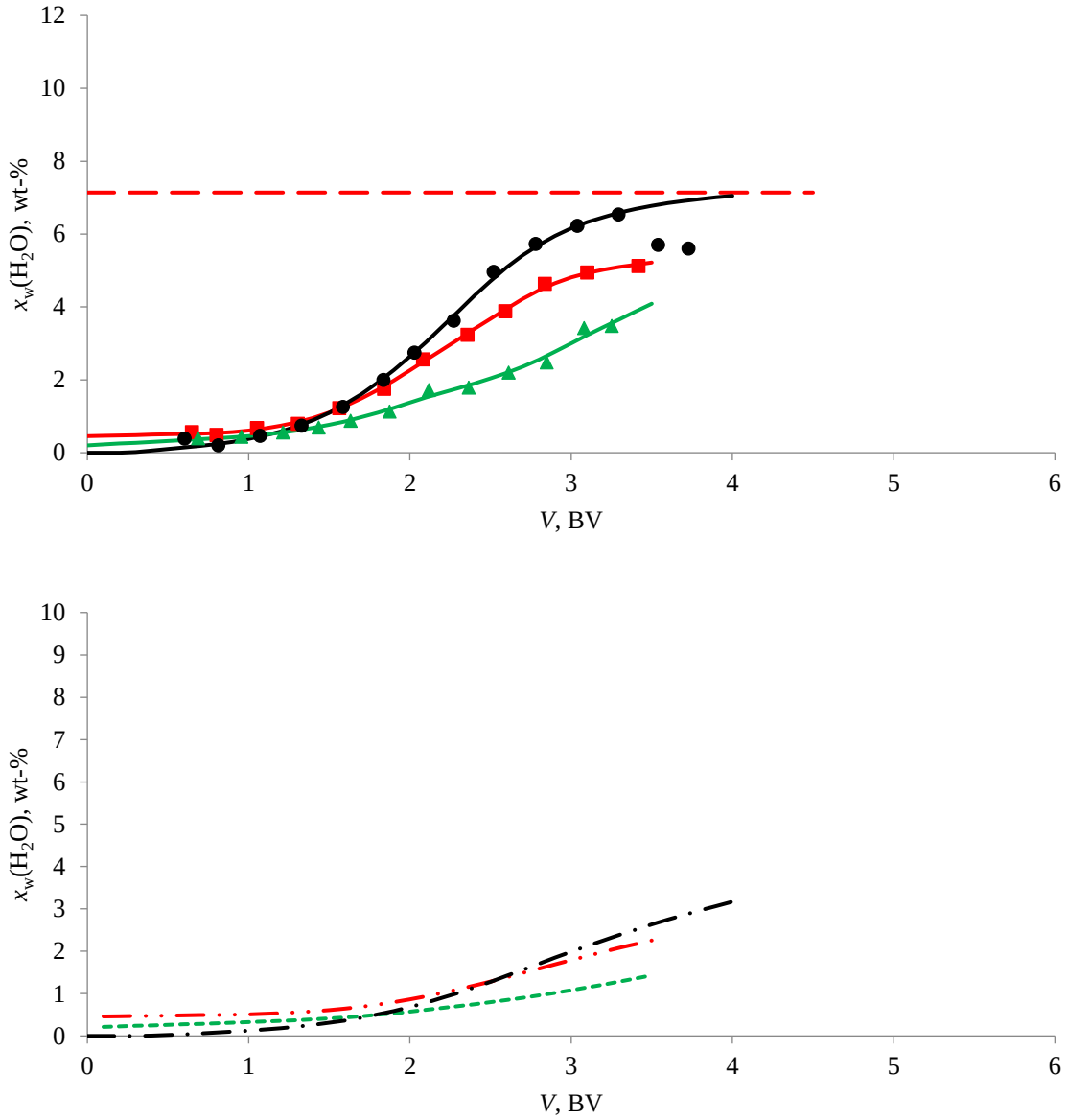

Figure 35 Measured (solid markers), fitted (solid lines) and cumulative (dotted lines) water content of [DBNH][OAc] at column outlet during 1st loading (●, ▬ ·), 2nd loading (■, ▬ ··), and 3rd loading (▲, ▪▪) of a cyclic experiment. Dashed red line (▬ ▬) represents the feed solution. Separation material: used zeolite 4A (Alfa Aesar, 0.4–0.8 mm particles). Experimental setup: see figure 13a. T_{column} = 80 °C, T_{feed} = 60 °C, $\dot{V}$ = 1 BV/h.

The breakthrough curves for each loading were different (figure 35). The breakthrough curve of the 2nd loading had a similar S-shape as the curve of the 1st loading, but the water content in the end was different. In the 1st loading, the water content was 6.5 wt-% at 3.3 BV, but in the 2nd loading water content at 3.4 BV was only 5.1 wt-%. Therefore, also the cumulative

water content was slightly lower in the 2nd loading (2.2 wt-% at 3.4 BV) compared to the 1st loading (2.5 wt-% at 3.4 BV).

On the other hand, the first two samples from the 2nd loading contained slightly more water (0.5–0.6 wt-%) compared to the first two samples of the 1st loading (0.2–0.4 wt-%). The difference is small, but it might suggest that there was some residual water left in the column after the 1st regeneration step as predicted by the drying experiment (figure 33). However, due to the inaccuracies related to water content determination by GC, not very detailed conclusions can be made.

The breakthrough curve of the 3rd loading had a different shape compared to the two previous ones and water content remained at an even lower level. At 3.3 BV, the water content was only 3.5 wt-%, which is about 1.5 %-units lower than in the 2nd loading and 3 %-units lower than in the 1st loading.

The results would suggest that lower water contents are reached as the adsorption cycle is repeated. Such behaviour could be explained by some water-binding component being adsorbed onto the zeolite during loading. The adsorbed component could then have caused more water molecules to be attracted onto the zeolite in the next loading step.

However, a more likely reason for the decreasing water contents is in the feed solution. As mentioned earlier, the same feed solution was used for all three loadings. The solution was kept at 60 °C when it was pumped to keep the viscosity of the solution at a low-enough level. Because the duration of the experiment was long (17 h 30 min), the feed vessel was also heated for a long time (10 h 50 min). As the level of the feed solution came down in the feed vessel, some condensed vapor was observed on the walls of the feed vessel. The condensed vapor suggests that some part of the feed liquid evaporated. If the evaporated substance was water, the water content in the liquid phase would have lowered, which would explain the lowering water contents.

To study if water evaporation did take place in the feed vessel, a sample of the condensed vapor was taken and analysed. The sample contained 12.2 wt-% water, which is 5.1 %-units higher than the water content of the feed solution. It seems therefore that some water did

evaporate away from the feed solution. The evaporated substance was not pure water, but most likely a mixture of DBN and water. This conclusion is supported by the fact that neutral DBN has been observed to evaporate first from [DBNH][OAc] when it is distilled (Ahmad, et al., 2016; Ostonen, et al., 2016b). In this case, it seems that the evaporating DBN took some water with it away from the liquid phase. Because the feed water concentration was measured before the 1st loading, the actual water content in the other two loadings was probably somewhat lower.

Due to water evaporation, direct comparison between the three consecutive loadings cannot be made. However, there seems to be no dramatic change in the water removal performance of the zeolite in the first three loadings. Very low water contents (<0.6 wt-%) were achieved initially in all three loadings, which also suggests that there was little water left in the zeolite after regeneration. It therefore seems that cyclic operation is possible, although more studies are needed to see if the performance of the zeolite changes over a longer period.

The process would be easier to operate, and continuous flow with would be easier to achieve, if the capacity of the adsorbent was higher. Therefore, alternative adsorbents should be explored and studied. Finding suitable adsorbents might be difficult, because as shown in this work, water removal from [DBNH][OAc] is based on size exclusion and the pore size of the adsorbent needs to be <5 Å. Due to the very small pore size requirement, there are few alternative adsorbent candidates. Some suitable alternatives might be found from metal-organic frameworks (MOFs), which are said to have higher surface areas than zeolites and good thermal and mechanical stability (Küsgens, 2010). Many of them have pores between 5 and 35 Å in diameter (Farusseng, et al., 2009) and their pore size is said to be adjustable (Küsgens, 2010). However, they are not widely available and finding a MOF with a suitable pore size and sufficient chemical stability might be difficult.

8.2.6 Stripping experiments

Stripping was studied as an alternative water removal method to the adsorption process. The idea of stripping was to remove water from [DBNH][OAc] by blowing dry air through the IL. The technique has been applied earlier for water removal from ILs with nitrogen as the stripping gas (Ren, et al., 2010). Air is usually much cheaper and more readily available,

which is why it was chosen as the stripping gas in this case. The glass column setup presented in figure 12b with a few modifications was used for the stripping experiments. The column was emptied from any solid separation material and filled partially with [DBNH][OAc] and air flow was switched to upwards flow. Otherwise, the setup remained the same.

The stripping experiment was done by adding 36.2 g (37.0 mL) of [DBNH][OAc] at 10.6 wt-% water content to the column (figure 36). There was 4.3 cm of empty space above the liquid in the column to allow the liquid to expand as air was bubbled through it. The column was heated to 50 °C. Air was blown through the column at 1 bar and 24–30 sccm. Samples from the liquid phase were taken at regular intervals by stopping the air flow, removing the top of the column and pulling out 0.5 mL of the liquid with a pipette.

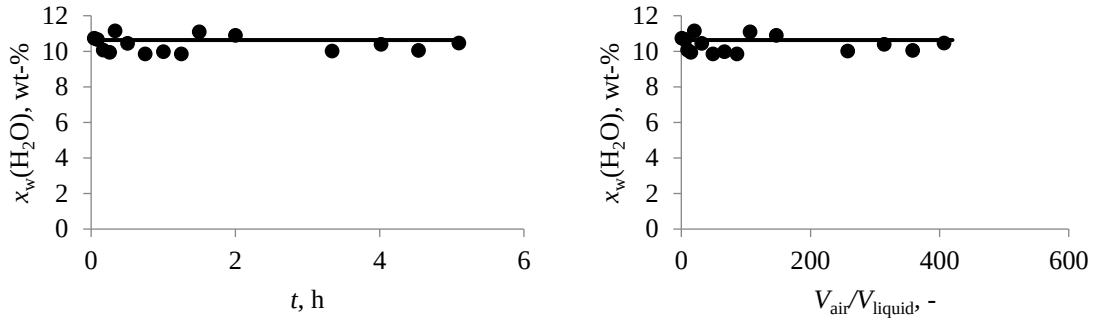

Figure 36 Water content of [DBNH][OAc] initially (▬) and during a stripping experiment (●). Experimental setup: see figure 12b. T = 50 °C, $\dot{V}_{air}$ = 24–30 sccm. V_{air} is in sccm and V_{liquid} in mL.

No water removal took place during the experiment (figure 36). One reason might be insufficient contact between air and the IL, because the setup was very simple and there was no mixing or packing material inside the column. However, a more likely reason for the lack of water removal was the low air flow. Higher flows could not be used, because liquid would end up in the column outlet if the flow was increased.

To allow for higher air flows, another stripping experiment was carried out with the same setup, but with less IL in the column. 9.0 g (10.1 mL) of [DBNH][OAc] at 14.2 wt-% water content was added to the column, which meant that there was 15.4 cm of empty space in the

column. Conditions were otherwise the same as in the previous experiment, but air was blown through the column at 540 sccm.

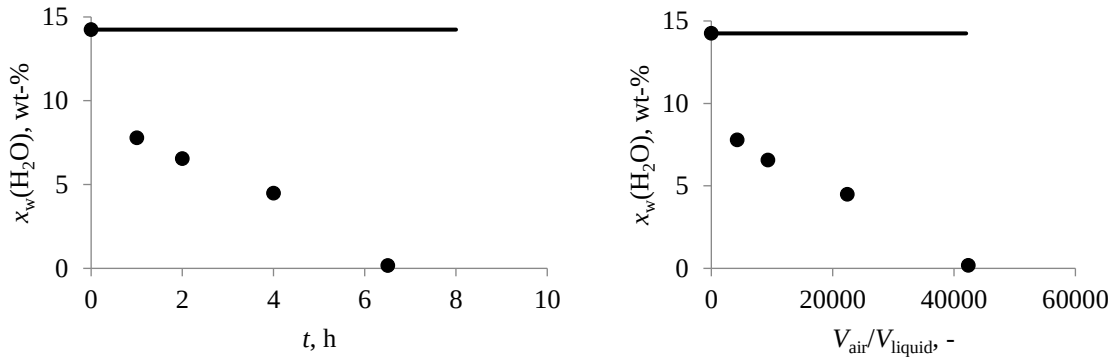

Figure 37 Water content of [DBNH][OAc] initially (▬) and during a stripping experiment (●). Experimental setup: see figure 12. T = 50 °C, $\dot{V}_{air}$ = 540 sccm. V_{air} is in sccm and V_{liquid} in mL.

A higher air flow was able to remove water from [DBNH][OAc] (figure 37). After 6.5 h of blowing, the water content had lowered to 0.17 wt-%. Interestingly, the water content lowered almost linearly apart from the first two points. If water removal was limited by the activity of water (vapor pressure), the shape of the water removal curve would probably have been similar to figure 32. As the water content becomes lower, the activity of water in [DBNH][OAc] also becomes lower (Ahmad, et al., 2016). Therefore, one would expect faster water removal at high water contents (>10 wt-%) and slower water removal at low water contents (<5 wt-%). Such behaviour was not observed, which suggests that there was something else limiting the water removal.

The limiting factor was most likely mass-transfer between gas and liquid phases. As mentioned earlier, the setup was very simple and contact between the two phases was not optimized. Also visually some of the air bubbles in the IL were quite large (d ~ 1 cm), which means that the surface area between the two phases was not very large.

Despite being able to remove water almost completely, a lot of air was used compared to the amount of liquid (V_{air}/V_{liquid} ~ 42 000). This makes the process seem unattractive as blowing such high air volumes would require a large amount of energy. On the other hand, in a more

sophisticated setup with better contact between the phases, significantly less air would most likely be required.

In addition to high air demand, another potential issue with stripping is the discoloration of [DBNH][OAc]. The colour gradually changed from yellow to brown during the stripping (figure 38).

a) b)

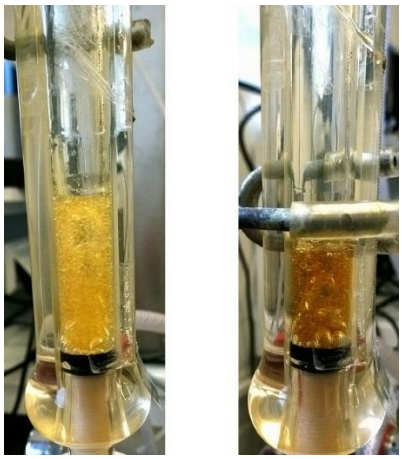

Figure 38 Colour of [DBNH][OAc] during a stripping experiment. a) after 30 min b) after 6 h. T = 50 °C, $\dot{V}_{air}$ = 540 sccm.

The colour change was probably caused by oxidation of [DBNH][OAc]. Therefore, air might not be the optimal stripping gas because it contains 21 % oxygen, which can oxidize [DBNH][OAc]. On the other hand, some drops of brown liquid were also found in the column outlet tubes. It therefore seems that in addition to water, some part of the IL ended up in the stripping gas. The brown substance was probably DBN or some degradation product of it, because it is the evaporative component of [DBNH][OAc] (Ahmad, et al., 2016; Ostonen, et al., 2016b). If DBN evaporated, the chemical composition of the liquid phase changed, and it is likely that its cellulose dissolving power was affected too. However, no analysis of the chemical composition of the liquid phase in the column or in the outlet tubes was made.

To avoid changing the chemical composition of [DBNH][OAc], the stripping gas could be saturated with the evaporative component (DBN). This way, the amount of DBN in the liquid phase would not decrease during stripping as it would not be able to move to the gas phase.

It might also lower the stripping gas demand, because DBN would make the gas phase more polar and thus attract water molecules more strongly from the liquid phase. On the other hand, due to excess DBN in the system, some DBN from the gas phase might move to the liquid phase. This would change the DBN:HOAc-ratio of the liquid phase, which might then affect the cellulose dissolving power of the IL.

Even if the stripping gas was saturated with DBN, oxidation might still be an issue if air is used as the stripping gas. DBN would also need to be recovered from the gas stream and reused to minimize chemical consumption. Recovering could be done by a cold trap, which would condense DBN away from the gas phase. However, using a cold trap might be difficult, because the boiling point of DBN (95–98 °C at 100 kPa) (Sigma-Aldrich, 2016) is very close to the boiling point of water (100 °C). Another option would be to use molecular sieves, which would capture water selectively away from the gas stream.

8.3 SEM-EDS studies

SEM-EDS analyses were carried out to see if the surface structure or elemental composition of the zeolites changes when they are in contact with [DBNH][OAc]. All samples were the same type 3A zeolite (Alfa Aesar, 1–2 mm). Samples that had been in contact with the IL were compared to a fresh, unused sample.

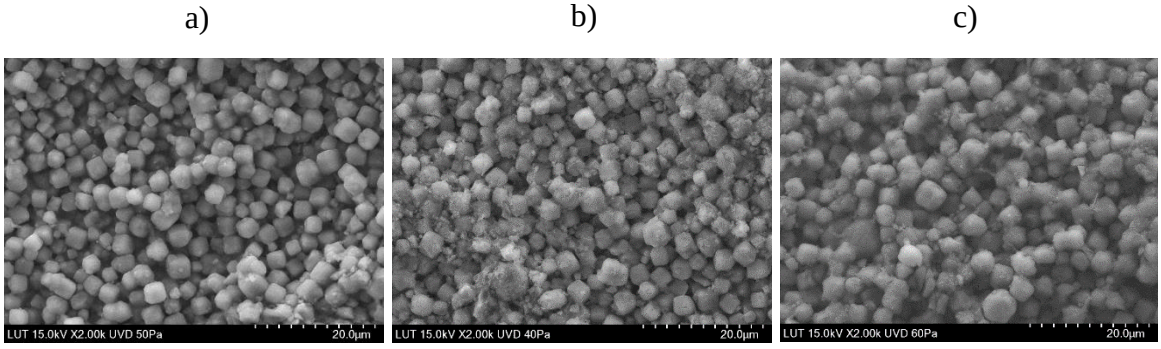

Figure 39 SEM images of type 3A zeolite samples. a) fresh zeolite, b) zeolite used in seven loading experiments, c) zeolite used in a kinetic experiment. U = 15 kV, detector = UV.

Some surface degradation was observed in the samples that had been in contact with [DBNH][OAc] compared to fresh zeolite (figure 39). It might have been caused by small particles coming off the surface, which has been reported for silica and alumina adsorbents

in ILs (Clare, et al., 2008). Degradation was observed for samples subject to low mechanical stress (figure 39b) as well as samples subject to high mechanical stress (figure 39c). Therefore, the degradation may not be purely mechanical abrasion.

EDS analysis was carried out to see if changes in the elemental composition had taken place. If there was some residual IL in the zeolite it was expected to show up as nitrogen and carbon in the EDS analysis.

Table VI Elemental composition of type 3A zeolite samples as determined by EDS. a) fresh zeolite, b) zeolite used in seven loading experiments, c) zeolite used in a kinetic experiment. U = 5 kV.

Element	Fraction in sample a), wt-%	Fraction in sample b), wt-%	Fraction in sample c), wt-%
C	4.6	5.7	4.4
N	-	1.1	-
O	41.4	43.2	41.5
Na	4.5	3.5	4.8
Mg	2	1.8	1.6
Al	11.7	12	12.9
Si	22.4	23.6	23.9
P	0.6	-	-
K	11.4	7.5	9.9
Fe	1.4	1.7	1

No significant changes in elemental composition were observed (table VI). The Si/Al ratio was also similar in all of the samples (1.90–1.96), which suggests that there indeed was no change in the chemical composition of the zeolite. Small amounts of carbon, magnesium and iron were observed in all the samples, although zeolites should not contain them (Helfferich, 1995). The elements are present most likely due to the clay binder, that is used to produce granulated zeolite particles (Helfferich, 1995). Small amount of nitrogen was found in sample b), which suggests that some IL was left in it due to insufficient washing.

To see if a longer contact time would cause more severe degradation, 5.1 g of fresh type 3A zeolite was kept in contact with a [DBNH][OAc] solution containing 8.6 wt-% water for 34 days at 60 °C. The solution and the zeolite were in a 50 mL glass bottle, which was occasionally (~twice a week) gently turned over. The idea was to keep mechanical stress to a minimum.

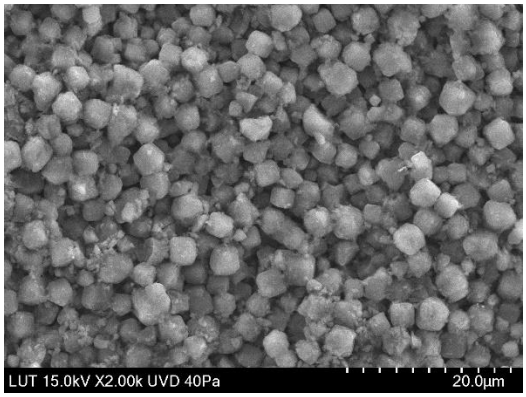

Figure 40 SEM image of type 3A zeolite sample that has been in contact with [DBNH][OAc] for 34 days. U = 15 kV, detector = UV.

Some surface degradation was observed also for the zeolite sample after a long contact time with the IL (figure 40). It therefore seems that the surface degradation is caused by a combination of mechanical and chemical stress.

However, even the long contact time sample was able to remove water. The water of content of the IL solution where the zeolite was kept had lowered from 8.6 wt-% to 3.9 wt-%, which means that the water content of the zeolite was 0.23 g(H_2O)/g(dry zeolite) according to equation (3). The water content is quite high, because as mentioned earlier, the maximum water vapor adsorption capacity for type 3A zeolite is reported to be 0.19 g(H_2O)/g(dry zeolite) at 50 °C (Lin, et al., 2015). In any case, it can be concluded that minor degradation of the zeolite in [DBNH][OAc] does take place, but the zeolite still retains its water adsorption capacity. Further studies should be conducted on whether degradation and the possible zeolite particles cause issues in the Ioncell-F process.

9 CONCLUSIONS

Removal of water from a superbase-based ionic liquid (IL) was studied in this work. Background of the work was in the production of cellulose-based textile fibres by a novel process called Ioncell-F. The process is based on direct dissolution of cellulose by an ionic liquid solvent called [DBNH][OAc]. The dissolution and fibre spinning part of the process is well-established and the quality of the produced fibres is high. A less-studied part of the process is solvent recycling and reuse, which is crucial for the economic feasibility of the process. Several impurities and substantial amounts of water need to be removed from the IL before it can be reused in the process. Because the composition of most impurities is not known at the present moment, the main focus of this work was on water removal.

Most of the water can be removed by evaporation, but at low water contents (<10 wt-%), the IL starts to decompose and evaporate. Therefore, another technique is needed to lower the water content of the IL to a low-enough level (<4 wt-%) to restore its cellulose dissolving power.

This work consisted of a literature part and an experimental part. General properties of ionic liquids and the Ioncell-F process were first introduced in the literature part. Methods to separate water, organic and inorganic impurities from ionic liquids were reviewed next and finally some solvent recycling concepts for Ioncell-F were introduced.

Two different water removal techniques were developed in the experimental part. One of the techniques is based on adsorption and the other on stripping with air. The main focus was on developing the adsorption-based process. Adsorbent screening was done first with equilibrium batch experiments and kinetic experiments, and the adsorbents with best water removal capacity were chosen for dynamic adsorption experiments. The effect of temperature, feed solution water content, flow rate and regeneration on water removal were studied in the dynamic experiments. A cyclic experiment was also carried out to demonstrate how the process would be operated in an industrial environment. Scanning electron microscopy (SEM) was used to study surface degradation of the adsorbents during the experiments.

In addition to adsorption studies, simple stripping experiments were also carried out to see if water could be removed by stripping with air. The stripping setup or conditions were not optimized.

It was found out that organic ion exchange resins, non-functionalized PS-DVB adsorbents, aluminium oxide, or type 13X zeolites were not able to remove water from [DBNH][OAc]. Type 3A, 4A and 5A zeolites (molecular sieves) on the other hand were able to remove water from the IL. Types 3A and 4A showed similar performance whereas type 5A had a smaller water adsorption capacity. It was concluded that the water removal by zeolites was based purely on size exclusion and only adsorbents with a pore diameter of <10 Å could be used.

Type 3A and 4A adsorbents were chosen for dynamic adsorption experiments and were found to behave similarly. The kinetics of water adsorption were found to be slow and low flow rates had to be used in the experiments. It was speculated that as the IL propagates through the adsorption column, the mass transfer resistance increases, which decreases the rate of adsorption. The phenomenon was thought to be caused by the decreasing water content of the IL. Increasing temperature and using a smaller particle size zeolite were found to enhance the kinetics and to increase the mass transfer rate.

The capacities of the zeolites were found to be low for the purpose and frequent regeneration was required to reach low-enough water contents. A separate washing step was also required to remove the IL from the column before the actual regeneration. It was however demonstrated that a continuous total flow might be achievable with two columns in parallel.

Minor zeolite surface degradation was observed by SEM in samples that had been in contact with the IL. However, no significant change in water removal capacity was observed when the zeolites were reused.

Stripping with air was studied briefly and it was demonstrated to remove water almost completely from [DBNH][OAc]. However, large amounts of air were needed, some part of the IL evaporated, and the IL developed a dark brown colour during the process. The evaporated part was thought to be mostly DBN, and the discoloration was thought to be caused by IL oxidation. It was speculated that a more advanced experimental setup with

better mixing would decrease the air demand. It was also speculated that IL oxidation could be avoided by using an oxygen-free gas as the stripping gas, and that IL evaporation could be avoided by saturating the stripping gas with the evaporative component (DBN). Cold traps and molecular sieves were suggested as methods for removing water from the used stripping gas.

As a simpler process, stripping is a more attractive option for water removal compared to adsorption. However, if the issues mentioned above cannot be solved, adsorption might also be a viable option. The benefits of adsorption are the wide availability and low price of the zeolite adsorbents, relatively simple operation and equipment, and moderate processing conditions in the loading step. The major drawback on the other hand is the relatively low capacity of the zeolite, which requires regeneration after about 3–5 BV of feed depending on the feed solution water content. The zeolite also requires washing after loading, which means that in addition to dehydrated [DBNH][OAc], the process produces 5–6 BV of dilute [DBNH][OAc] per cycle. The washing liquid needs to be either returned to the evaporation stage, or the IL recovered in a separate process step.

The performance of the adsorption process could be improved by using smaller particle size zeolites, which would produce a sharper breakthrough curve and maybe allow higher flow rates and/or lower temperatures to be used. Lower temperature (<70 °C) during loading would be desirable to avoid degradation and discoloration of the IL. However, a smaller particle size zeolite would still have the same capacity as the larger particle size zeolites, which is why alternative adsorbents should be studied.

Of course, other techniques such as pervaporation should not be forgotten nor should the fact that water is just one component that needs to be removed from [DBNH][OAc]. Ideally, organic or inorganic impurities would be removed simultaneously with water, which would decrease the number of process steps. Therefore, studies with a more representative feed solution should be made and the behaviour of impurities studied.

The most important results of this work were that water can be removed from [DBNH][OAc] by at least two mechanisms: size exclusion and stripping. This knowledge can be used in the

future to design new types of separation processes. The mechanisms are also most likely applicable for other ionic liquids and other processes utilising them.

References

Abu-Eishah, S. I., 2011. Ionic Liquids Recycling for Reuse. In: S. T. Handy, ed. *Ionic Liquids - Classes and Properties.* Rijeka: InTech, p. 239–272.

Ahmad, W. et al., 2016. Feasibility of thermal separation in recycling of the distillable ionic liquid [DBNH][OAc] in cellulose fiber production. *Chemical Engineering Research and Design,* Volume 114, p. 287–298.

Anthony, J. L., Maginn, E. J. & Brennecke, J. F., 2001. Solution Thermodynamics of Imidazolium-Based Ionic Liquids and Water. *Journal of Physical Chemistry B,* Volume 105, p. 10942–10949.

Belyakova, L. D., Schevchenko, T. I., Davankov, V. A. & Tsyurupa, M. P., 1986. Sorption of Vapors of Various Substances by Hypercrosslinked "Styrosorb" Polystyrenes. *Advances in Colloid and Interface Science,* Volume 25, p. 249–266.

Bentivoglio, G. et al., 2006. Cellulose Processing with Chloride-Based Ionic Liquids. *Lenzinger Bericthe,* Volume 86, p. 154–161.

Binder, J. B. & Raines, R. T., 2010. Fermentable sugars by chemical hydrolysis of biomass. *Proceedings of the National Academy of Sciences of the United States of America,* Volume 107, p. 4516–4521.

Blanchard, L. A. & Brennecke, J. F., 2001b. Recovery of Organic Products from Ionic Liquids Using Supercritical Carbon Dioxide. *Industrial & Engineering Chemistry Research,* Volume 40, p. 287–292.

Blanchard, L. A., Gu, Z. & Brennecke, J. F., 2001a. High-Pressure Behavior of Ionic Liquid/CO2 Systems. *Journal of Physical Chemistry B,* Volume 105, p. 2437–2444.

Bulota, M. et al., 2016. The effect of hydration on the micromechanics of regenerated cellulose fibres from ionic liquid solutions of varying draw ratios. *Carbohydrate Polymers,* Volume 151, p. 1110–1114.

Caes, B. R. et al., 2013. Simulated Moving Bed Chromatography: Separation and Recovery of Sugars and Ionic Liquids from Biomass Hydrolysates. *ChemSusChem,* Volume 6, p. 2083–2089.

Clare, B. R. et al., 2008. Purification or contamination? The effect of sorbents on ionic liquids. *Chemical Communications,* p. 2689–2691.

Clare, B., Sirwardana, A. & MacFarlane, D. R., 2009. Synthesis, Purification and Characterization of Ionic Liquids. In: B. Kirchner, ed. *Ionic Liquids.* Berlin: Springer, p. 1–40.

CRC Press, 2017. Entahalpy of Vaporization. In: J. R. Rumble, ed. *CRC Handbook of Chemistry and Physics, 98th Edition (Internet Version 2018).* Boca Raton: CRC Press/Taylor & Francis.

Davis, J. H., 2004. Task-Specific Ionic Liquids. *Chemistry Letters,* Volume 33, p. 1072–1077.

Davis, M. E., 1991. Zeolites and Molecular Sieves: Not Just Ordinary Catalysts. *Industrial & Engineering Chemistry Research,* Volume 30, p. 1675–1683.

de Dardel, F., 2016. *Ion Exchange Basics.* [Online] Available at: http://dardel.info/IX/IX_Intro.html [Accessed 20 September 2017].

Deng, Y. et al., 2009. Phase Diagram of [Amim]Cl + Salt Aqueous Biphasec Systems and Its Application fo [Amim]Cl Recovery. *Journal of Chemical & Engineering Data,* Volume 54, p. 2470–2473.

Dibble, D. C. et al., 2011. A facile method for the recovery of ionic liquid and lignin from biomass pretreatment. *Green Chemistry,* Volume 13, p. 3255–3264.

Ebner, G., Schiehser, S., Potthast, A. & Rosenau, T., 2008. Side reactions of cellulose with common 1-alkyl-3methylimidazolium-based ionic liquids. *Tetrahedron Letters,* Volume 49, p. 7322–7324.

El-Sayed, M. M. H., Hani, H. A. & Sorour, M. H., 2014. Polymeric Ion Exchangers for the Recovery of Ions from Brine and Seawater. *Chemical Engineering & Process Techniques,* Volume 2, p. 1020.

Enders, F., Zein El Abedin, S. & Borissenko, N., 2006. Probing Lithium and Alumina Impurities in Air- and Water Stable Ionic Liquids by Cyclic Voltammetry and In Situ Scanning Tunneling Microscopy. *Zeitschrift für Physikalische Chemie,* Volume 220, p. 1377.

Farusseng, D., Aguado, S. & Pinel, C., 2009. Metal-Organic Frameworks: Opportunities for Catalysis. *Angewandte Chemie, International Edition,* Volume 48, p. 7502–7513.

Feng, D. et al., 2011. Separation of ionic liquid [Mmim][DMP] and glucose from enzymatic hydrolysis mixture of cellulose using alumina column chromatography. *Applied Microbiology and Biotechnology,* Volume 91, p. 399–405.

Fernández, J. F. et al., 2011. Recovery of Ionic Liquids from Wastewater by Nanofiltration. *Journal of Membrane Science & Technology,* 1(Special Issue 4).

FIBIC Oy, 2014. *FIBIC FuBio Cellulose programme report.* [Online] Available at: https://www.slideshare.net/FIBIC/cellulose-webv2 [Accessed 22 September 2017].

Fox, D. M. et al., 2008. Flammability and Thermal Analysis Characterization of Imidazolium-Based Ionic Liquids. *Industrial & Engineering Chemistry Research,* Volume 47, p. 6327–6332.

Gabrus, E., Nastaj, J., Tabero, P. & Aleksandrzak, T., 2015. Experimental studies on 3A and 4A zeolite molecular sieves regeneration in TSA process: Aliphatic alcohols dewatering-water desorption. *Chemical Engineering Journal,* Volume 259, p. 232–242.

Gregor, H. P., Sundheim, B. R., Held, K. M. & Waxman, M. H., 1952. Studies on Ion-Exchange Resins. V. Water Vapor Sorption. *Journal of Colloid Science,* Volume 7, p. 511–534.

Gutowski, K. E. et al., 2003. Controlling the Aqueous Miscibility of Ionic Liquids: Aqueous Biphasic Systems of Water-Miscible Ionic Liquids and Water-Structuring Salts for Recycle, Metathesis, and Separations. *Journal of the American Chemical Society,* Volume 125, p. 6632–6633.

Haerens, K., Van Deuren, S., Matthijs, E. & Van der Bruggen, B., 2010. Challenges for recycling ionic liquids by using pressure driven membrane processes. *Green Chemistry,* Volume 12, p. 2182–2188.

Hämmerle, F. M., 2011. The Cellulose Gap (The Future of Cellulose Fibers). *Lenzinger Berichte,* Volume 89, p. 12–21.

Hauru, L. K. J., Hummel, M., Michud, A. & Sixta, H., 2014. Dry jet-wet spinning of strong cellulose filaments from ionic liquid solution. *Cellulose,* Volume 21, p. 4471–4481.

Helfferich, F. G., 1995. *Ion Exchange.* Mineola: Dover Pubilcations.

Hellstén, S., 2017. *Ioninen neste,* [e-mail]. sanna.hellsten@aalto.fi. 18 December 2017: s.n.

Holbrey, J. D. & Seddon, K. R., 1999. The phase behaviour of 1-alkyl-3-methylimidazolium tetrafluoroborates; ionic liquids and ionic liquid crystals. *Journal of the Chemical Society, Dalton Transactions,* p. 2133–2139.

Hummel, M. et al., 2016. Ionic Liquids for the Production of Man-Made Cellulosic Fibers: Opportunities and Challenges. In: O. J. Rojas, ed. *Cellulose Chemistry and Properties: Fibers, Nanocelluloses and Advanced Materials.* Berlin: Springer, p. 133–168.

Iborra, M. et al., 2000. Drying of Acidic Macroporous Styrene-Divinylbenzene Resins with 12–20 % Cross-Linking Degree. *Industrial & Engineering Chemistry Research,* Volume 39, p. 1416–1422.
Islam, M. M., Okajima, T., Kojima, S. & Ohsaka, T., 2008. Water electrolysis: an excellent approach for the removal of water from ionic liquids. *Chemical Communications,* p. 5330–5332.
Joshi, S. & Fair, J. R., 1991. Adsorptive Drying of Hydrocarbon Liquids. *Industrial & Engineering Chemistry Research,* Volume 30, p. 177–185.
Katritzky, A. R. et al., 2002. Correlation of the Melting Points of Potential Ionic Liquids (Imidazolium Bromides and Benzimidazolium Bromides) Using the CODESSA Program. *Journal of Chemical Information and Modelling,* Volume 42, p. 225–231.
Khan, I. et al., 2014. Assessing the activity coefficients of water in cholinium-based ionic liquids: Experimental measurements and COSMO-RS modeling. *Fluid Phase Equilibria,* Volume 361, p. 16–22.
Kirchner, B., 2009. *Ionic Liquids.* Berilin: Springer.
Kiser, D. L., 1987. *Removal of water from aqueous alcohol mixtures.* US, Patent No. 4696720 A.
König, A. et al., 2008. Ultra-purification of ionic liquids by melt crystallization. *Chemical Engineering Research and Design,* Volume 86, p. 775–780.
Krossing, I. et al., 2006. Why Are Ionic Liquids Liquid? A Simple Explanation Based on Lattice and Solvation Energies. *Journal of the American Chemical Society,* Volume 128, p. 13427–13434.
Küsgens, P., 2010. *Metal-organic frameworks for water adsorption applications in the automotive filtration industry.* Doctoral dissertation, Technische Univerisität Dresden, Fakultät Mathematik und Naturwissenschaften: s.n.
Kuzmina, O., 2016. Methods of IL Recovery and Destruction. In: O. Kuzmina & J. P. Hallet, eds. *Application, Purification and Recovery of Ionic Liquids.* Amsterdam: Elsevier, p. 205–248.
Laatikainen, M. et al., 2007a. Modelling of size-exclusion chromatography of electrolytes on non-ionic nanoporous adsorbents. *Journal of Chromatography A,* Volume 1149, p. 245–253.
Laatikainen, M. et al., 2007b. Chromatographic separation of a concentrated HCl-$CaCl_2$ solution on non-ionic hypercrosslinked polystyrene. *Reactive & Functional Polymers,* Volume 67, p. 1589–1598.
Lei, Z., Chen, B., Koo, Y.-M. & MacFarlane, D. R., 2017. Introduction: Ionic Liquids. *Chemical Reviews,* Volume 117, p. 6633–6635.
Lemus, J. et al., 2012. Developing criteria for the recovery of ionic liquids from aqueous phase by adsorption with activated carbon. *Separation and Purification Technology,* Volume 97, p. 11–19.
Li, B., Filpponen, I. & Argyropoulos, D. S., 2010a. Acidolysis of Wood in Ionic Liquids. *Industrial & Engineering Chemistry Research,* Volume 49, p. 3126–3136.
Li, C. et al., 2010b. Phase Behavior for the Aqueous Two-Phase Systems Containing the Ionic Liquid 1-Butyl-3-methylimidazolium Tetrafluoroborate and Kosmotropic Salts. *Journal of Chemical & Engineering Data,* Volume 55, p. 1087–1092.
Lin, R. et al., 2015. Isotherms for Water Adsorption on Molecular Sieve 3A: Influence of Cation Composition. *Industrial & Engineering Chemistry Research,* Volume 54, p. 10442–10448.
Maase, M., Massonne, K. & Vagt, U., 2005. BASIL™—BASF's Processes Based on Ionic Liquids. *Chemfiles,* Volume 5, p. 4.

Mai, N. L., Ahn, K. & Koo, Y.-M., 2014. Methods for recovery of ionic liquids - A review. *Process Biochemistry,* Volume 49, p. 872–881.
Mai, N. L. et al., 2012. Recovery of ionic liquid and sugars from hydrolyzed biomass using ion exclusion simulated moving bed chromatography. *Journal of Chromatography A,* Volume 1227, p. 67–72.
Mallakpour, S. & Dinari, M., 2012. Ionic Liquids as Green Solvents: Progress and Prospects. In: A. Mohammad & D. Inamuddin, eds. *Green Solvents II: Properties and Applications of Ionic Liquids.* Dordrecht: Springer, p. 1–33.
McCabe, W. L., Smith, J. C. & Harriot, P., 1993. *Unit Operations of Chemical Engineering.* 5th edition ed. Singapore: McGraw-Hill.
Michud, A. et al., 2014. *Process for the production of shaped cellulose articles.* s.l. Patent No. WO 2014163062.
Nandan, D., Venkataramani, B. & Gupta, A. R., 1993. Ionic Hydration and Water Sorption Isotherms for Ion Exchange Resins. *Langmuir,* Volume 9, p. 1786–1793.
Neves, C. M. S. S. et al., 2014. Enhancing the adsorption of ionic liquids onto activated carbon by the addition of inorganic salts. *Chemical Engineering Journal,* Volume 252, p. 305–310.
Ostonen, A. et al., 2016b. Experimental and Theoretical Thermodynamic Study of Distillable Ionic Liquid 1,5-Diazabicyclo[4.3.0]non-5-enium Acetate. *Industrial & Engineering Chemistry Research,* Volume 55, p. 10445–10454.
Ostonen, A., Uusi-Kyyny, P., Pakkanen, M. & Alopaeus, V., 2016a. Dew points of pure DBN and DBU and vapor-liquid equilibria of water + DBN and water + DBU systems for cellulose solvent recycling. *Fluid Phase Equilibria,* Volume 408, p. 79–87.
Palomar, J., Lemus, J., Gilarranz, M. A. & Rodriquez, J. J., 2009. Adsorption of ionic liquids from aqueuous effluents by activated carbon. *Carbon,* Volume 47, p. 1846–1856.
Parviainen, A. et al., 2013. Predicting Cellulose Solvating capabilites of Acid-Base Conjugate Ionic Liquids. *ChemSusChem,* Volume 6, p. 2161–2169.
Parviainen, A. et al., 2015. Sustainability of cellulose dissolution and regeneration in 1,5-diazabicyclo[4.3.0]non-5-enium acetate: a batch simulation of the IONCELL-F process. *RSC Advances,* Volume 5, p. 69728–69737.
Pucheault, M. & Vaultler, M., 2009. Task Specific Ionic Liquids and Task Specific Onium Salts. In: B. Kirchner, ed. *Ionic Liquids.* Berlin: Springer, p. 83–126.
Purolite, 2018. *Macronet™ MN200.* [Online] Available at: http://www.purolite.com/product/mn200 [Accessed 23 April 2018].
Ranke, J. et al., 2007. Design of Sustainable Chemical Products – The Example of Ionic Liquids. *Chemical Reviews,* Volume 107, p. 2183–2206.
Ren, S., Hou, Y., Wu, W. & Liu, W., 2010. Purification of Ionic Liquids: Sweeping Solvents by Nitrogen. *Journal of Chemical & Engineering Data,* Volume 55, p. 5074–5077.
Rodríquez, H. et al., 2009. Biphasic liquid mixtures of ionic liquids and polyethylene glycols. *Physical Chemistry Chemical Physics,* Volume 11, p. 10916–10922.
Rosenau, T. et al., 2002. Cellulose solutions in N-methylmorpholine-N-oxide (NMMO) – degradation processes and stabilizers. *Cellulose,* Volume 9, p. 283–291.
Schäfer, T., Rodrigues, C. M., Afonso, C. A. M. & Crespo, J. G., 2001. Selective recovery of solutes from ionic liquids by pervaporation – a novel approach for purification and green processing. *Chemical Communications,* p. 1622–1623.
Scott, R. P. W., 2003. *Priciples and Practice of Chromatography.* [Online] Available at: http://faculty.ksu.edu.sa/Dr.almajed/Books/practical%20HPLC.pdf [Accessed 27 September 2017].

Scurto, A. M., Aki, S. N. V. K. & Brennecke, J. F., 2003. Carbon dioxide induced separation of ionic liquids and water. *Chemical Communications*, p. 572–573.

Shahriari, S., Neves, C. M. S. S., Freire, M. G. & Coutinho, J. A. P., 2012. Role of the Hofmeister Series in the Formation of Ionic-Liquid-Based Aqueous Biphasic Systems. *The Journal of Physical Chemistry B*, Volume 116, p. 7252–7258.

Sigma-Aldrich, 2016. *1,5-Diazabicyclo[4.3.0]non-5-ene Safety Data Sheet.* [Online] Available at: https://www.sigmaaldrich.com/MSDS/MSDS/DisplayMSDSPage.do?country=FI&language=EN-generic&productNumber=136581&brand=ALDRICH&PageToGoToURL=https%3A%2F%2Fwww.sigmaaldrich.com%2Fcatalog%2Fproduct%2Faldrich%2F136581%3Flang%3Dfi
[Accessed 20 5 2018].

Sigma-Aldrich, 2017. *Physical Properties of Solvents.* [Online] Available at: https://www.sigmaaldrich.com/content/dam/sigma-aldrich/docs/Aldrich/General_Information/labbasics_pg144.pdf
[Accessed 13 09 2017].

Sigma-Aldrich, 2018. *Molecular Sieves - Technical Information Bulletin.* [Online] Available at: https://www.sigmaaldrich.com/chemistry/chemical-synthesis/learning-center/technical-bulletins/al-1430/molecular-sieves.html
[Accessed 4 April 2018].

Sinegra, J. A. & Carta, G., 1987. Sorption of Water from Alcohol-Water Mixtures by Cation-Exchange Resins. *Industrial & Engineering Chemistry Research*, Volume 26, p. 2437–2441.

Sixta, H. et al., 2015. Ioncell-F: A High-strength regenerated cellulose fibre. *Nordic Pulp & Paper Research Journal*, Volume 30, p. 43–57.

Sklavounos, E. et al., 2016. Ionic Liquids: Recycling. In: *Encyclopedia of Inorganic Chemistry.* s.l.:John Wiley & Sons, p. 1–16.

Solà Cervera, J. L. & König, A., 2010. Recycling Concept for Aluminum Electrodeposition from the Ionic Liquid System EMIM[Tf2N]-AlCl3. *Chemical Engineering & Technology*, Volume 33, p. 1979–1988.

Strathmann, H., 2011. Membranes and Membrane Separation Processes, 1. Principles. In: *Ullmann's Encyclopedia of Industrial Chemistry.* Weinheim: Wiley, p. 413–456.

Sun, J. et al., 2017. Efficient dehydration and recovery of ionic liquid after lignocellulosic processing using pervaporation. *Biotechnology for Biofuels*, Volume 10, p. 154.

Suomen Standardisoimisliitto, 1982. *SFS 3017 - Veden metallipitoisuudet. Määritys atomiabsorptiospektrometrisesti liekkimenetelmällä. Erityisohjeita natriumille ja kaliumille.* s.l.:s.n.

Swatloski, R. P., Spear, S. K., Holbrey, J. D. & Rogers, R. D., 2002. Dissolution of Cellose with Ionic Liquids. *Journal of the American Chemical Society*, Volume 124, p. 4974–4975.

Tan, S. S. Y. T. & MacFarlane, D. R., 2009. Ionic Liquids in Biomass Processing. In: B. Kirchner, ed. *Ionic Liquids.* Berlin: Springer, p. 311–340.

Taubert, A., 2009. Heavy Elements in Ionic Liquids. In: B. Kirchner, ed. *Ionic Liquids.* Berlin: Springer, p. 127–160.

The Dow Chemical Company, 2017. *DOWEX Ion Exchange Resins - DOWEX Resins as Organic Solvent Desiccants.* [Online] Available at: http://msdssearch.dow.com/PublishedLiteratureDOWCOM/dh_0060/0901b803800609a0.pdf?filepath=liquidseps/pdfs/noreg/177-01722.pdf&fromPage=GetDoc
[Accessed 19 September 2017].

Thomas, W. J. & Crittenden, B., 1998. *Adsorption Technology and Design.* Oxford: Elsevier.
Tiihonen, J., Laatikainen, M., Markkanen, I. & Paatero, E., 1999. Sorption of Neutral Components in Ion-Exchange Resins. 1. Effect of Cross-Link Density and Counterion on Selective Sorption of Water-Ethanol Mixtures in Sulfonated PS-DVB Resins. *Industrial & Engineering Chemistry Research,* Volume 38, p. 4832–4842.
Tomé, L. I. N. et al., 2014. ‘‘Washing-out’’ ionic liquids from polyethylene glycol to form aqueous biphasic systems. *Physical Chemistry Chemical Physics,* Volume 16, p. 2271–2274.
Toteja, R. S. D., Jangida, B. L., Sundaresan, M. & Venkataramani, B., 1997. Water Sorption Isotherms and Cation Hydration in Dowex 50W and Amberlyst-15 Ion Exchange Resins. *Langmuir,* Volume 13, p. 2980–2982.
Trindade, J. R. et al., 2007. Salting out effects in aqueous ionic liquid solutions: Cloud-Point Temperature shifts. *Journal of Physical Chemistry B,* Volume 111, p. 4737–4741.
Trinh, L. T. P. et al., 2013. Recovery of an ionic liquid [BMIM]Cl from a hydrolysate of lignocellulosic biomass using electrodialysis. *Separation and Purification Technology,* Volume 120, p. 86–91.
Tsyurupa, M. P. & Davankov, V. A., 2006. Porous structure of hypercrosslinked polystyrene: State-of-the-art mini-review. *Reactive & Functional Polymers,* Volume 66, p. 768–779.
Vakkilainen, E. K., 2005. *Kraft recovery boilers - Principles and practise.* Helsinki: Suomen Soodakattilayhdistys r.y..
Vekariya, R. L., 2017. A review of ionic liquids: Applications towards catalytic organic transformations. *Journal of Molecular Liquids,* Volume 227, p. 44–60.
Wakai, C., Oleinikova, A., Ott, M. & Weingärtner, H., 2005. How Polar Are Ionic Liquids? Determination of the Static Dielectric Constant of an Imidazolium-based Ionic Liquid by Microwave Dielectric Spectroscopy. *The Journal of Physical Chemistry B,* Volume 109, p. 17028–17030.
Walger, E., Hellstén, S., Witos, J. & Sixta, H., 2017. Identification of accumulated carbohydrate degradation products during the processing of cellulose using an ionic liquid solvent: Towards solvent recycling. *253rd American Chemical Society National Meeting & Exposition - Valorization of Renewable Resources & Residuals into New Materials & Multiphase Systems - Division of Cellulose and Renewable Materials.*
Wang, H., Gurau, G. & Rogers, R. D., 2012a. Ionic liquid processing of cellulose. *Chemical Society Reviews,* Volume 41, p. 1519–1537.
Wang, X. et al., 2012b. Recovery of ionic liquids from dilute aqueous solutions by electrodialysis. *Desalination,* Volume 285, p. 205–212.
Wei, G.-T., Yang, Z. & Chen, C.-J., 2003. Room temperature ionic liquid as a novel medium for liquid/liquid extraction of metal ions. *Analytica Chimica Acta,* Volume 488, p. 183–192.
Wilkes, J. S., Levisky, J. A., Wilson, R. A. & Hussey, C. L., 1982. Dialkylimidazolium Chloroaluminate Melts: A New Class of Room-Temperature Ionic Liquids for Electrochemistry, Spectroscopy and Synthesis. *Inorganic Chemistry,* Volume 21, p. 1263–1264.
Wu, B., Liu, W., Zhang, Y. & Wang, H., 2009. Do We Understand the Recyclability of Ionic Liquids?. *Chemistry - A European Journal,* Volume 15, p. 1804–1810.
Wu, B., Zhang, Y. M. & Wang, H. P., 2008. Aqueous Biphasic Systems of Hydrophilic Ionic Liquids + Sucrose for Separation. *Journal of Chemical & Engineering Data,* Volume 53, p. 983–985.
Wymore, C. E., 1966. *Dehydration of organic liquids with carboxylate cation exchange resins.* US, Patent No. 3235610A.

Yu, G. et al., 2012. Viscosity of ionic liquids: Database, observation, and quantitative structure-property relationship analysis. *AIChE Journal*, Volume 58, p. 2885–2899.
Öhman, F., Delin, L., Simic, N. & Pelin, K., 2014. *Electrolysis of sodium sulphate – efficient use of saltcake and ESP dust in pulp mills.* [Online] Available at: http://www.aforsk.se/sites/default/files/13-347.pdf [Accessed 18 October 2017].

APPENDIX I DERIVATION EQUATION (3)

Solid phase water content is calculated from the amount of water that has been removed ($m_{\mathrm{H_2O,removed}}$) by a gram of dry solid (m_{solid}):

$$q_{\mathrm{e}} = \frac{m_{\mathrm{H_2O,removed}}}{m_{\mathrm{solid}}} \tag{4}$$

If it is assumed that only water is adsorbed, the amount of removed water is calculated from the mass of the liquid phase before ($m_{\mathrm{IL,i}}$) and after ($m_{\mathrm{IL,e}}$) contact with the solid.

$$m_{\mathrm{H_2O,removed}} = m_{\mathrm{IL,i}} - m_{\mathrm{IL,e}} \tag{5}$$

Mass of the liquid phase after contact with the solid can be calculated from its water content ($x_{\mathrm{w}}(\mathrm{H_2O})_{\mathrm{e}}$) and from the mass of the pure IL component ($m_{\mathrm{IL,pure}}$).

$$m_{\mathrm{IL,e}} = \frac{m_{\mathrm{IL,pure}}}{1 - \frac{x_{\mathrm{w}}(\mathrm{H_2O})_{\mathrm{e}}}{100}} \tag{6}$$

Mass of the pure IL component is assumed to stay constant, because only water is assumed to be adsorbed. Its mass can be calculated from the initial mass of the liquid phase ($m_{\mathrm{IL,i}}$) and the initial water content ($x_{\mathrm{w}}(\mathrm{H_2O})_{\mathrm{i}}$).

$$m_{\mathrm{IL,pure}} = m_{\mathrm{IL,i}}\left(1 - \frac{x_{\mathrm{w}}(\mathrm{H_2O})_{\mathrm{i}}}{100}\right) \tag{7}$$

Equations (6) and (7) can then be combined and placed into equation (5).

$$m_{\mathrm{H_2O,removed}} = m_{\mathrm{IL,i}} - \frac{m_{\mathrm{IL,i}}\left(1 - \frac{x_{\mathrm{w}}(\mathrm{H_2O})_{\mathrm{i}}}{100}\right)}{1 - \frac{x_{\mathrm{w}}(\mathrm{H_2O})_{\mathrm{e}}}{100}} = m_{\mathrm{IL,i}}\left(1 - \frac{1 - \frac{x_{\mathrm{w}}(\mathrm{H_2O})_{\mathrm{i}}}{100}}{1 - \frac{x_{\mathrm{w}}(\mathrm{H_2O})_{\mathrm{e}}}{100}}\right) \tag{8}$$

Finally, by placing equation (8) to equation (4), the form presented in equation (3) is obtained.